MODELLING AND SIMULATION OF MODULAR REFINERY FOR PRODUCTION OF FUELS WITH LOW ENVIRONMENTAL POLLUTION

Prepared by

Mbinzi Kita Deddy Ngwanza

(#1569064)

MSc Eng (Wits)

A thesis submitted to the Faculty of Engineering and the Built Environment, University of the Witwatersrand, Johannesburg, in fulfilment of the requirements for the degree of Master of Science in Engineering

Supervisor: Dr DiakanuaNkazi

Johannesburg, May 2020

Declaration

I declare that this thesis is my own unaided work. It is being submitted for the Degree of Masters of Science to the University of the Witwatersrand, Johannesburg. It has not been submitted before for any degree or examination in any other University.

Mbinzi Kita Deddy Ngwanza

10th day of May year 2020

Abstract

Production and upgrading of fuels and petrochemicals, used worldwide, are based on a type of refinery (characteristics, capacity), market, consumption demands, and development of engine technology. Although the composition of crude oil differs by origin, the key operations (units) performed are same. Crude oil distillation, cracking and reforming constitute the operations' key in oil refineries to produce useful product. Each process has attracted more researches since the discovery of method separating crude oil cuts. The complexed operations that occur in the production of fuels' and their impact on environment are reflected, paving the way for many additional researches.

Industrial processes cover a wide range of operations that deal with solids, liquids and gases as feeding process or product. This requires a contribution from Chemical Engineering science to solve any problem occurs during the operations. Modelling and simulation are tools that are combined or useful on their own to solve real-life troubleshooting situations, and/or upgrade researches. These can bring great advantages to the industrial process.

Due to the need of upgrading petroleum refining products, this research aimed to develop models and simulate the main refining units. Design data based on the characteristics of crude oil, operating parameters of the involved units, and other essential data were calculated and collected, and then entered into the Aspen Plus simulation software to generate the modular refinery model. The results of the full simulation were studied and allowed to obtain the composition of different products and to determine conditions of petroleum products. This study shows that it is definitely possible to predict impact of sulphur on environment. Different information on the modular refinery in this study were obtained and used for the simulation. Simulation was performed using data such as the number of trays (24), a reflux of 0.61, total catalyst flowrate of 6.92 m^3/h, 36.42 m^3/h and 44.01 m^3/h respectively for the hydrotreater, the reformer and the cracker; and the composition of distillate, the bottom and the feed rate for paraffins, naphtenes and aromatics.

Dedications

To my family members

Publications

- Paper accepted for publication by International Journal of Research and Review:

Mbinzi K. Deddy Ngwanza, D. Nkazi, H. Ngwanza and H Mukaya, 2018. "Review of Catalytic processes design and modelling: Fluid Catalytic Cracking unit and Catalytic Reforming unit". International Journal of Research and Review 2018 - reviewed and accepted for publication.

Conference(s) and seminar(s)

Date	Place	Nature of presentation	Event
28 September 2017	Richard Ward Building, Wits University	Poster	Engineering Research Day
31 August 2018	Richard Ward Building, Wits University	Oral presentation	Oil and Gas group research meeting

Acknowledgements

Prima facie, I am grateful to God for the good health and wellbeing that were necessary to complete this study.

I would like to pay particular tribute to the following key persons who have worked closely with me in various ways during this period. You have assisted me more then you thought.

I place on record, my sincere thank you to Dr Diakanua Nkazi, for his supervision, inspiring guidance and support throughout this Masters journey.

I express my gratitude to the National Research Foundation for the financial assistance throughout my second year of research.

I am also grateful to staff of the School of Chemical and Metallurgical Engineering of University of the Witwatersrand for providing me with all the necessary facilities and technical support for this research project.

I thank Mr Bruce Mothibedi for assisting me on the use of Wits-CHMT computer lab facilities for simulation.

I owe more thanks to family. Words cannot express how grateful I am to my mother, Anne Mulenga, and father, Norbert Ngwanza, for all the sacrifices that you have made on my behalf. I thank my uncle and aunty, respectively Charles and Lorraine Ngwanza for his dedication for the success of my studies.

Also I would like to thank my brothers and sisters for their endless support. Thanks to Tiemele Aka, Olayile Ejekwu and Swathi Burla for their inputs during brainstorming time. Lastly, I would like to thank my fiancée Pamela Kabila for her endless love and support.

Table of content

List of Figures

List of Tables

List of Symbols

accumulation of mass on the stage while W_i is liquid holdup at stage i for component j	$\frac{d(W_i x_{i,j})}{d\theta}$
Active surface area of the stage and surface area of the down corner	A_{Ti} and A_{Di}
Actual composition of vapour entering n^{th}tray	$Y_{n-1,j}^{T}$
Actual number of tray	N_{actual}
Actual Reflux	R_{actual}:
Adsorption terms for the metal function and for the acid function respectively	θ and Γ
Ammonia	NH_3
Antimony	Sb
Area of heat transfer pertaining to the convection	A_{conv}
Area of heat transfer pertaining to the radiant	A_{rad}
Average molecular weight	M
Characterization factor	K_W
Cold stream inlet temperature	t_1
Cold stream outlet temperature	t_2
Commercial cobalt-molybdenum on alumina	Co-Mo/γ-Al_2O_3
Composition of component (i) in Feed	$\boldsymbol{z_i}$
Composition of light component in feed	Z_F
Constant mass transfer coefficient	k_L
density difference between aqueous and	$\Delta\rho$

organic phases, kg/m^3	
Catalyst to Oil Ratio	COR
Density of liquid at stages i	ρ_{Li}
Density of the catalyst	ρ_{Cat}
Density of the mixture	ρ_G
Diameter of the tower	D_T
Dioxide of carbon	CO_2
Drop radius, m	r
Efficiency	ε
Equilibrium coefficient for component j	K_j
European emission standards	Euro 1/2/3/4/5
Factor used to correct the departure from true counter current flow	F_T
Feed	$\boldsymbol{F}$
Feed quality	$\boldsymbol{q}$
Feed rate of input stream	F
Flow rate of catalyst	Q_{cat}
Flux of A into the liquid through the liquid film as a function of driving force	N_A
Fractional recovery of light in the bottom	δ
Fractional recovery of light in the distillate	β
From molecule with five carbon to molecule with twelve carbon	C5-C12
From molecule with one carbon to molecule with four carbon	C1-C4
Fugacity coefficient of the vapour phase	Φ_i
Gravity, m/s^2	g
Heat transfer rate	Q
Heat transfer surface area[m^2]	A

Height of column	H_{tower}
Hot stream inlet temperature	T_1
Hot stream outlet temperature	T_2
Hydrocarbon molecule	R
Hydrogen sulphide	H_2S
Independent variables for the *i*th stage of multicomponent distillation problem	$x_{i,j}$,L_i, $V_i$and T_i
Iron	Fe
Liquid enthalpy for *j*th component on *i*th stage	$h_{i,j}$
Liquid flow from the process	L_i
Liquid flow into the process	$L_{i\,feed}$
Liquid height of the stage	h_{Ti}
Log mean temperature difference ΔT_M	ΔT_{LM}
Mean Average Boiling Point	Mid-BP
Mean temperature difference	ΔT_M
Minimum reflux	R_{min}
Molar density	ρ_m
Molar enthalpies of inlet and outlet streams	h_i, h_{i+1}, $h_{i-1}$and h_{Fi}
Mole flow of liquid from and entering stage i	L_i and L_{i-1}
Mole flow of vapours from and entering stage i	V_i and V_{i+1}
Mole fraction of *j*th component in liquid phase on *i*th stage	$x_{i,j}$
Mole fraction of light component in bottom	X_B
Mole fraction of light component in distillate	X_D

Mole fractions in feed	f
Mole fractions in liquid and vapour	x and y
Mole ratio of light component in feed	Z_F
Molecular weight of gas	M_G
Molecular weight of the products	M_B
Molecular weight of the reactants	M_A
Murphree vapour efficiency for j^{th}component on n^{th}tray	
Nitrogen Oxides	NOx
Overall transfer coefficient	U
Parts per million	Ppm
Phase equilibrium constant of jth component on ith stage	$K_{i,j}$
Polycyclic Aromatic Hydrocarbons	PAH
Position of vapour in phase equilibrium with liquid on n_{th} tray with composition X_{nj}, Y_{nj} actual composition vapour leaving n^{th}tray	Y_{nj}^{*}
Rates constants of catalytic reforming reactions	K_{e1},k_{f1},K_{e2},k_{f2}, $-r_{naphthene-cracking}$, k_{f3}, $-r_{paraffin-cracking}$, k_{f4}
Rates equations of catalytic reforming reactions	r
Reflux ratio	R
Relative volatility	α
Residence time	t_C
Respectively fugacity coefficient of pure components in liquid phase and activity coefficients and	v_j^0 and γ_i
Respectively the heat of mixing, external heat source and the heat losses	Q_M, Q_S and Q_{loss}

Settling rate	V
Side stream	S_i
Specific enthalpy of the feed	h_f
Specific enthalpy of the feed	h_i
Sulphur	S
Sulphur Dioxide	SO_2
The heat flux in the radiant section	q_r
The heat flux which occurs in the convection section	q_c
Theoretical number of tray	N_{theory}
Total bottom amount	B
Total distillate amount	D
Total distillate flow rate	D
Total liquid flow rate from *i*th stage	L_i
Total vapour flow rate of *i*th stage	V_i
Valve sizing coefficient	C_V
Vapour enthalpy for *j*th component	$H_{i,j}$
Vapour velocity	V
Viscosity of oil, kg/m^{1}s	μ_0
Volume average boiling point	T_V
Volume of reactor	$V_{reactor}$
Volume of the catalyst	V_{Cat}
Weight percent	wt%

List of Abbreviations

Abbreviation	Meaning
ADU:	Atmospheric Distillation Unit
AG:	Atmospheric Gasoil
API gravity:	American Petroleum Institute gravity
BP:	Boiling Point
BPD:	Barrels per day
CF2/3:	Clean Fuels 2/3
CDU:	Crude oil Distillation Unit
CRU:	Catalytic Reforming Unit
D:	Distillate
DEA-RSA:	Department of Environmental Affairs, Republic of South Africa
EPA:	United States Environmental Protection Agency
EU:	European Union
FCCU:	Fluid Catalytic Cracking Unit
FUG:	Fenske-Underwood-Guilliland
HDAs:	Hydrodeasphatenization
HDM:	Hydrodemetallization
HDNi:	Hydrodenickelation
HDS:	Hydrodesulphurization
HDV:	Hydrodevanadization
HK:	Heavy Key
HN:	Heavy Naphtha
HNK:	Heavy Non-Key
HTU:	HydroTreatment Unit
IEA:	International Energy Agency
K:	Kerosene
LK:	Light Key
LN:	Light Naphtha

LNK:	Light Non-Key
LPG:	Liquefied Petroleum Gas
MESH:	Mass balance, Equilibrium, Summation and Heat relations
Mid-BP:	Mean Average Boiling Point
PetroSA:	Petrol, oil and gas corporation of South Africa
PIONA:	Paraffin, Isoparaffin, Olefin, Naphtene and Aromatic
PM:	Particle Matter
PNA:	Paraffin, Naphtene and Aromatic
PONA:	Paraffin, Olefin, Naphtene and Aromatic
R:	Reflux
RON:	Research Octan Number
RVP:	Reid vapor pressure
SAPIA:	South African Petroleum Industry Association
SARA:	Saturated Aromatic, Resine and asphaltene
TBP:	True Boiling Point
VDU:	Vacuum Distillation Unit
VG:	Vacuum Gasoil
VGO:	Vacuum Gasoil
WSHV:	Weight Hourly Space

CHAPTER 1

INTRODUCTION

1.1. Background and motivation

In this century, due to several lifestyles changes, the use and demand of petroleum products in various fields (industry, transport, heating, electricity, …) has grown rapidly, making petroleum the most important consumed substances in modern society (Khim, 2013; Ejikeme-Ugwu, 2012; Speight, 2006). In fact, with 80% of global demand for transportation fuels met by petroleum products, crude oil is the most widely used energy source in the world (Behmiri and Manso, 2014). However, crude oil is responsible for emissions of Carbon Dioxide (CO_2), Sulphur Dioxide (SO_2), Nitrogen Oxides (NO_x) and Particulate Matter (PM). As a consequence, global warming, stratospheric ozone depletion and climate change are due to these emissions. Harmful emissions have therefore posed a pollution problem to the world that requires scientific research to provide alternative and safe energy sources.

In many developing and transition countries, transport activities account for more than 50 % of urban air pollution (PCFV, 2015). Developed countries have made significant investments in cleaner and more efficient transport to reduce emissions (PCFV, 2015). Similar environmental approaches have been adopted by encouraging the use of cleaner fuels and vehicle emissions standards.

This research project focuses on modelling and simulation of a modular refinery to mitigate negative emissions and provide cleaner fuels. A project of this nature is particularly necessary of the aging of South Africa's refining infrastructure, which has a negative impact on crude oil production processes (Wakeford, 2012). Recognizing the ever-increasing demand for oil products for both local and export consumptions, researchers consider that the environmental benefits of cleaner fuels are essential for reducing the greenhouse gas emissions responsible for global warming. Thus, a mathematical modelling process in this research provides a basis for a process intervention to mitigate the unsustainable costs currently affecting South African refineries.

Pollution and clean fuels issues have taken prominent place in international debates, and South Africa is no exception. Desired levels of reduction of harmful emissions are critical in this debate. Ranked 14th in 2018 by the International Energy Agency (IEA), South Africa is one of the largest countries contributing to global greenhouse gas emissions and among the largest in Africa (McSweeney and Timepley, 2018). From 27.8 million tonnes in 1971, South Africa has increased its production of CO_2 from fuel combustion-oil by 60.30% in2014 (I.E.A., 2016). This position is largely due to the economy's dependence on fossil fuels.

According to the manufacturers companies, the main drivers of energy efficiency are new environmental regulations coupled with costs of reducing emissions. Improving the energy efficiency of companies means that their carbon footprints that allow to improve their position in face of the challenges and costs resulting from CO_2 regulations (Bunse, Vodicka, Schönsleben, Brülhart and Ernst, 2011). The influence of the quality of air emissions from various sources should therefore begin to focus on the production of clean fuels at source. Various industries are faced the need to produce environmentally friendly fuels, so that the scientific level researchers must look for scientific leads to this end. This research is therefore aimed at proposing formulae and processes that can leverage existing scientific and chemical provisions and enhance further capabilities for refinement. An understanding of the composite constituents of existing fuels is critical to provide a starting point for this research.

Refining is normally a combination of separation and purification processes that take into account the required constituents of natural elements and organisms. Humans have been using the separation process for a long time since the earliest civilizations. They developed the extraction of metals from ores, flowers perfumes, plants dyes, and potash from ashes of burnt plants, salt from sea water evaporation, refining of rock asphalt, and liquors distillation (Seader *et al.*, 2011). Separation processes and the use made of these extracts have always resulted in determining the quality, the nature and the impact of the final product. An understanding of the composition of petroleum will serve to further demonstrate the importance of these separation processes.

Petroleum is an extremely complex product among hydrocarbon compounds and the use of its various components depends on the separation process used. Several complex and intensive

processes are used to extract these components in order to formulate the final products. The process of separation, conversion and treating is called crude oil refining process (Speight, 2006; Yusuf, 2013). Crude oil processing comprises first, the separation process such as atmospheric distillation and vacuum distillation; second, cracking and reforming processes to reduce heavier hydrocarbons and increase hydrocarbon's octane number; finally, a hydro-treatment process for stabilizing and upgrading petroleum products (Jones and Pujadó, 2006; Yusuf, 2013). The balance of use and formulae used in these processes determines the quality of the final product.

Certainly, fuel requirements are central to the operation of various industries. However, There is a need to improve refining products and process in order to meet the environmental fuel requirements, improve internal combustion and for economic reasons. The modelling and simulation of chemical processes such as the crude distillation unit (CDU), the fluid catalytic the cracking unit (FCCU), the cracking reformer unit (CRU), and hydro-treatment unit (HTU) can alleviate problems by using software. In fact, HTU modelling helps meet environmental requirements because it is the process that removes sulphur, nitrogen and aromatic; and modelling of the CRU makes it to meet economic requirements as the aim of the process is to upgrade the octane number in gasoline. The output of modelling could predict the process behaviour and optimize the production process by improving operability and profitability controls (Rao *et al.*, 2004; Liu, 2015). A continuous search for enhancement and optimisation of processes to produce more environmentally friendly fuels is therefore critical.

The aging of South Africa's refining infrastructure affects the Crude oil processing operations, and the processes review will help to improve the production of oil products. In fact, the last significant changes fuels industry production in Southern Africa took place in 1980 when PetroSA synthetic fuel facility was commissioned and Sasol shut down the synthetic fuel production (Putter, 2015). Notably, the first South African crude oil refineries were built in the1950s. It is becoming increasingly difficult to meet the modern standards of oil refining industry sector. In South Africa, as well as in the rest of the world, demand for oil products has increased as follows: Petrol by 35% and Diesel by 80% since 1990 (Putter, 2015). Production of fuels with low environmental effect will be a solution of greenhouse effect and global warming. Current South African refineries cost more to maintain and may become unsustainable in the future.

1.2. Research aims

The aims of this project are to review the refining process for the production of petroleum products with low environmental impact and simulate what enhances the production of environment. To achieve these aims, this project will focus on the following objectives:

- To Model and simulation of Crude oil Distillation Unit (CDU);
- To investigate the Modelling and simulation of Catalytic Reforming Unit (CRU);
- To investigate the Modelling and simulation of Catalytic Cracking unit (FCCU);
- To investigate the Modelling and simulation of Hydrotreatment Unit (HTU).

There is compelling evidence world that it is more necessary than ever for the industry to use cleaner fuels due to the rate of pollution that caused the emission of gasses that led to the greenhouse effect. Chemical processes did not significantly reduce these emissions, which required a more in depth study of the scientific and chemical processes used by the industry to create viable options leading to creation of chemicals and fuels that have acceptable levels of impact on the environment. The South African environment is not immune to the need for cleaner fuels.

1.3. Research keys questions

This research seeks to answer the following main questions:

How can existing processes of modular refinery simulation and modelling be mathematically manipulated to improve the refining of environmentally friendly fuels?

The sub questions emanating for the main research question are as follows:

1. Can existing processes of refinement be improved?
2. Can existing equations used in the refinement processes be updated to fit the environment friendly requirement?
3. How can modelling and simulation of modular refinery achieve desired levels of fuel purity?

1.4. Expected outcomes

Following outcomes resulted from this research effort:

- Design of a modular refinery with distillation, catalytic cracking, catalytic reforming and hydrotreatment as principal operations
- Formulation of mathematical model for each unit considered.
- Simulation of the modular refinery obtained after design
- Environmental analyse of data obtained after simulation

1.5. Outline of the dissertation

The dissertation is structured as follows:

Chapter 1: This chapter provides a brief introduction to problems related to refining process and implicit environmental aspects; briefly motivates the study and provides the aims of the research. This chapter also outlines the steps followed to complete the project.

Chapter 2: This chapter summarize the theoretical underpinnings of the project, examining each unit of the study and the environmental aspects of refinery production.

Chapter 3: This chapter discusses the Methodology used in this research and presents an overview of elements of the refinery design and the presentation of modelling software used.

Chapter 4: This chapter presents the results obtained from the simulation of the designed model.

Chapter 5: This chapter provides a summary and the conclusion of the study. In addition, it provides recommendations for future work.

CHAPTER 2

LITERATURE REVIEW

This chapter presents a review of the literature on finding cleaner energy through simulation and modelling. Science and technology make extensive use of simulation and modelling to improve various processes such as petroleum refining. In this chapter the review will include general information on the origin and production of crude oil, an understanding of the constituent products of crude oil, process description as well as the environmental consequences of refining. An understanding of physical and chemical characteristics of crude oil, a modular refinery, a description of refining process, a presentation of the overall design and environmental regulations of refinery are required to build a model for crude oil separation plant. Each of these topics is reviewed in this chapter.

2.1. Crude oil

Crude oil naturally exists in the form a mixture of hydro carbonates, organic compounds and small amounts of metals. The nomenclatural culture around crude oil is based on their origins and composition. The metamorphosis of organic matter in the earth's crust is responsible for the creation of crude oil, which is then refined to generate the petrochemicals used for various fuel and energy needs. What follows is a detailed description of the constituencies of crude oil.

2.1.1. Basics of crude oil

As stated above, crude oil is a mixture of a myriad of hydrocarbons compounds from light hydrocarbons such as methane, ethane, etc., to very heavy components. So called petroleum, name taken from the Latin word meaning "rock oil"(Fagan, 1991). Throughout this study reference to oil is synonymous to petroleum. The main constituents of petroleum are carbon and hydrogen, besides that there are smaller amounts of non-hydrocarbon constituents such as sulphur, nitrogen, oxygen and some trace elements (vanadium, nickel, iron and copper). In general, crude oil contains on average 84% carbon, 14% hydrogen, 1%-3% sulphur, and less than 1% each of nitrogen, oxygen, metals, and salts (Cheremisinoff and Rosenfeld, 2009). Based on

the predominant proportion of similar hydrocarbon molecules crude oils are generally classified as paraffinic, naphthenic, or aromatic. Mixed-base crudes contain varying amounts of each type of hydrocarbon. Refinery crude base stocks usually consist of mixtures of two or more different crude oils.

The composition of the numerous compounds of the crude oil depends on the geographical location of exploitation. Although the chemical compositions are surprisingly uniform, their physical characteristics vary considerably (Gary and Handwerk, 2001). Oil and natural gas were formed hundreds of years ago from the prehistoric plants and animals. Deep organic matter in the earth's crust is converted to hydrocarbons over millions of years and is composed of oil and gas (Speight, 2002; Tissot and Welte, 1984; Vanmali, 2014). This is caused by the thermal maturation which occurs under extreme pressure and high temperature.

South Africa relies on imports feed for its refineries to attain the country's liquid fuels needs because of low levels of proven crude oil reserves and low crude oil production. Over 60% of products refined locally are produced from imported crude oil from the following countries (Ratshomo and Nembahe, 2015):

- Saudi Arabia: about 50%
- Nigeria: 24%
- Ghana: 5%
- Various producers: 7%

2.1.2. Crude oil properties

A complete analysis of crude oils is difficult because of their complex composition with different hydrocarbon components creating complex mixtures. Fractionation and elemental analyses applied to the fraction obtained are thus used to reach elemental analysis. Fractionation is a separation process applied to mixtures to run a stepwise process of reducing transient mixtures to the final product required. Although, according to Wauquier (1994), the heaviest crude oil fractions such as asphaltenes cannot be isolated and completely characterised by modern analytical methods. The high boiling point of components is significantly influenced by physical

properties such as API gravity, which quantifies asphaltenes and resins in terms of percentage (Fahim, Al-Sahhaf and Elkilani, 2012).

Various researches and studies on analytical techniques have largely contributed to characterization of petroleum in order to level the complexity of the qualitative and quantitative determination of crude oil composition (El-Hadi, 2015; Liu, 2015). Understanding the composition of crude oil provides a premise for this study extrapolate the implicit impact of modelling and simulation when refinement optionsare sought.

Widely used for classification based on temperature range, the boiling point fractionation is directly ralated to the size and complexity of the crude components (Klein, 2005). Based on the boiling point range and the number of carbon atoms, the fractionated products of the crude oil sample are classified as shown in Figure 2.1:

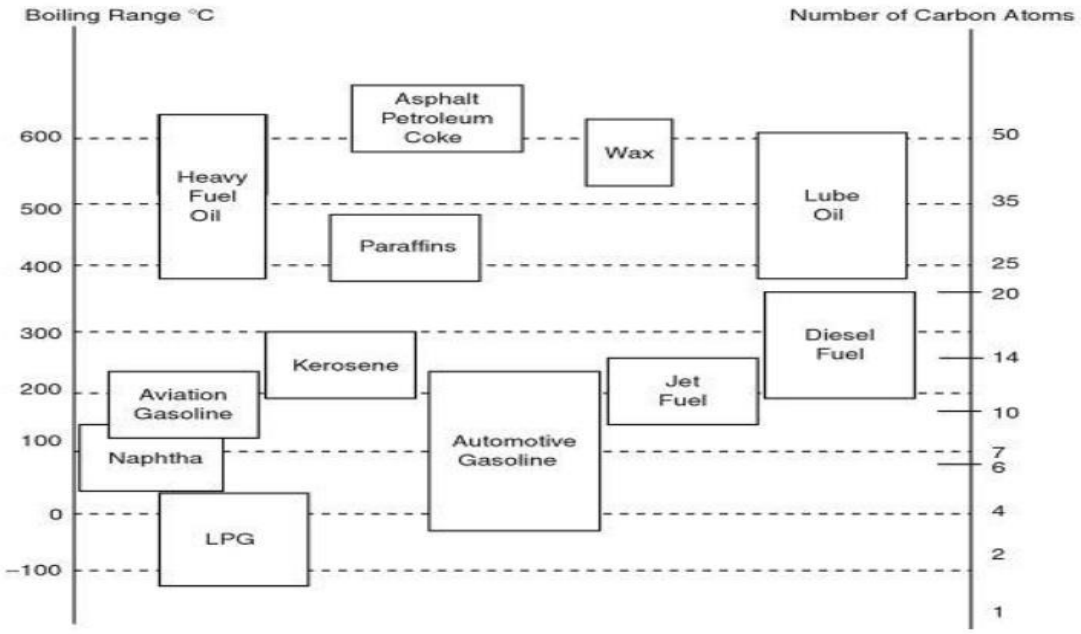

Figure 1: Petroleum products with carbon numbers and boiling point (Fahim *et al.*, 2010)

El-Hadi (2015), Liu (2015), McCain Jr (1990), Merdignac and Espirat (2007), Odebunmi, Ogunsakin and Ilukhor (2002), Riazi (2005) and, Yasin, Bhanger, Ansari, Naqvi, Ashraf, Ahmad and Talpur (2013) are amongst several researches that have proposed common analytical

methods and techniques used to identify the crude oils and petroleum products' characteristics. According to these researches, a conclusive characterization can be summarized by finding:

- Physico-chemical proprieties: Specific gravity, API gravity, Sulphur content, Pour point, Total acid content, water content, Kinematic viscosity and boiling point.
- Compositional analysis: PONA, PNA, PIONA, SARA, elements analysis.

Crude oil with high viscosities and high API gravities contains a large amount of sulphur and sulphur compounds (Eβer, Wassersceid and Jess, 2004). Refering to this category, crude oil may also be classified as sweet crude if it contains less than 0.5% or as sour crude if it contains more than 0.5% sulphur impurity (Wlazlowski, Hagströmer and Giulietti, 2001).

Notions of the proprieties of crude oil are from the basis of the characterization of the feed that will be further used in this study.

2.2. Modular refinery

Due to economic considerations, expansion of distribution facilities, location, environmental regulations, removal of price control, desired products and commodities and chemical processing, petroleum refineries have increased significantly in size and particularity for each refinery, as well as many refineries of very small size have shut down in the 20th century (Ibsen, 2006; Gary and Handwerk, 2001). According to Cross, Desrochers and Shimizu (2013) there are probably no more than two identical refineries although some may share a number of common features and processes because of specificity of refineries processing crude oil. The multiplicity of refineries in their variegated processes of use results in efficiencies; although they are sometimes detrimental to environment.

It is difficult to make general comparisons between refineries because of differences in processing flow, type of crude oil fed and products slate chosen, such as a 500,000.00 Barrels Per Day (BPD) refinery and 2,000.00 BPD refinery produce a different variety of products (Ibsen, 2006).

A conventional refinery is a plant made up of different complex processing units that contribute to production of various petroleum products. These units are costly to build and maintain sustainably. This type of refinery has to use a large space and is often built near coasts for easy transport and access to other countries (Moses, 2011).

According to Cenam (2014) and Moses (2011) a modular refinery consists of module-based equipment built to be easily and quickly transported, configured and customized as needed, anywhere in the world. In another a modular refinery is a conventional refinery built in a fragmented way (Brown et al, 2003). Modular refineries are made up of discrete parts which are assembled into modules in less time during their construction. Assembling off-site, the modules are delivered to the refinery site where connection is made quickly and easily. Modular refineries offer customized products and a variety of sizes with a capacity ranging from 500.00 to 30,000.00 BPD of crude oil inlet. These are considered as mini refineries easy to relocate that efficiently produce primary fuels (for consumption) as well as raw materials (petrochemical industries). In general, the averages quantities of products made from a barrel of crude oil are (EIA, 2014):

- Gasoline: 46%
- Diesel fuel and heating oil: 26%
- Jet Fuel: 9%
- Liquefied Petroleum: 6%
- Asphalt: 3%
- Other products: 10%

The Table 1 below highlights the difference between conventional and modular refinery:

Table 1: Conventional versus Modular Refineries (Moses, 2011)

CONVENTIONAL	MODULAR
Constructed on site	Skid-mounted on modules
Configuration could be any of topping, cocking, cracking, hydro-skimming, … process	Mostly installed as topping or hydro-skimming
Caters for all range of products	Products mostly restricted to production of middle distillates, naphtha and lights
Could process all crude types depending on processing severity	Utilization of heavy crudes yield higher proportion of low value fuels oils

In Africa, South Africa has the second largest oil refining capacity; with rising fuel demand since 2002, due in part to increased gasoline and diesel consumption in the transport sector (Ratshomo and Nembahe, 2015). This demand may put pressure on the production of volumes at the expense of quality.

2.3. Process description

This section deals with process description, for establish the basic conventions used in crude oil refining. This descriptive process provides a basis for justifying the need for production and refining options that reduce negative emissions. In their various sizes, refineries have a potential to pollute. This is due to the uniformity of the basic approaches to the process. Regardless of the variance in the sizes of refineries, they operate in three basic processes: separation (fractional distillation), conversion (cracking and reforming) and treatment (Kane, 2006).

The fractional distillation process is the step of atmospheric and vacuum distillation. It is based on the separation of crude oil components into different fractions or cuts using distillation principles. In addition, it is essential in the refining process, required better control of cuts, and has a great impact on the performance and quality of petroleum product (Yang and Barton, 2015;

López *et al.*, 2009). The objective here is to obtain C1-C4, naphtha/gasoline, kerosene, diesel and atmospheric gasoil (Parkash, 2010).

With the aim of generating new hydrocarbons adapted to the desired products, the conversion step can either break or combine molecules. From heavy hydrocarbons to smaller molecules, the cracking process can be achieved by the thermal cracking or/and fluid catalytic cracking (FCC), then converting heavy hydrocarbons (gas oils, residues) into lighter petroleum fractions (gasolines, LPG) (Han *et al.*, 2004; Barbosa *et al.*, 2013). By often using naphtha as feed catalytic reforming gives high yields of aromatics compounds such as benzene, toluene and xylenes (Taskar, 1996). A combination process, such as alkylation and polymerization, links the molecules together to form a larger molecule. From the light olefins available, larger amounts of paraffinic high octane products can be made through alkylation although polymerization produces highly photo-reactive olefins that contribute to visual pollution of the air and to the production of ozone (Gary, Handwerk and Kaiser, 2007). The culmination of the cracking stage is to prepare the resulting products for the next treatment.

The treatment step, also called purification process, has the role of eliminating impurities such as sulphur compounds, nitrogen, metals and other impurities that can poison the catalysts and responsible for pollution that is an environmental constraint (Fahim *et al*., 2010; Ferreira *et al.*, 2010). Any formula-based intervention should also target this stage of the process because it is similar to the quality of the products obtained prior the blending stage.

The last phase in the process involves blending and this is the stage at which the product is finalized for consumption. It is at this stage that the composition of the products indicates the subsequent environmental impact. This stage must thus be achieved when everything is done to minimize impurities in the final products placed on the market.

This research will focus on the some of the main units shown in the flow process below (Figure 2) which include: Crude oil Distillation Unit (CDU), Catalytic Reforming (Cat Ref), Catalytic Cracking (Cat Crack), Hydrotreatment, and Blending Unit.

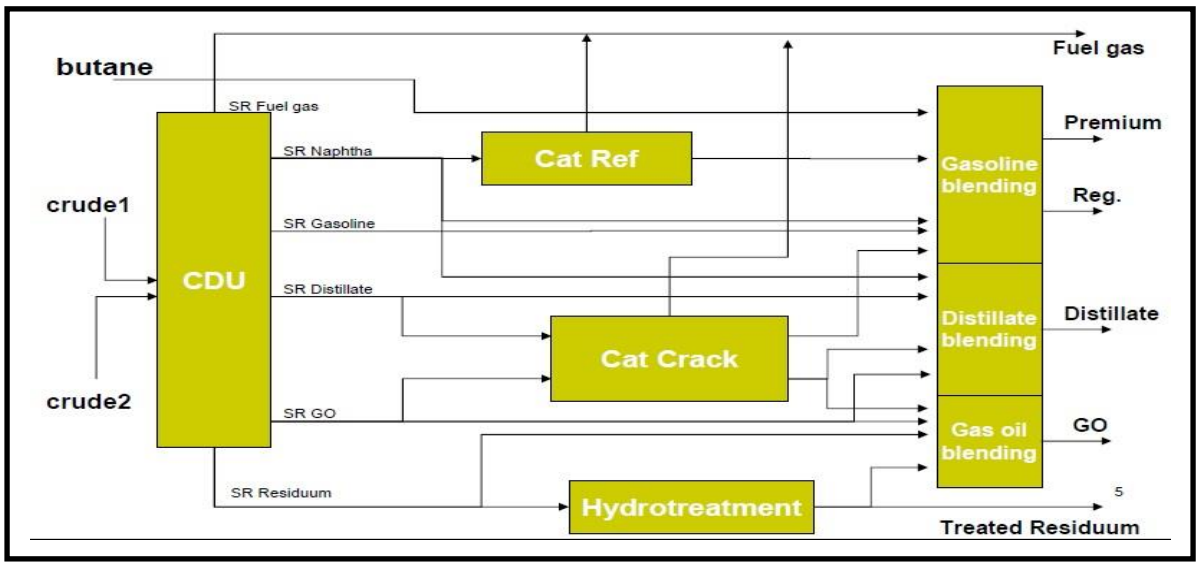

Figure 2: Flow diagram of a typical petroleum refinery (Alattas, Grossman and Palou-Rivera, 2012)

2.3.1. Crude oil Distillation Unit

Firstly, crude oil is fractionated in the atmospheric column (ADU) in order to obtain following components: Off gas (LPG), naphtha, kerosene, atmospheric gasoil, diesel and the atmospheric residue. Then the last component, namely atmospheric residue, undergoes fractionation in order to obtain light, heavy gasoil and vacuum residue from long carbon chained molecules with very high boiling points. This study covers both atmospheric columns products and vacuum columns products.

Due to the composition of crude oil, it is important to follow some steps before starting the main step of separation. In order to prevent corrosion and downstream poisoning, it is necessary to eliminate the amounts of water and traces of inorganic accompanying oil, using a specific process named desalting and dehydration separation systems (Ilkhaani, 2009). The Oil needs to be heated using heat generating equipment (heater and preheater), which are furnaces or direct combustion; in order to heat all types of hydrocarbons (Fuente, 2015). In addition to the furnace, some devices are also used to transfer heat between a solid object and fluid, or between two or

more fluids, and this is called heat exchanger. Therefore, our research will consider desalting and heating as pre-treatment step of crude oil.

The most important unit of the refining process is the atmospheric distillation unit (ADU). The efficiency of this unit determines the processing at the subsequent steps of refining. The heated crude oil (350^{o}C-400^{o}C) is fed into the bottom of the column from where different components come out as separate streams. The upper distillates will be gas and naphtha, the middle distillates will contain kerosene, heavy and light gasoil, the lower distillates will be sent to the reboiler in order to increase the degree of fractionation and overall efficiency and finally the atmospheric residue will be injected to a furnace as required by the vacuum distillation unit (VDU). The VDU operates in a range of 370 to 425^{o}C temperature and pressure range of 350 to 1400.00 kg/m^2 (EPA, 1995). Products from the VDU are light vacuum gas oil, heavy vacuum gas oil and vacuum residue (used to make asphalt). These details will be taken into account in the configuration process.

2.3.2. Fluid Catalytic Cracking Unit

According to Sadeghbeigi (2000), the cracking unit is the key of the conversion process used in refinery. The thermal cracking was the primitive way used to crack crude oil, but because of the production of higher octane number gasoline, it was replaced by catalytic cracking (Hug, 1998). During fluid catalytic cracking of petroleum, heavy hydrocarbons are converted to valuable petroleum gasoline, olefin compounds (ethylene, propylene) having a carbon chain of more than 100 through fluidized catalytic cracking process (Han *et al.*, 2000; Barbosa *et al.*, 2013). Notably, heavy hydrocarbons are high-molecular weight hydrocarbons fractions with a high-boiling point. This study focuses on heavy gas oil such as atmospheric gas oil (AG) and vacuum gas oil (VG) which constitute the feedstock of FCCU.

The foregoing products are both converted using catalysts made by combination of materials to display a plurality of functions that behave as a liquid when fluidized (Sadeghbeigi, 2012). The catalysts are a combination of acidic functions in amorphous and crystalline matrices, metal impurity traps, combustion enhancers, sulphur oxide traps, octane boosters and olefins promoter additives (Sadeghbeigi, 2012). What happens during catalytic cracking in a fluid medium is that the feed is brought into contact with the catalyst at a temperature of about 500^{o}C and at

moderately low pressures. Catalysts have four major components: zeolite, matrix, binder, and filler (Doronin *et al.*, 2007). The zeolites are chosen as particularly useful catalysts for gasoline because zeolites give high percentages of hydrocarbons with between 5 and 10 carbon atoms. Zeolite will therefore be the catalyst used in this study.

The main objective of the petroleum refinery is the production of fuels, which cannot be achieved without valorization of fractionation products (Ancheyta, 2011). Fluid catalytic cracking is one of the processes for upgrading production by conversion using catalysts. In particular, the catalytic reforming is also a conversion process which uses catalysts whose components have great similarities with the components present in the FCCU catalysts. Therefore, the next section will deal with the process where chemical conversions take place to the production of usable petrochemicals, thus addressing with the CRU.

2.3.3. Catalytic Reforming Unit

The CRU is a very important aspect of the process in terms of converting low-octane naphtha to high-octane naphtha without any changing the number of carbons in the molecule, as well as the producing a high yield of aromatics (benzene, toluene, and xylenes) in petroleum-refining and petrochemical industries (Liang *et al.*, 2005; Taskar, 1996). Hydrogen and lighter hydrocarbons are also obtained as by-products. This must be taken into account in order to optimize the amount of gasoline produce by the modular refinery.

The reforming feedstock is a complex mixture of normal and branched paraffins, five- and six-membered ring naphthenes, and single-ring aromatics, having carbon number ranging from 6 to 11. A good reforming feed must have high naphtene and aromatic hydrocarbon content. However, heavy fractions have good reforming, they have a strong tendency of coke formation and lighter fractions have poor reforming capacity. The process built into our research must take into account this important parameter.

During the catalytic process a number of conversion reactions occur, such as dehydrogenation of naphthenes to aromatics and paraffins to olefins, dehydrocyclization of paraffins and olefins to aromatics, isomerization of normal paraffins to isoparaffins, hydrocracking of paraffins and naphthenes to lower hydrocarbons. The success of those different reactions helps to transform

low octane number to high octane number and aromatics into rich benzene. To achieve our research aim, certain pressure and temperature conditions must be respected as shown in Table 2.

Table 2: Conditions of reforming process (Jechura, 2017)

REACTION	PRESSURE	TEMPERATURE
Isomerization	Indeterminate	Intermediate
Dehydrocyclization	Low pressure	High temperature
Dehydrogenation	Low pressure	High temperature
Hydrocracking	High pressure (70-140 kg/cm^2)	High temperature (400-815ºC)

Reforming conditions can be low or high for any reaction that occurs during the process. The temperature is high when it is between 480 and 510ºC. AS for the pressure, it is high when it is between 200 and 300 psig, and between 50-200 psig when it is low.

2.3.4. Hydro Treatment Unit

The final products should be adjusted to the specification of different streams such as light naphtha, kerosene and low Sulphur fuel oil, to suit the environment in which they are used (Fahim *et al.*, 2010; Ferreira *et al.*, 2009). In fact, HTU stabilizes and upgrades petroleum products by separating them from less desirable products and eliminating unwanted elements (EPA, 1995). The feed of HTU is mixed with hydrogen before being introduced to the furnace in order to increase the temperature from 316 to 427^{o}C, and then the mixture inlets a fixed bed reactor, named hydrotreater, in which sulphur and nitrogen are converted to sulphide and ammonia under a pressure between 100-3000 psi (Albahri, 2001). The products of this unit are sent to a stripper for further removal of hydrogen and ammonia, and the hydrogen is separated from the effluent before being recycled. Then desulphurized product is ready for further processing.

Although this section has provided insights into the processes involved in refining and in the production of petrochemicals, products the next section will focus on modelling and simulation.

2.4. Background in Modelling and simulation of each unit of refinery

Simulation can be defined as usage of mathematical model to generate a certain description of process behaviors. The main advantage of the simulation is to give a real view of the process behavior (Rahim and Ben-Rahla, 2012).

Aspen Hysys was developed by AspenTech, a leading supplier of software that optimizes process manufacturing for the energy, chemicals, pharmaceuticals, engineering and constructions, and other industries that manufacture and produce products from chemical processes (AspenTech, 2009).

This section serves to highlight further investigation of the different refinery units for which the models used were based on the process illustrated in the Figure 2.

2.4.1. Crude oil Distillation Unit

In the pursuit of improving and developing rigorous models several researches and various approaches have been advanced, especially in computer science. Such research has improved and developed many tools, such as Aspen Plus (Aspentech), PRO/II (SimSci-Esscor), PROMS and design IITM (ChemShare), which have been a feature of simulation and modelling (Li, Hui and Li, 2005).

In 2009, Haydary and Pavlík developed a mathematical description of crude oil distillation column using the theoretical stage method as described in Figure 3. Considering the steady state, equations of the mass balance of components, the enthalpy balance and vapour-liquid equilibrium are proposed from each theoretical step as follows:

$$L_{i-1}x_{i-1,j} + V_{i+1}y_{i+1,j} + F_i f_{i,j} - L_{i,j}x_{i,j} - V_i y_{i,j} = 0 \qquad (2.1)$$

$$L_{i-1}x_{i-1,j} + V_{i+1}y_{i+1,j} + F_i f_{i,j} - L_{i,j}x_{i,j} - V_i y_{i,j} = \frac{d(W_i x_{i,j})}{d\theta} \qquad (2.2)$$

$$W_i = \rho_{Li} A_{Ti} h_{Ti} + \rho_{Li} A_{Di} h_{Di} \qquad (2.3)$$

V_i and V_{i+1} are the mole flow of vapours from and entering stage i, L_i and $L_{i-1}$are the mole flow of liquid from and entering stage i, x, y and f represent the mole fractions in liquid, vapour and

feed, respectively, and $\frac{d(W_i x_{i,j})}{d\theta}$ represents accumulation of mass on the stage while W_i is liquid holdup at stage i for component j. ρ_{Li} is the density of liquid at stages i, A_{Ti} is the active surface area of the stage,A_{Di} is the surface area of the down corner, h_{Ti} is the liquid height of the stage.

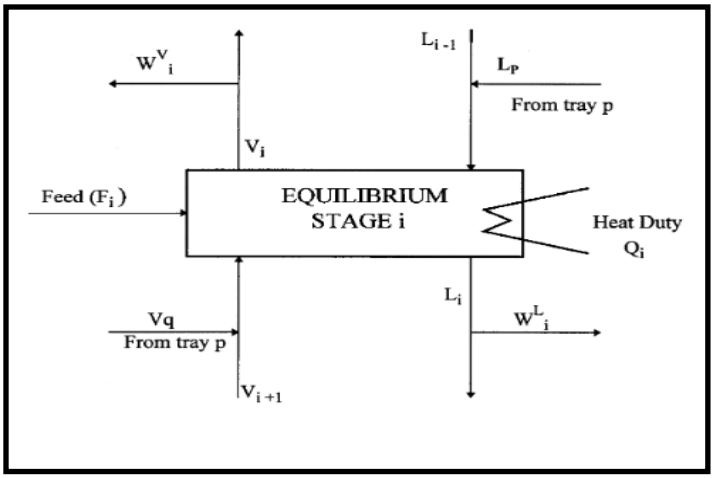

Figure 3: Schematic diagram of an equilibrium stage (Kumar *et al.*, 2001)

Equations below give enthalpy balance of stage i where h_i, h_{i+1}, $h_{i-1}$and h_{Fi} are the molar enthalpies of inlet and outlet streams; Q_M, Q_S and Q_{loss} represent respectively the heat of mixing, external heat source and the heat losses; and $\frac{d(W_i h_i)}{d\theta}$ represents the accumulated heat on stage i (Haydary and Pavlík, 2009).

$$L_{i-1}h_{i-1} + V_{i+1}h_{i+1} + F_i h_{Fi} - L_i h_i - V_i h_i + Q_M - Q_S - Q_{loss} = 0 \qquad (2.4)$$

$$L_{i-1}h_{i-1} + V_{i+1}h_{i+1} + F_i h_{Fi} - L_i h_i - V_i h_i + Q_M - Q_S - Q_{loss} = \frac{d(W_i h_i)}{d\theta} \qquad (2.5)$$

Equations (6) gives the proposed Vapour–liquid equilibrium equation:

$$y_j = K_j x_j \qquad (2.6)$$

$$K_j = \frac{\nu_j^0 \gamma_i}{\Phi_i} \qquad (2.7)$$

Where K_j (equation 2.7) is the equilibrium coefficient for component j; ν_j^0, γ_i and Φ_i are respectively the fugacity coefficient of the pure components in the liquid phase, the activity coefficients and the fugacity coefficient of the vapour phase.

Known as MESH, mass balance, equilibrium, summation and heat relations are used to develop a multicomponent distillation model suited for crude oil fraction at each stage, taking into account variables such as total liquid and total vapour flow rates, mole fractions of the components, and temperature (Haydary and Pavlík, 2009, Kumar *et al.*, 2001).

In some cases, the nonlinear equations of systems have been solved using the Newton–Raphson method by a correct choice of independent variables. This choice of variables makes the proposed model numerically stable and robust, and has helped the authors to demonstrate the stability and efficiency of the technique. The formulation founded by Kumar, Sharma, Chowdhury, Ganguly and Saraf (2001) uses $x_{i,j}$,L_i, V_i and T_i as independent variables for the ith stage of multicomponent distillation problem, and the mass balance, energy balances and summation equations are given below:

$$DC_{i,j} = V_{i+1}K_{i+1,j}x_{i+1,j} + L_{i-1}x_{i-1,j} - L_i x_{i,j} - V_i K_{i,j} x_{i,j} \quad (2.8)$$

$$DH_i = V_{i+1}\sum K_{i+1,j}x_{i+1,j}H_{i+1,j} + L_{i-1}\sum x_{i-1,j}h_{i-1,j} - L_i\sum x_{i,j}h_{i,j} - V_i\sum K_{i,j}x_{i,j}H_{i,j} \quad (2.9)$$

$$DV_i = V_i - V_i\sum K_{i,j}x_{i,j} \quad (2.10)$$

$$DL_i = L_i - L_i\sum x_{i,j} \quad (2.11)$$

With D: Total distillate flow rate

$H_{i,j}$: Vapour enthalpy for jth component

$h_{i,j}$: Liquid enthalpy for jth component on ith stage

$K_{i,j}$: Phase equilibrium constant of jth component on ith stage

L_i: Total liquid flow rate from ith stage

V_i: Total vapour flow rate of ith stage

$x_{i,j}$: Mole fraction of jth component in liquid phase on ith stage

2.4.2. Catalytic reforming unit

Simulation catalytic reforming unit developed by Askari, Karimi *et al.* (2012) used the Hysys-refinery software, and Esfahan oil refinery operating data (temperature, pressure, catalyst age and volume, and recycle rate) for the validation of the model. Askari *et al.* (2012) used continuous catalytic semi-regeneration (Figure 3) and the process feed had over 300 chemical compounds of naphthenes, aromatics and paraffins in the carbon range of C5 to C12, with 22500 bbl/day gasoline with octane number 45 as the feed flow rate and 18200-16700 bbl/day gasoline as final product rate with an octane number between 88-95.5.

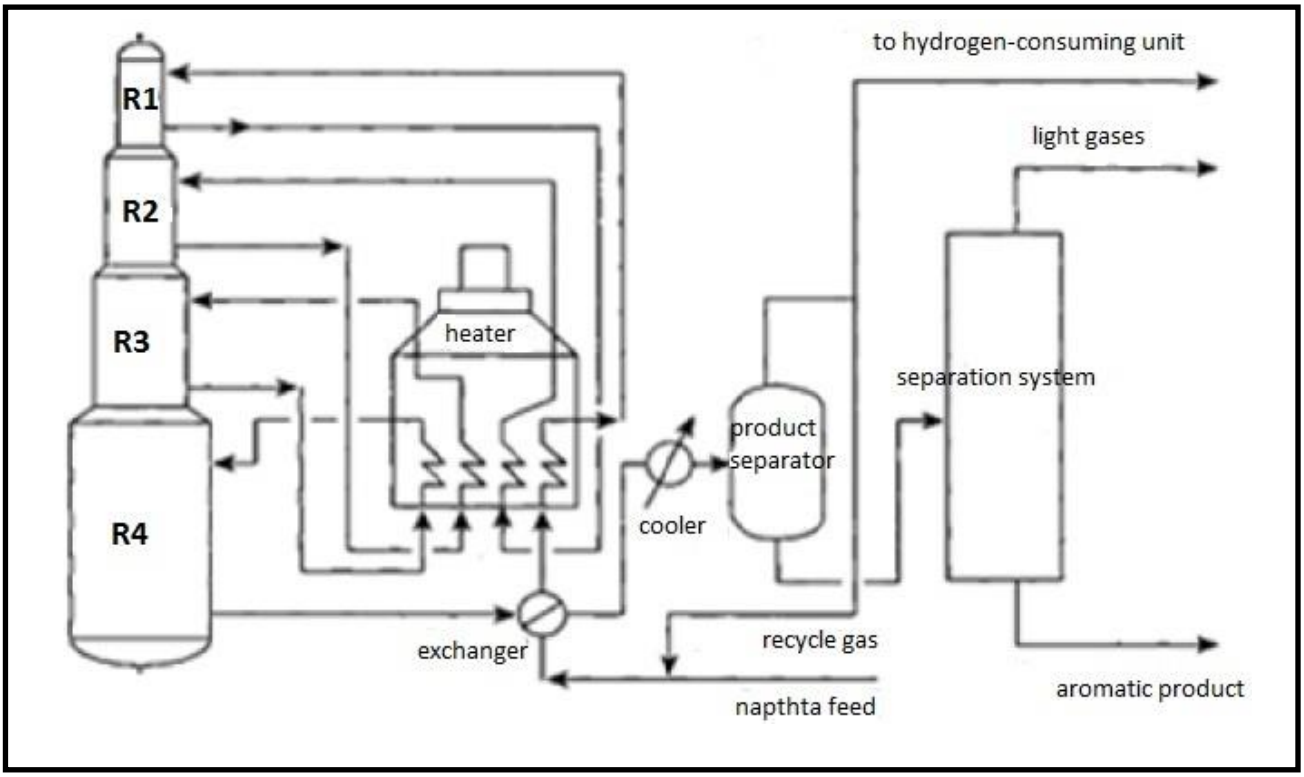

Figure 4: Catalytic reforming flowsheet (semi-regenerative) (Askari *et al.*, 2012)

The simulation of catalytic reforming unit considers temperature [^{o}C] and pressure [bar], measured delta [^{o}C], catalyst volume [m3], catalyst age days and recycle rate as input parameters. With four reactors in series using Smith model (first kinetic model), catalytic reforming unit classifies reactions into four groups below (Askari *et al.*, 2012):

- Naphthenes to paraffins:

$$Naphthenes + H_2 \leftrightarrow Paraffin \qquad \text{(Reaction 1)}$$

Rates constants:

$$K_{e1} = e^{(-7.12+\frac{8000}{T})}, \text{atm}^{-1} \quad (2.12)$$

$$k_{f1} = e^{(35.98-\frac{59600}{T})}, \frac{moles}{(hr)(lbcat)(atm)^2} \quad (2.13)$$

- Naphthenes to aromatics:

$$Naphthenes \leftrightarrow Aromatics + 3H_2 \quad \text{(Reaction 2)}$$

Rates constants:

$$K_{e2} = e^{(46.15-\frac{46045}{T})}, \text{atm}^3 \quad (2.14)$$

$$k_{f2} = e^{(23.21-\frac{34750}{T})}, \frac{moles}{(hr)(lbcat)(atm)^2} \quad (2.15)$$

- Hydrocracking of naphthenes:

$$C_nH_{2n}(naphthene) + \frac{n}{3}H_2 \leftrightarrow \frac{n}{15}\sum_{i=1}^{5} C_iH_{2i+2} \quad \text{(Reaction 3)}$$

Rates constants:

$$-r_{naphthene-cracking} = \frac{k_{f3}}{P_t}P_p \quad (2.16)$$

$$k_{f3} = e^{(42.97-\frac{62300}{T})}, \frac{moles}{(hr)(lbcat)} \quad (2.17)$$

- Hydrocracking of paraffins:

$$C_nH_{2n+2}(paraffin) + \frac{n-1}{3}H_2 \leftrightarrow \frac{n}{15}\sum_{i=1}^{5} C_iH_{2i+2} \quad \text{(Reaction 4)}$$

Rates constants:

$$-r_{paraffin-cracking} = \frac{K_{f4}}{P_t}P_p \quad (2.18)$$

$$k_{f4} = e^{(42.97-\frac{62300}{T})}, \frac{moles}{(hr)(lbcat)} \quad (2.19)$$

where k, K, t,p and n is rate constant, equilibrium constant, temperature (oR), partial pressure (atm) and number of octane atoms, respectively.

Arani *et al.* (2010) used Hougen-Watson Langmuir-Hinshelwood approach to derive below reaction rate expressions.

- Isomerization of paraffins: rate equation:

$$r = ke^{-\frac{E}{RT}}\frac{(P_{ip} - P_{np}/K_{ip\leftrightarrow np})}{(P_{H_2}\Gamma)} \quad (2.20)$$

- Dehydrocyclization of paraffins: rate equation:

$$r = ke^{-\frac{E}{RT}}\frac{(P_{np} - P_N P_{H_2}/K_{np\leftrightarrow N})}{(P_{H_2}\Gamma)} \quad (2.21)$$

- Deshydrogenation of naphtenes: rate equation:

$$r = ke^{-\frac{E}{RT}}\frac{(P_{np} - P_A {P_{H_2}}^3/K_{N\leftrightarrow A})}{(P_{H_2}\theta)} \quad (2.22)$$

- Cracking of paraffins: rate equation:

$$r = ke^{-\frac{E}{RT}}\frac{P_{ip}}{\Gamma} \quad (2.23)$$

- Hydro-dealkylation of aromatics: rate equation:

$$r = ke^{-\frac{E}{RT}}\frac{P_A}{\Gamma} \quad (2.24)$$

Where θ and Γ is adsorption terms for the metal function and for the acid function respectively.

The equations of reactors dynamic model (masse balance (2.25) and energy balance (2.26)), furnace model (2.27), heat exchange model (2.28 and 2.29) and octane number expression (2.30) were simulated using MATLAB in SIMULINK via the diagram below.

$$-\frac{dF_i}{dw} + \sum_{j=1}^{n_r}\gamma_{i,j}r_j = \frac{\varepsilon}{\rho_b}\frac{d(C_i)}{dt} \quad (2.25)$$

$$\frac{dT}{dt} = \frac{-(\sum_{i=1}^{n_c}F_i C_{pi})\frac{dT}{dw} - \sum_{j=1}^{n_r}r_j(\sum_{i=1}^{n_c}H_i\gamma_{i,j})}{(C_{pcata} + \frac{\varepsilon}{\rho_b}\sum_{i=1}^{n_c}c_i C_{pi})} \quad (2.26)$$

$$\frac{d(m_w C_{p_w} T_w + m_f C_{p_f} T_{f,m})}{dt} = q - \left(T_{f,out} - T_{f,in}\right) C_{p_f} \dot{m}_f \quad (2.27)$$

$$\frac{d(C_{p,cold}\, M_{cold}\, T_{cold,o})}{dt} = F_{cold}\left(H_{cold,i} - H_{cold,o}\right) - q \quad (2.28)$$

$$\frac{d(C_{p,hold}\, M_{hot}\, T_{hot,o})}{dt} = F_{hot}\left(H_{hot,i} - H_{hot,o}\right) - q \quad (2.29)$$

$$RON = \sum_{r=1}^{n} b_r W_r \quad (2.30)$$

Finally, Askari *et al.* (2012) showed that if the feed increased by more than 20% of the current value, the flow rate and the octane number of the final products would be increased as well. In addition, the variation in temperature and pressure, under the operating conditions of the reactors unit, had no effect on the octane number or the flow rate of the final product. The comparison between simulation data (from Hysys-refinery software) and experimental results could confirm the ability of the software to simulate the catalytic reforming unit. But, its effect on catalyst deactivation rate must be investigated. On the other hand, Arani *et al.* (2010) implemented a simulation model that was compared with experimental data obtained from the operation data sheets of a refinery plant in Iran, revealing a high level fitness between experimental data and the model.

The current project will model the catalyst deactivation rate based on Smith model by using a semi-generative catalytic reforming unit, with gasoline being the main product.

2.4.3. Fluid Catalytic Cracking Unit

Pahwa and Gupta (2016) describe FCCU as a process mainly consisting of two basic units:

- Reactor: in which the hot catalyst is brought in contact with the feed (gas oil),
- Regenerator: in which the coke deposited on the catalyst is burned off for regenerating the catalyst.

Between these two units, the riser is the most important part of the FCC process from a modelling point of view. The FCC riser is the unit that was simulated in the study by Pahwa and Gupta (2016), using the Eulerian-Eulerian approach for the description phases, the gas and solid

energy equations (with Ranz-Marshal correlation for single particles) and four lump kinetic scheme will be used for its simplicity (Table 3). Below is the general rate equation:

$$R_{i,r} = k_r C_i^n \quad (2.31)$$

Where, k_r is rate constant for rth cracking reaction, C_i is concentration of ith species (kmol/m3).

Table 3: Kinetic parameters for the four-lump model (Pahwa and Gupta, 2016)

Reaction	**Pre-exponential factor** $(m^3/m_{cat}^3.s)$	**Activation energy E** $(kJ/kmol)$
Gasoil (VGO) to Gasoline	0.06	68316
Gasoil (VGO) to Light Gases	0.04	89303
Gasoil (VGO) to Coke	0.0076	64638
Gasoline to Light Gases	0.0042	52768
Gasoline to Coke	0	115566

A model based on the main FCC processes was developed in the Bhende and Patil (2014) study working on the feed and preheating system, riser, stripper, reactor, regenerator and fractionation. For simplicity, the model assumed the riser as a reactor in which all complex reactions occurred under isothermal, constant-holdup, constant-pressure, and constant density conditions. FCC reactor is assumed to be a continuous stirred-tank reactor operating under pressure, and fractionator as a multi-component non-ideal distillation column. The following are the proposed mathematical equations.

- For riser:

$$N_A = K_L(C_A^* - C_1) \quad (2.32)$$

$$F_V = F_A - (A_{MT} N_A M_A)/P_A \quad (2.33)$$

Total continuity: $\frac{d(\rho V)}{dt} = 0 = F_B \rho_B + M_A N_A A_{MT} - F_L \rho$ (2.34)

Where k_L the constant mass transfer coefficient, N_A flux of A into the liquid through the liquid film as a function of driving force.

- For reactor:

$$F = C_V\sqrt{\frac{P-PD}{\rho}} \quad (2.35)$$

$$\tilde{n} = MP/RT = \{[yM_A + (1-y)M_B]P\}/RT \quad (2.36)$$

Total continuity: $V\ (d\rho/dt) = \rho_o F_0 - P_\rho$ (2.37)

Where $C_V$valve sizing coefficient, M average molecular weight, M_A molecular weight of the reactants, M_B molecular weight of the products.

- For fractionator:

$$E_{nj} = (Y_{nj} - Y^T_{n-1,j})/(Y^*_{nj} - Y^T_{n-1,j}) \quad (2.38)$$

Total continuity: $\frac{d(M_n)}{dt} = L_{n+1} + F^L_n + F^V_{n-1} + V_{n-1} - V_n - L_n - S^L_n - S^V_n$ (2.39)

Where Y^*_{nj} position of vapour in phase equilibrium with liquid on nth tray with composition X_{nj}, Y_{nj} actual composition vapour leaving n^{th} tray, $Y^T_{n-1,j}$actual composition of vapour entering n^{th} tray, E_{nj} Murphree vapour efficiency for j^{th}component on n^{th} tray.

The proposed model was able to predict and describe the overall conversion, products yields, process temperature and pressure. The outcome of the predicted simulator data, from Aspen v7.3 environments were closely agreed with the industrial data.

2.4.4. Hydro-treating unit (HTU)

Jurallah (2012) used trickle bed reactor to develop an unconventional kinetic model of the crude oil HTU process. Commercial cobalt-molybdenum on alumina (Co-Mo/γ-Al2O3) was proposed as the catalyst. In this treatment process, the main reactions are the following:

Hydrodesulphurization (HDS), hydrodenitrogenation (HDN), hydrodeasphaltenization (HDAs), hydrodemetallization (HDM), that include hydrodevanadization or HDV and hydrodenickelation or HDNi).

HDs: $R - S + H_2 \rightarrow R + H_2S$ (Reaction 4)

HDN: $R - NH_2 + H_2 \rightarrow RH + NH_3$ (Reaction 5)

HDM: $R - M + H_2 \rightarrow RH + M$ (Reaction 6)

HDAs: $R - Asph + H_2 \rightarrow RH + Asph - R(smaller\ hydrocarbons)$ (Reaction 7)

R represents the hydrocarbon molecule.

The general process modelling system (gPROMS) was used to model and simulate the process using below equations, based on:

- Mass balance equations in gas phase:

Hydrogene: $\frac{dP_{H_2}^G}{dz} = -\frac{RT}{u_g} k_{H_2}^L a_L (\frac{P_{H_2}^G}{h_{H_2}} - C_{H_2}^L)$ (2.40)

H_2S: $\frac{dP_{H_2}^G}{dz} = -\frac{RT}{u_g} k_{H_2}^L a_L (\frac{P_{H_2S}^G}{h_{H_2S}} - C_{H_2S}^L)$ (2.41)

- Mass balance equations in liquid phase:

Hydrogene: $\frac{dC_{H_2}^L}{dz} = \frac{1}{u_l} [k_{H_2}^L a_L \left(\frac{P_{H_2}^G}{h_{H_2}} - C_{H_2}^L\right) - k_{H_2}^S a_s (C_{H_2}^L - C_{H_2}^S)]$ (2.42)

H_2S: $\frac{dC_{H_2S}^L}{dz} = \frac{1}{u_l} [k_{H_2S}^L a_L \left(\frac{P_{H_2S}^G}{h_{H_2S}} - C_{H_2S}^L\right) - k_{H_2S}^S a_s (C_{H_2S}^L - C_{H_2S}^S)]$ (2.43)

$\frac{dC_i^L}{dz} = -\frac{1}{u_l} k_i^S a_s (C_i^L - C_i^S)$ (2.44)

Where i = sulfur, nitrogen, asphaltene, vanadium or nickel

- Mass balance equations in solid phase:

Hydrogene: $k_{H_2}^S a_s\left(C_{H_2}^L - C_{H_2}^S\right) = \rho_B \sum \eta_j r_j$ (2.45)

H_2S: $k_{H_2S}^S a_s\left(C_{H_2S}^L - C_{H_2S}^S\right) = -\rho_B \eta_{HDS} r_{HDS}$ (2.46)

$k_i^S a_s\left(C_i^L - C_i^S\right) = -\rho_B \eta_i r_i$ (2.47)

Where i = sulfur, nitrogen, asphaltene, vanadium or nickel and j = HDS, HDN, HDAs, HDV and HDNi.

Daneshvar and Fatemi (2011) presented a non-isothermal three-phase heterogeneous model to describe the hydro-treatment of diesel in a trickle-bed reactor. The model was based on mass balance equations in gas phase (H_2, H_2S andNH_3), liquid phase (S, A, NB, NNBand HC) and solide phase (for HDS, HDN and HDAs reactions), energy balance and chemical reaction kinetics (2.48, 2.49, 2.50, 2.51, 2.52, 2.53) as proposed by Jurallah (2011).

Korsten and Hoffmann: $r_{HDS} = K_{HDS} \frac{(C_S^S)(C_{H_2}^S)^{0.45}}{(1+ K_{H_2S} C_{H_2S}^S)^2}$ (2.48)

Murali and Voolapalli: $r_{HDS} = K_{HDS} \frac{(C_S^S)^{1.64}(C_{H_2}^S)^{0.55}}{(1+ K_{H_2S} C_{H_2S}^S)^2}$ (2.49)

Cheng and Fang: $r_{HDS} = K_{HDS} \frac{(C_S^S)^2(C_{H_2}^S)^{0.6}}{1+ K_{H_2S} C_{H_2S}^S}$ (2.50)

Non-basic (HDN): $r_{HDN_{NB}} = k_{HDN_{NB}} (C_{N_{NB}}^S)^{1.5}$ (2.51)

Basic (HDN): $r_{HDN_{NB}} = k_{HDN_{NB}} (C_{N_{NB}}^S)^{1.5} - k_{HDN_B} (C_{N_B}^S)^{1.5}$ (2.52)

Forward and reverse reaction (HDA): $r_{HDN_{NB}} = k_f p_{H_2}^G C_A^S - k_r (1 - C_A^S)$ (2.53)

The model of Murali and Voopalli was consistent with experimental results compared with other kinetics models of HDS.

2.5. Environmental aspects of refinery production

According to I.E.A. (2016) South Africa recorded a 60.3% increase in the production of CO_2 from fuel oil combustion, resulting in an increase of 27.8 million tons in 1971 to 69.1 million tons, between 1990 and 2014. Although South Africa accounted for 38% of CO_2 emissions from fuel combustion throughout Africa in 2011, this represented only 1% of the global total. This position is largely due to the economy's dependence on fossil fuels, especially the electricity and heating sector. In addition, according to Naré and Kamakaté (2017), road transport is one of the leading sources of outdoor air pollution in Western and Southern Africa due to the use of vehicles. In fact, for transport of people and goods in Sub-Saharan Africa, motor vehicles are increasingly used (Thambiran and Diab, 2011). Large vehicle emissions result from rapid urbanization and motorization makes cities pollution hotspots.

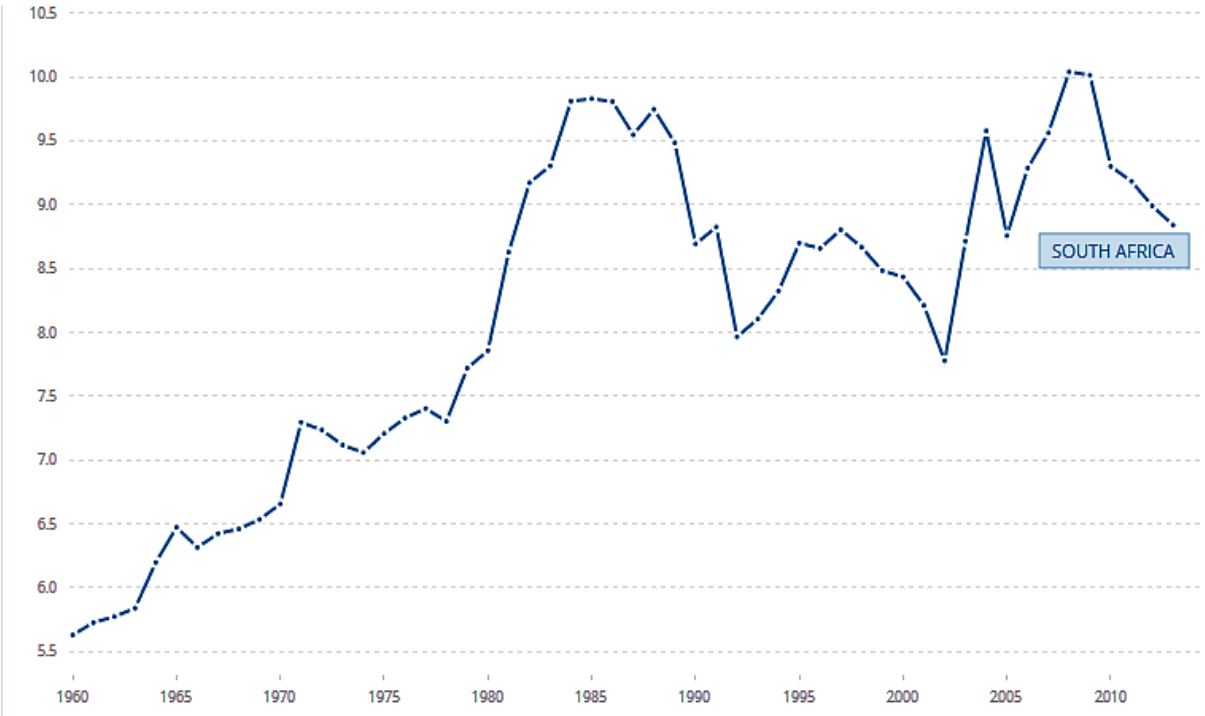

Figure 5: South African CO2 Emissions (Metric tons per capita) per year
Source: (World Bank Group, 2012)

Crude oil input contributes largely to the use of energy generation in the form of fuel refinery. As sulphur contents and densities increase in crude oils, the quality of processed crude oils is expected to deteriorate slowly in the future (Gary and Handwerk, 2001). In terms of sulphur content, the production of clean diesel and gasoline may be more energy. This results in additional CO_2 emissions as more advanced processing capacity is required due to the increased complexity refining. With fuel consumption of 43% and 41% respectively for diesel and gasoline, both are the dominant fuels used in South Africa in 2016 as shown in the Figure 4. In fact, the demand for fuel has increase by +5.6% in 2014 for South Africa, making the country the largest consumer of oil products in Southern Africa (Naré and Kamakaté, 2017).

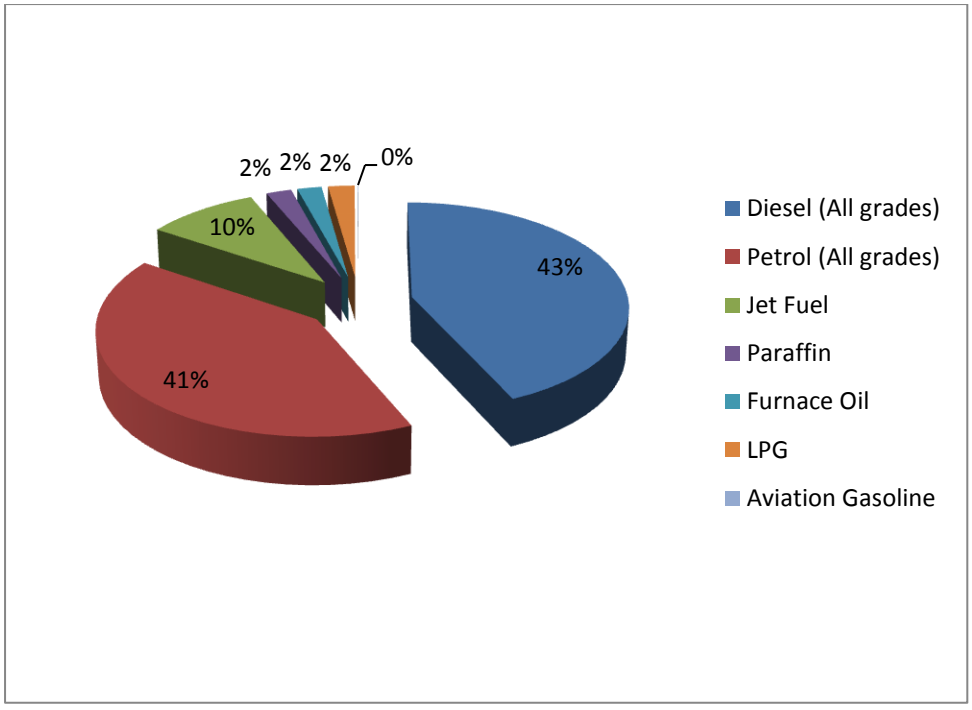

Figure 6: Fuels sales consumption in South Africa during year 2016
Source: SAPIA, 2016

With respect to cleaner fuels, the refining industry in South African is influenced by number of regulations, such as those of Japan, Australia, USA, New Zealand, Europe, China and India fuel specifications. South Africa is committed to reducing emissions by 34% by 2020 and 42% by 2025 under the Copenhagen Accord (DEA-RSA, 2010). South Africa is also amongst G20 countries that adopted and implemented clean fuel standards for gasoline and diesel to reduce sulphur content in order to jointly move toward world-class tailpipe emissions standards as rapidly as possible (Kodjak, 2015). The current format of refineries in the country comply with Euro 2 standards, with regulators requiring refineries upgraded to Euro 5 as illustrated in the Tables 4 and 5.

Table 4: Proposed Petrol specifications (Source: SAPIA, 2016)

Petrol	**Units**	**Current National specification**	**Clean Fuels 2 (CF2)**	**Clean Fuels 3 (CF3)**
Vehicle emissions standards SANS specifications roughly equivalent to EU		"Euro 2"	"Euro 4"	"Euro 5"
Sulphur max	ppm (m/m)	500	50	10
Research Octane Number (RON)		95, 93, 91	95, 93, 91	95, 93, 91
Benzene max	vol %	5	2	1
Aromatic content max	vol %	50	45	42
Olefins max	vol %	-	24	21
RVP (summer) max	Kpa	75	65 (+5 ethanol)	65 (+5 ethanol)

Table 5: Proposed Diesel specifications (Source: SAPIA, 2016)

Diesel	**Units**	**Current National specification**	**Clean Fuels 2 (CF2)**	**Clean Fuels 3 (CF3)**
Vehicle emissions standards SANS specifications roughly equivalent to EU		"Euro 2"	"Euro 4"	"Euro 5"
Sulphur max	ppm (m/m)	500/50	50/10	10
Polycyclic Aromatic Hydrocarbons (PAH), max		na	11	11
T90, max T95, max	^{o}C	362 na	na 360	Na 360

Initially planned to be upgraded in July 2017, refineries in South Africa are expected to produce Euro 5 compliant fuels. However, this deadline has been suspended because of the negotiation between government and the petroleum industry.

The new regulation stipulates that sulphur content in gasoline and diesel must remain below 10 ppm. The immediate option to meet growing regulatory demand for low carbon fuels in South Africa could be import or progress and scientific research. It is on the basis of this concrete reality that this study wishes to contribute to the environmental wellbeing of South Africa by positing a viable formula for the reduction of oil pollutants.

Previous research on the environmental challenges of petroleum refineries has conducted recently, including the reduction of sulphur content in fuels. Useful tools, such as software, were then developed to manage desulfurization of fuels (especially gas oil). Shakri *et al.* (2007) are among the researchers who have developed a process model and sulphur reduction reactor called hydrodesulphurization. Based on the Fotrand codes the model was able to simulate using the HYSYS environment and implement it via the HYSYS customization function. A deep hydrodesulphurization took place in the trickle bed reactor during simulation of dimensional

model of heterogeneous reactor. The study consisted of two sections: based on Hougen Watson rate, the first was a simulation of hydrodesulphurization of a trickle bed reactor and a simulation of the hydrodesulphurization process, based on the design and implementation of the hydrodesulphurization model. As results of simulation, a ratio of H_2/Oil equal to 55.7 gave a better performance and the increase in temperature highly affected the sulphur concentration.

De la Paz-Zavala *et al.* (2013) have developed a kinetic model of hydrodesulphurization of diesel. The objective was to reach a low sulphur diesel and apply it to commercial units. Commercial catalysts, straight run gasoil, light cycle oil, light cracked gasoil and feedstock proprieties were experimental data used for modelling. Simulation analysis, based on temperature, space velocity and pressure, of the model obtained in order to compare predictions and industrial applications.

Another study that dealing with sulphur problems in transport fuels (road and air) was published in 2003 by Song. This study provided an insight into new contributions to deep desulfurization of refinery streams without lower octane number or gasoline loss. Two streams were targeted: gasoline for a reduction of 330 to 30 ppm and gasoline for a reduction of 500 to less than 15 ppm. In conclusion, Song stated that new and more effective approaches, catalyst studies and processing researches are needed for the production of ultra-clean and affordable fuels, in line with government regulations.

CHAPTER 3

METHODOLOGY FOR DESIGN AND SIMULATION OF PROCESS UNITS

3.0. Introduction

This section covers the methodology used to model and simulate a modular refinery for the production of fuels with low environmental pollution. First, a description of the five main steps to model the unit process will be presented. The processes involving refinery design, modelling and simulation will be addressed and the required formulas proposed to compliment the methodology.

3.1. Methodology

The modelling of the refining process will be carried out in two major stages: design of main refining unit and simulation by Aspen; spit in five steps. This stage involves the performance of each unit process based on such process variables such as feed flow rate, temperature, products and feed composition. The following steps will be conducted in order to propose the model for the unit process:

Step1: Assessment of each unit process variables as shown in the Figure below:

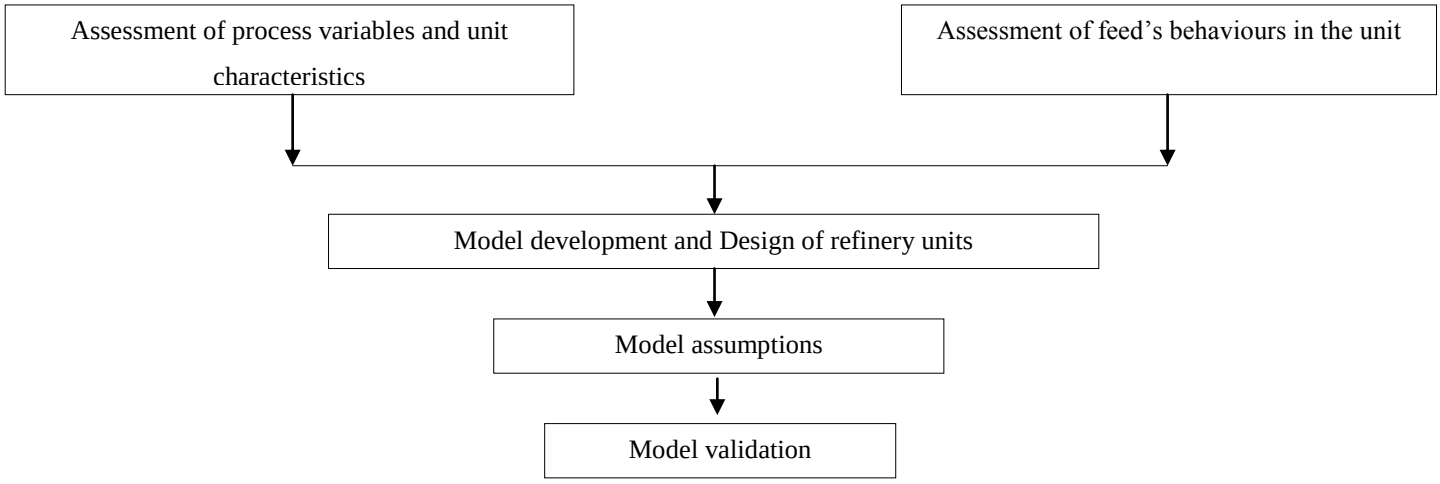

Figure 7: Steps to be followed for the development of refinery's process

Step 2: Theoretical assumptions and Characteristic equations of each unit

Step 3: Process modelling

Step 4: Process simulation using Aspen

Step 5: Case studies and model validations

3.2. Modular refinery design basis and Process description

a) Crude oil Distillation Unit

To design the modular refinery, this project assumed that the feed of crude oil was preheated, desalted, heated in the furnace and then fed to the distillation unit. Fractionation takes place in the atmospheric column (ADU) purposed to obtain: Off gas (LPG), naphtha, kerosene, atmospheric gasoil, diesel and the atmospheric residue. The last component made of long carbon chained molecules with high boiling points will be further fractionated in the vacuum distillation column (VDU) into light, heavy gasoil and vacuum residue.

- ***Process design***

Desalting design

In order to remove water and soluble salts from oil stream, desalting plants are often installed in crude oil production units (Vafajoo, Ganjian and Fattahi, 2012).

Gravitational separation is the commonly used method to separate oil and water; this is also applied to the electrostatic desalter which relies mainly on gravity separation governed by Stokes law (Dreher, 2016). An expression describing the settling velocity of spherical sediments in a fluid medium:

$$v = \frac{2r^2 \Delta\rho\, g}{9\mu_0} \qquad (3.1)$$

where v: settling rate, kg/s/m2

r: drop radius, m

$\Delta\rho$: density difference between aqueous and organic phases, kg/m3

g: gravity, m/s^2

μ_0: viscosity of oil, kg/m.s

Table 6 shows how varying operating parameters of separation process (desalting process) in different CDU function.

Table 6: Range or optimum of operating parameters in different researches

Research	**Operating range**				
	Temperature (°C)	**Retention time (min)**	**Wash water (%)**	**pH**	**Efficiency (%)**
Dreher, 2016	100-250	10-30	5-10	2.5-13.2	95-99
Fetter-Pruneda, Borrell-Escobedo and Garfias Vázquez, 2005	135	30	-	-	95-99
Cournoyer, Couture, Couture, Ferland, Fontaine, Gervais, Giroux, Laplante, Lapointe-Garant, Morin and Vallières, 2005	135	30	5-10	-	85-95
Vafajoo, 2012	98-133	10-30	2.5-5	2.5-12	97.3-97.9

This study focussed on optimization of efficiency as a key parameter in design and reduction of salt and water concentration in crude oil.

Furnace design

Steam or hot air coupled with a hot coil is mainly used to heat all types of hydrocarbons. The equipment used to heat oil at industrial level or to serve as thermal reactor is a furnace or direct combustion (Fuente, 2015). The design of the furnace depends on its function: the heating, the type of fuel and the method of injecting combustion air. The basic design of the furnace is determined by the area of heat transfer pertaining to the radiant (A_{rad}) and convection (A_{conv}).

The sum of these two areas results in the total area of a furnace (Fuente, 2015). In order to determine the radiant and convection area, the following equations was used (Fuente, 2015):

$$A_{rad} = \frac{0.5\ Q}{q_r} \qquad (3.2)$$

$$A_{con} = \frac{0.5\ Q}{q_c} \qquad (3.3)$$

where q_r: The heat flux in the radiant section is, quantified as 37.6 kW/m2

q_c : The heat flux which occurs in the convection section, quantified as 12.5 kW/m2

Q : The heat required by the inlet cold stream to reach the desired temperature or absorbed duty from heat balance or heat duty desired temperature

In this study the design of the use of furnace was adopted from Fuente, (2015) as indicated in the literature above.

Heat exchanger design

The design of heat exchanger is used in the pre-heating unit, as device used to transfer heat between a solid object and a fluid, or between two or more fluids.

According to Kemp (2007), the Equation 3.4 which represents a simple equation that calculates the ΔT for heat exchanger matches, is quite useful for gases and viscous liquids with poor overall heat transfer coefficients (U), or fouling heat exchanger surfaces. It is the general formula that describes the heat transfer (Q) which occurs through heat exchangers and gives a better value for the ΔT for such fluids (Kemp, 2007; Sinnot, 2005, Fuente, 2015).

$$Q = UA\Delta T_M \qquad (3.4)$$

where Q : Heat transfer rate [W] : From the energy balance

U : Overall transfer coefficient [W/ (m2.K)]: Estimation of heat transfer coefficient which depends on configuration and media used in the Shell and Tube side: L-L, Condensing vapour-L, Gas-L, Vaporizers. Selected from Backhurst, Coulson, Harker, and Richardson (1999).

A : Heat transfer surface area [m2]

ΔT_M: mean temperature difference [K]

$$\Delta T_M = F_T \Delta T_{LM} \qquad (3.5)$$

where F_T: Factor used to correct the departure from true counter current flow

ΔT_{LM} : Log mean temperature difference ΔT_M, K

$$\Delta T_{LM} = \frac{(T_1 - t_2) - (T_2 - t_1)}{\ln(\frac{T_1 - t_2}{T_2 - t_1})} \qquad (3.6)$$

where T_1: Hot stream inlet temperature [K]

T_2: Hot stream outlet temperature [K]

t_1: Cold stream inlet temperature [K]

t_2: Cold stream outlet temperature [K]

It is important to note that ΔT_{LM} is the logarithmic average of the temperature difference between the hot and cold streams at each end of the exchanger and has a direct correlation on the amount of heat transferred for a counter current flow heat exchanger.
The parameter calculated and used in this study is the area, which was the main parameter for simulation.

Distillation column design

Feeding location, number of trays or column diameter, trays design or packing type, distance between trays or packings height, total column height, operating conditions, and mechanical design are some of the parameters required for complete design and optimization of distillation. Among these parameters, the determination of the theoretical stages and the feed location are one of the first steps in distillation design (Green and Perry, 2007; Caballero, 2014).

The crude oil column design requires some input data such as crude oil true boiling point (TBP), density or API gravity, molecular weight and viscosity, as well as required specifications such as column pressure. Product specification can be determined in terms of fix or distillation point, pumping around entitlements and column top temperature (Pant and Kunzru, 2015).

The process design of distillation column includes the following steps: specify the separation and determination of the material and energy balance optimization; set a column pressure; determine the minimum reflux and the minimum number of stages; find the optimal feeding stage; Select three ratios of actual reflux preceding minimum reflux (Kister, 1992). Calculations during process design can be abridged or rigorous, it is therefore important to re-exanimate some steps

and to graphically analyze the design. This procedure ensures optimal design and the absence of pinched regions (Kister, 1992).

Most distillation processes in industry are used to separate more than two components. As in the case of distillation of two components, the same type of distillation columns, reboilers, condensers, heat exchangers and so on, is used on multicomponent separations. The cuts obtained after distillation are called key components among which the light key (LK), heavy key (HK) and other components called non-keys (NK) exist. The process also produces light non-key (LNK), more volatile non-key, and the heavy non-key (HNK), less volatile heavy key (Manjumdor and Das, 2012). The design process consists of calculation steps in the distillation of multicomponent systems, which is performed using several short-cut methods. These generally involve an estimation of the following parameters: minimum number of trays, minimum reflux rate and the number of stages (Manjumdor and Das, 2012; Ibrahim, 2014). A widely used approximate method is commonly referred to as the Fenske-Underwood-Gilliland method or FUG (Manjumdor and Das, 2012).

This study relates to a distillation that contains inter alia atmospheric distillation as a vacuum distillation unit in two different columns. So, the design of the columns is therefore focused on the calculations of the following parameters (Douglas, 1998; McCabe and Warren, 1993).

- Determination of process operations variables :

Some parameters such as feed rate, composition, purity of the distillate and the bottom, and quality of the feed are assumed to be known. Determination of the distillate and bottoms is done by oerforming overall material and component balances.

$$F\ Z_F = X_D D + X_B B \quad (3.7)$$

$$F = D + B \quad (3.8)$$

where, F: Feed rate of input stream

Z_F: Composition of light component in feed

X_D: Mole fraction of light component in distillate

X_B: Mole fraction of light component in bottom

D: Total distillate amount

B: Total bottom amount

As crude oil contains more than two components, X_D and X_B are light-key and heavy-key component.

- Determination of minimum reflux ratio

The determination of minimum reflux ratio is done either analytically, using Underwood Equations, or graphically, using the McCabe-Thiele method.

The use of the McCabe-Thiele method implies the following assumptions: constant molar overflow; heat effects are negligible; for every mole of vapour condensed, another mole of liquid is vaporized; and the liquid and vapour leaving the tray is in equilibrium with the vapour and liquid entering the tray (Douglas, 1988). A diagram Y-X (Y representing the vapour phase and X the liquid) is plotted if no equilibrium curve is given, which can be can be obtained by relating the relative volatility (α) to the composition of the liquid (McCabe and Warren, 1993):

$$Y = \frac{\alpha X}{1+(\alpha-1)X} \quad (3.9)$$

This shows the bubble-point and dew point of a binary mixture at constant pressure. An equilibrium line describes the compositions of the liquid and vapour in equilibrium at a fixed pressure.

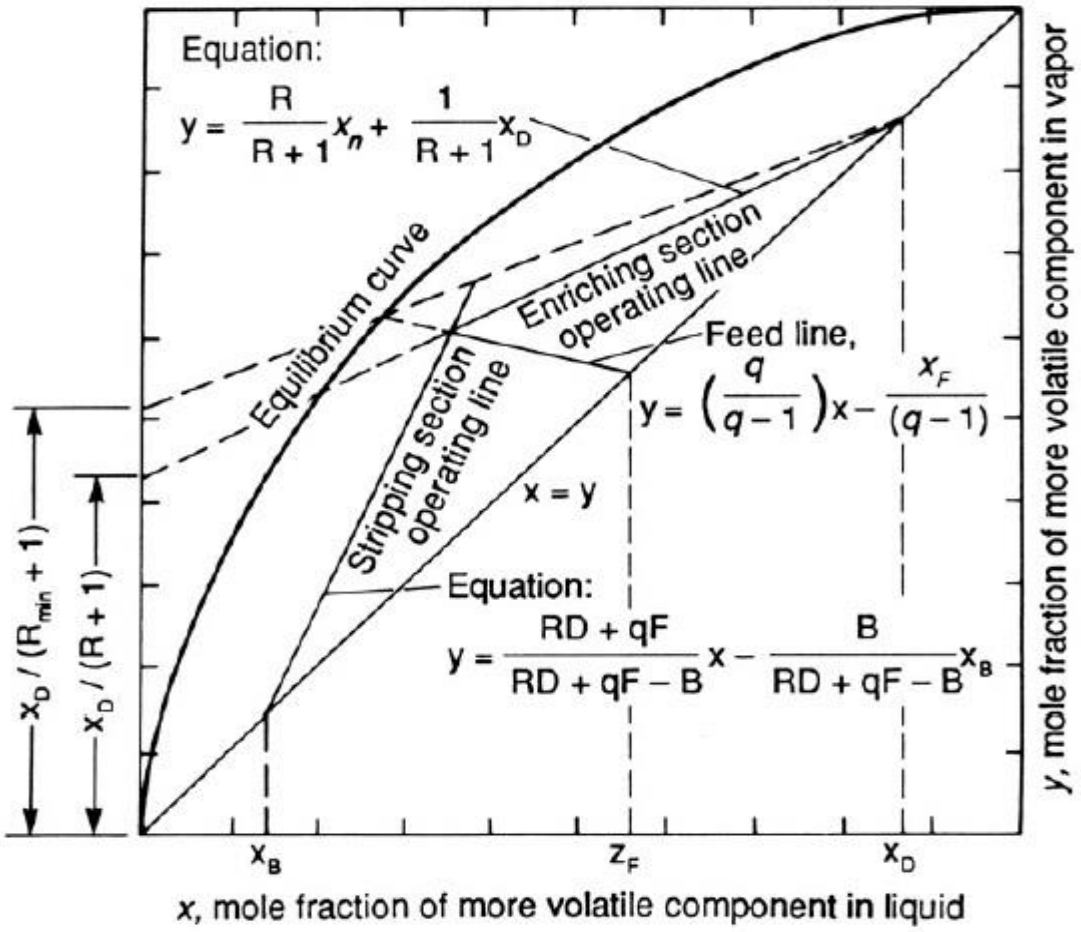

Figure 8: Operating line and construction and minimum reflux construction (Douglas, 1988)

The drawing of figure 8 above is described as follows (Douglas, 1988):

- The equilibrium line at the bisector of x and y indicates an azeotropic mixture.
- Draw the bisector which is the diagonal line of the points (0.0,0.0) to (1.0,1.0).
- Construction of Feed Line (q-Line) by locating the point on the bisector that corresponds to the feed composition. This point can be extended with a slope of $q/(q-1)$ where q is the feed quality. The feed line can be directly plotted through the following equation:

$$Y = \frac{q}{q-1}X - \frac{Z_F}{q-1} \quad (3.10)$$

- Draw the operating line for the enrichment section called upper operating line. First find the desired top product composition (on the x-axis) and locate the corresponding point on bisector. Connect this point to the point where the equilibrium curve and the feed line intersect. The Y intercept of this line is equal to$X_D/(R+1)$. Minimum reflux can be determined using the following equation:

$$R_{min} = \frac{X_D}{Y_{intercept}} - 1 \qquad (3.11)$$

- Draw the operating line for the stripping section called lower operating line. First find the desired bottom product composition (on the x-axis) and locate the corresponding point on bisector. Draw a line from this point at the intersection of the equilibrium curve and the feed line. The slope of this line is equal to $Vb_{min}/(R+1)$; where Vb_{min} is the boiling point, corresponding to the minimum reflux of the fractional amount of liquid returned to the column of liquid leaving.

- Determination of the actual reflux ratio

The distillation columns are mostly designed to operate between 1.2 and 1.5 times the minimum reflux ratio because this range corresponds approximately to the zone of minimum operating cost. Based on the first estimates, the operating reflux is therefore equated as following (Douglas, 1998):

$$R_{actual} = 1.2\, R_{min} \quad (3.12)$$

$$R = L/D \qquad (3.13)$$

Analytically, the minimum reflux ratio is approximated by the Underwood equation as stated above (Douglas, 1988). With respect to mass balances and VLE equations, the following equation can be used for multi-component systems with constant relative volatility and ∅ can be calculated derived from the equation.

$$\boldsymbol{F(1-q) = \sum((\alpha_i\ z_i)/\ (\alpha_i\ - \emptyset))} \quad (3.14)$$

where $\boldsymbol{F}$: Feed

$\boldsymbol{q}$: Feed quality

$\boldsymbol{\alpha_i}$: Relative Volatility

$\boldsymbol{z_i}$: Composition of component (i) in Feed

Considering the equation (3.14), ∅ can be obtained in a polynomial expression. This expression can be used to solve for ∅. Only ∅ between the relative volatilities of the components should be considered. The ∅ can be used to get the minimum amount of vapour (V_{min}):

$$\boldsymbol{V_{min}} = \sum((\boldsymbol{\alpha_i}\ \boldsymbol{Dx_i})/\ (\boldsymbol{\alpha_i}\ - \emptyset))\ (3.15)$$

From a mass balance and the definition of reflux:

$$\boldsymbol{L_{min}}\ =\ \boldsymbol{V_{min}} - \boldsymbol{D} \quad (3.16)$$

$$\boldsymbol{R_{min}}\ =\ \boldsymbol{V_{min}}\ /\ \boldsymbol{D} \quad (3.17)$$

- Determination of the minimum number of trays and theoretical number of trays

The upper and lower operating line and the actual reflux ratio can be used to determine the number of trays. From the plotting point to $X_D/(R+1)$ and from the line plot X_D, the equation of the upper line is:

$$Y = \frac{R}{R+1}X + \frac{X_D}{R+1}\ (3.18)$$

By connecting the point to $X_B$to the intersection of the feed line and the upper line, the equation of the lower operating line can be drawn:

$$Y = \frac{V_B+1}{V_B}X + \frac{X_B}{V_B}\ \ (3.19)$$

From composition of the distillate (projection of X_D on the forty Five Degree line), the horizontal is drawn to the equilibrium curve. This line represents the first tray. From intersection of the previous horizontal line and the equilibrium curve, drop vertically until the upper operating line is obtained. As for the first horizontal a second horizontal is drawn to determine the next tray. Continue doing same operation until the liquid compositions ends the desired bottom composition. The theoretical number of trays is equal to the total numbers of steps.

Analytically, a simplified approximate equation can be used to determine the number of trays. Fenske is an expression of the minimum number of trays, assuming total reflux and constant relative volatility. This equation takes into account the reflux ratio (Douglas, 1988).

$$N = \frac{\ln SF}{\ln\left(\frac{\alpha}{\sqrt{(1+1/R*Z_F)}}\right)}\ \ (3.20)$$

where:

$$SF = \beta * \frac{\delta}{((1-\delta)*(1-\beta))} \quad (3.21)$$

β: Fractional recovery of light in the distillate

δ: Fractional recovery of light in the bottom

α: Relative volatility

R: Reflux ratio

Z_F: Mole ratio of light component in feed

- Determination of the actual number of trays

The actual number of trays is determined by taking the quotient of the number of theoretical trays to the tray efficiency in the range of 0.5 to 0.7. These values depend on the type of trays used and the internal flow rate of liquid and vapour (Douglas, 1998):

$$N_{actual} = N_{theory}/\varepsilon \quad (3.22)$$

- Determination of principal dimensions of the column (Diameter/Height):

According to the design guideline, the height of the column should not exceed 60m (Price, 2003). The ratio of height to diameter ratio should be less than 20 to 30 (Douglas, 1988).

The tower height may be related to the number of trays in the column. The formula below indicates that a gap of 0.61 m between trays will be sufficient, which includes an additional 1.52 to 3.05 m at both ends of the tower; this will includes a 15% excess allowance of space (Douglas, 1988):

$$H_{tower} = 2.3\ N_{actual} \quad (3.23)$$

The diameter of a tower is relatively insensitive to changes in operating temperature or pressure. Determination of the column diameter needs to consider the vapour velocity (V) which is the main determinant of the diameter and can be derived from the flooding velocity. A velocity 50-

80% of flooding is chosen to limit column from as stated by Douglas. The desired vapour velocity is dependent on the limitations of undesired column flooding. This equation allows for a twelve % surplus in area (Douglas, 1998):

$$D_T = 0.0164\sqrt{V}\left(\frac{M_G}{\rho_m}\right)^{0.25} \quad (3.24)$$

where

$$V = \frac{1.2}{\sqrt{\rho_G}} \quad (3.25)$$

D_T: Diameter of the tower

V: Vapour velocity

M_G: Molecular weight of gas

ρ_m: Molar density

ρ_G: Density of the mixture

b) Fluid Catalytic Cracking Unit

- ***Process description***

The FCCU includes preheating the feed, feed nozzles, riser, catalyst separation, striping section and regenerator valves. From CDU and VDU, the feed of FCCU passes through a vertical riser reactor where cracking reactions are carried out. The oil fed into this unit moves up in the riser, vaporizes and cracks at the same time to lighter products, carrying the catalyst powder along with it. The catalyst used is a zeolite which flows like a liquid because the pressure force is transmitted through the catalyst particles (Sadeghbeigi, 2000). The products in this unit are light gases, gasoline products and coke. The coke deposited on the catalyst and both are separated in the regenerator.

- ***Process design***

There are different reactors used for catalytic cracking such as three-phase fluidized bed reactor (using an upward flow of liquid as opposed to the gas), the continuous stirred tank reactor (for homogeneous reactions), the fixed/packed bed reactor and the fluidized bed reactor. The

fluidized bed reactor is the suitable for conversion of gas oils into gasoline. It allows regeneration of the short lifespan catalyst and offers better loss of catalyst.

In this study, the choice of the fluidized bed reactor takes into account the fact that the most appropriate option is the conversion of gasoil into gasoline. This is the essential part serving as the reactor in the FCC is the riser. The configuration of this reactor is vital to maintain the FCC pressure balance (Sadeghbeigi, 2000).

The riser temperature, catalyst flow rate, feed catalyst temperature and catalyst to oil ratio (COR) are parameters to be optimized in this section so the design focuses only on the catalyst.

- ***Catalyst design***

The catalyst design consists of calculating the weight and deactivation, as well as catalysts parameter and specifications as follows:

- Mass of the catalyst at any given time is given as follows:

$$m_{cat} = \rho_{Cat} V_{cat} \quad (3.26)$$

where:

$$V_{Cat} = t_c Q_{cat} \quad (3.27)$$

ρ_{Cat}: Density of the catalyst

V_{Cat}: Volume (flowrate) of the catalyst

t_C: Residence time

Q_{cat}: Flow rate of catalyst

Knowing that the amount of catalyst circulating between the regenerator and the reactor is about 5 kg of feedstock (i.e 4.66 kg per litre of feed stream) (Gary and Handwerk, 2007); and having determined the feed flow rate, the bulk catalyst mass per day can be determined. Also, the residence time is taken equal to 2 seconds according to Lee (2016).

- The Table 7 below presents a summary of the catalyst data and specifications that are used in this study:

Table 7: Summarized catalyst data (Bollas, Lappas, Iatridis and Vasalos, 2007)

Parameter	**Value**	**Parameter**	**Value**
Bulk density (kg/m3)	840	Re2O3 (wt%)	0.65
Mean particle diameter (μm)	80	Fe (wt%)	0.59
3 (Å)	24.26	Ni (ppm)	163
Al2O3 (wt%)	39.1	Sb (ppm)	<50

c) Catalytic Reforming Unit

- ***Process description***

The CRU consists of a feed of naphtha mixture removed with sulphur, nitrogen and heavy metals. In fact the feed goes into different reactors and is heated before passing through each reactor to maintain the energy required for endothermic reactions.

The design of this unit involves furnace design as in the case of CDU, catalyst design and reactors design.

- ***Process design***

In order to calculate the catalyst volume in each reactor ($V_{catalyst}$), the Weight Hourly Space Velocity (WHSV) of each reactor, respective catalyst density ($\rho_{catalyst}$) and the reactor feed flow rate from the mass balance can be applied to Equation 3.28 and 3.29 (Fuente, 2015):

$$WHSV\ (h^{-1}) = \frac{Reactor\ feed\ flow\ rate\ (kg/h)}{\rho_{catalyst}(kg/m^3)V_{catalyst}(m^3)} \quad (3.28)$$

$$V_{reactor}\ (m^3) = \frac{V_{catalyst}(m^3)}{1-\varepsilon} \quad (3.29)$$

Where ε is an industrial bed void fraction of 0.5 as stated by Korsten and Hoffman (1996).

d) Hydrotreatment Unit

- ***Process description***

The feed of this unit is mixed with hydrogen gas before being fed into a furnace to increase the temperature the range of 316 to 427^{o}C. The mixture enters a fixed bed reactor where sulphur and nitrogen are converted to hydrogen sulphide and ammonia. The hydrotreater operates at pressures between 70,307 to 210,921 kg/m^2 (Albahri, 2001).

- ***Process design***

The design of the process will consist of a calculation of the catalyst volume and WHSV as done in equation 3.28 and 3.29.

3.3. Modelling

3.3.1. Distillation

Due to the complexities of crude oil feed and petroleum products, it is essential to develop an appropriate algorithm for the simulation of multi-component mixture separation (Douani, Ouadjenia and Terkhi, 2007a; Sridhar and Lucia, 1990). The development and improvement of distillation modelling have been carried out in many researches and, at the same instance, tools such as Aspen Plus (Aspentech), PRO/II (SimSci-Esscor) and the IITM design (ChemShare), have been developed and used for common modelling (Li *et al.*, 2005).

Approximate, equilibrium and rate based methods are the three classes of simulation methods for distillation columns which have been developed according to different assumptions made during the development of models (Jelinet and Hlavecek, 1975; Gañí, R., Ruiz, C.A. and Cameron, 1986). Amongst these methods the equilibrium method, which is the most commonly used method, develops and solves the MESH equations (Material balance equation, Equilibrium phase equations, Summation equations and Heat balance equations) (Ramesh, *et al*., 2007). The model equations that describe multi-component separation processes are non-linear and interdependent, irrespective of the method used, and solutions are complex iterative and difficult to converge (Abdullah *et al*., 2007; Boston and Sullivan, 1974; Jaroslav, Hlavacek, and Kubicek 1973;

Ivakpour and Kasiri, 2008). The performed matrix method was used by Rosendo (2003) and Douani, *et al*. (2007) as solution of the MESH equations.

In this work, the degree of freedom analysis of distillation column will be mathematically modelled. Steady state simulation of distillation unit is considered as well as the MESH equations of input and output. The atmospheric distillation and the vacuum distillation are assumed to occur in the column.

a) Data and consideration

Inspired by Akpa and Umuze (2013), and Kumar *et al.* (2001), considering the system showed in the Figure 3, MESH equations for productions of Gas (i=1), Naphtha (N; i=2), Kerosene (K; i=3), diesel (i=4), light gasoil (LG; i=5), heavy gasoil (HG; i=6) and residue (i=7) are:

- Material balance (M equation):

$$F = \sum_{j=1}^{7} Stream_j \qquad (3.30)$$

$$\sum_{i=1}^{7} F\ Z_i = \sum_{\substack{i=1 \\ j=1}}^{7} X_i\ Stream_j \qquad (3.31)$$

- Equilibrium relationships (E equation):

$$Y_{i,j} = K_{i,j} X_{i,j} \qquad (3.32)$$

Where: $1 \leq j \leq N_t$ and $1 \leq i \leq 7$

N_t: Number of tray

7: Number of main constituents (cuts)

- Summation of mole fraction (S equation):

$$L_{i\ feed} = \sum_{i=1}^{7} L_i \qquad (3.33)$$

Where: L_i: liquid flow from the process

$L_{i\ feed}$: Liquid flow into the process

- Heat balance (H equation):

$$F * h_f + q = \sum_{i=1}^{7} S_i h_i \qquad (3.34)$$

Where: S_i: side stream

q: heat flow into

h_f: specific enthalpy of the feed

h_i: specific enthalpy of the feed

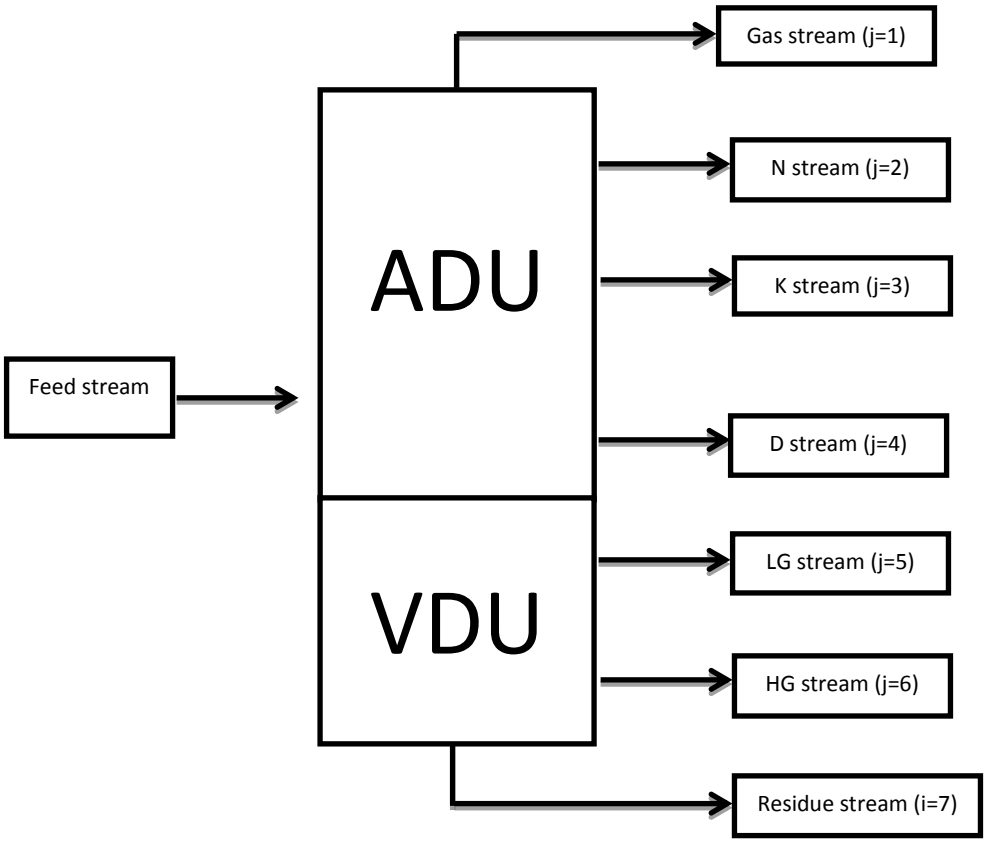

Figure 9: Scheme of Crude Oil Distillation Unit model

Following specifications will be needed for modelling of distillation unit:

- Number of actual plates
- Number of component
- Plate efficiency
- Number of effectives plates
- Actual feed: Result of design
- Type of boiler
- Type of condenser
- Feed temperature
- Feed flow rate
- Feed Enthalpy
- Feed composition

b) Assumptions

Here are assumptions that will be taken into account for modelling of distillation:

- The column is perfectly insulated, there is no heat lost
- Vapour of each tray is neglected
- Process will be considering as a binary distillation where components are: Light Key (LK which is gas) and Heavy Key (HK which is residue)
- The feed is a saturated liquid
- All the tray are ideal (100% of efficiency)
- The molar vaporisation of LK and HK are approximately equal
- Number of trays will be calculated during design of column and will exclude reboiler and condenser.
- Feed stage will be obtain by design calculation
- Perfect mixing of each stage
- Relative volatility of component remains constant throughout the column
- Condenser and reboiler dynamics are neglected

On the basis of the first three first assumptions, we can easily conclude that the vapour coming out of the first stage is equal to the one coming out of the second, equal to that coming out of the third, etc. This can be written as follow:

$$V_1 = V_2 = V_3 = \cdots = V_{residue} \qquad (3.35)$$

c) Procedure

The modelling of distillation will be taking into account 4 sections of the distillation column, as illustrated in figure 10:

- Reflux drum
- Top stage (N^{th} stage of distillation)
- n^{th} stage of distillation
- Feed section
- First stage
- Bottom stage

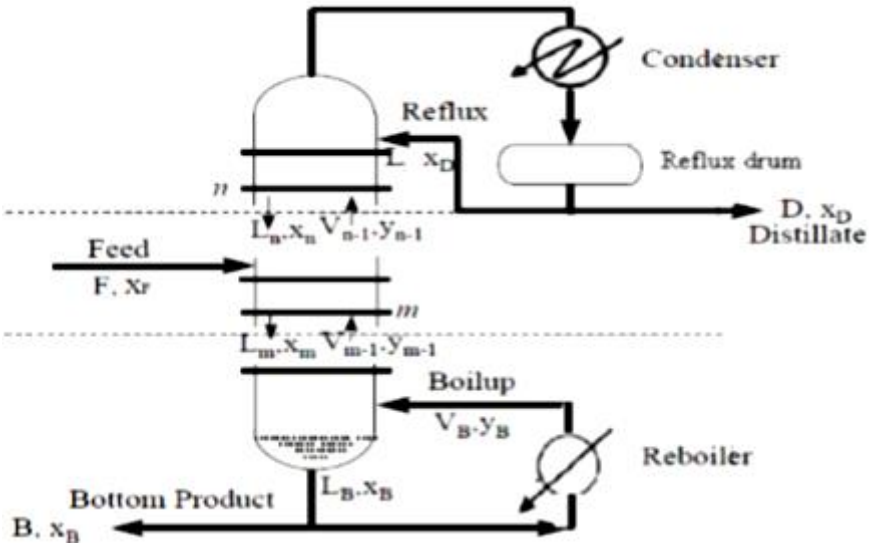

Figure 10: Material balance distillation column (Jinsa and Ajeesh, 2014)

The sections below, total mass balance of fluid retention and component mass balance of liquid phase modelling equations will be developed. Compositions of vapour (y) and liquid modelling equations will be next. All the equations obtain will be necessary to determine degree of freedom (f) given by relation 3.36:

$$f = Number\ of independants\ variables - Number\ of\ independants\ equations \quad (3.36)$$

3.3.2. Fluid Catalytic Cracking

The FCC unit plays an important economic role in today's petroleum refining. This has generated high interest in academia and industry in terms of modelling of FCC unit (Bhende and Patil, 2014). Feeding and catalytic effects, fluid dynamics and reaction kinetic are important parameters for modelling and simulation of the FCC unit (Heydari *et al*., 2010).

This work is inspired by Lumped models and, as model it will consider reactants and products as a set of hydrocarbons. It will be a block composed of 4-lump that are gasoline (G), vacuum gas oil (VGO), light gases (L) and coke (C).

a) Data

Following specifications will be needed for modelling of FCC unit:

- Feed
- Catalyst
- Catalyst to oil ratio
- Weight fraction of each components involve
- Ratio of molecular weight

b) Assumptions

Here are assumptions that will be taken into account for modelling of FCCU:

- Isothermal condition
- Constant hold-up
- Constant pressure
- Constant density
- Feed viscosity and heat capacities of all components are constant
- Perfect mixed
- Unreacted gases are off the top of reactor
- Vapour-phase dynamics very fast
- FCC riser is a conversion reactor and FCC reactor is a continuous stirred-tank reactor
- The coke deposit on the catalyst does not affect the fluid flow
- All cracking reactions are considered taking place in the riser

c) Procedure

Drawing of schematic diagram representing reactions scheme, that makes the equations from the constituted network.

3.3.3. Catalytic Reforming Unit

The modelling is frequently based on the type of kinetic model used and the number of reactive species (Askari *et al.*, 2012). This study will take account pseudo components to reduce complications. Naphtene, aromatic and paraffins are pseudo components considered by the Smith model and also used in this work.

Knowing that catalyst deactivation is defined as the ratio of the reaction rate at a time t and the reaction rate at the beginning start of a cycle.

The following assumptions will be taken into account for modelling of FCCU:

- Catalytic reforming proves is considered as an isothermal condition
- Reactions are represented by simple first order

Based on the reactions rate equations, the modelling procedure will consist of considering an initial rate with a certain temperature (T_0) and a rate at a certain temperature (T). Then the development will take place from there.

3.3.4. Hydrotreatment modelling

A couple of physical and chemical processes take place in a catalytic process and influence the overall reaction rate (Rivotti, 2009). The model is then more or less detailed depending on the number of phenomena taken into account in the process.

a) Data

Based on phenomena taking place in hydrotreatment following data were considered:

- Molar concentration
- Reaction rate constant
- Temperature range
- Pressure range
- WHSV ranges

b) Assumptions

The following parameters are the assumptions made for modelling of hydrotreatment:

- Reactions occurs in the kinetic area
- The order of reactions is the first
- Reactions of hydrogenolis are reaction of first order in quasi homogeneous conditions
- Pseudo homogene reactions
- Hydrogen is feed in excess, so its concentration is constant along the reactor
- Isothermal conditions along the reactor.

c) Procedure

Comparison of different models used. Here are models considered:

- Chang and Fang model
- Korsten and Hoffman model
- Murali and voolapali

3.4. Simulation of modular refinery

The computer simulation of this study was carried out using Aspen Hysys simulation software. With unique characteristics among chemical processes, petroleum refining processes are extremely complex and integrated. To manage the simulation of petroleum processes Aspen Hysys can be used. Aspen Hysys is an advanced process simulation environment for processes that provide special features to develop a model of petroleum process; and then use this model to study alternative modes of operation or optimize the existing operation (AspenTech, 2009).

3.4.1. Process simulation procedure

The computer simulation was carried out according to the following procedure:

- Data collection: Refinery process and operation data were collected from literature and Kutubu (crude assay).
- Construction of the modular refinery: Building the model of the refinery designed using the data collected.
- Computer simulation: Carried out using Aspen Hysys

3.4.2. Process simulation

The computer simulation software was used to carry out complete modelling and process simulation of the refinery in order to obtain reasonable design parameters. Reliable process operation data such as thermodynamic packages were provided by Aspen Hysys.

Mainly, process simulation involved the following simulation:

1. Defining feedstock
2. Selecting thermodynamic package
3. Specify modular refinery capacity
4. Assigning proper operation units and settings up input operating conditions

3.5. Environmental study

This section explains how the environmental results obtained were analysed as the study focused on the environmental impact of the fuels produced by a modular refinery.

The environmental study of this research is a combination of exploratory and experimental survey. The exploratory part is the research for studies related to environmental impact of refinery products; and experimental part being mainly based on the simulation of the designed modular refinery. According to Saunders et al. (2009), documentary data include written materials such as notices, correspondence (including emails), meeting minutes, annual sustainability reports, diaries, speech transcripts and administrative and public records. In our case, the document search process has taken following steps:

- Search for relevant keywords in databases (keyword was use to limit the search results);
- Search the databases again with the new references as keywords or relative information;
- Collect the most relevant argument and data from the search results, and make the comments on the information obtained.

The research process took place with the usage of the Internet by downloading documents or reports with environmental impacts as output from the refinery and by categorising the extracted literature (process or product pollution).

The reports and studies or research constituting documentary data are the following:

- Buckle et al (2008): This study showed that a modular refinery could be considered as a new and better technology, based on environmental, social and economic considerations stipulated by the United Nation framework Consideration on climate Change (UNFCC) in 1992.
- Adefarati and Chigbu (2017): This research concluded that the modular refinery would lead to an overall reduction in pollutants emissions. This will have an impact on the production of the conventional refineries by increasing the capacity. Most importantly, it would serve as a climate mitigating tool.
- Muhsin et al (2016): The optimisation of the crude oil hydrotreatment unit in this study was carried out in order to maximise sulphur removal in the product. Usage of Bootstrap aggregated neural network for modelling and optimising the process based on results such as the existence of a trace-off between sulphur removal and the production rate (for instance 40.00 m^3/h, which is the smallest feed makes the highest sulphur removal of 95.82%).
- Sharma (2018): This study used laboratory-scale reactor and industrial data to achieve its goal. Based on the development of the Graphical User Interface (GUI) to compare the sulphur concentration measured in the product and the expected sulphur concentration predicted.
- Shokri et al (2007): the results of this research have shown that the sulphur content decrease as the temperature increases while the pressure and H_2/oil ratio are constant. It has been observed that by increasing $H_2/$oil ratio to 55.7, the sulphur concentration decreases, but it increases again by increasing H_2/oil. 55.7 was then the optimal H_2/oil ratio.
- Al-Malki (2004): based on the use of the oxidation extraction technique for the reduction of sulphur in gasoline and diesel, this study showed that the technique is promising for the reduction of sulphur below of 100 ppm from the value of 1044 ppm with a total removal of 92%.
- Abubakar et al (2016): the study aims to reduce the sulphur content in crude oil from the Urals using oxidative desulphurization. The results obtained have shown that the

reduction in the sulphur content of refinery products increase with the increase in amount of oxidant. In fact, the content of gasoline, kerosene, diesel and residue sulphur were reduced respectively from 0.0805 to 0.0548 wt%, from 0.2086 to 0.1150 wt%, from 0.7754 to 0.2698 wt% and from 1.6426 wt% to 0.4110 wt%.

- Gupta (2006): the study concluded that gasoline yield increases with the increase in COR; however, the rate of increase in the gasoline yield decreases at higher COR values.
- Paul et al (2015): the researchers built a model to predict the conversion of feed oil and formation of gasoline. The results showed that when the COR is 4.5, the gasoline yield is 55.89. When the COR goes to 8.5, the yield is 58.9%.

Richmond (2006) defined qualitative data as data represented in verbal or narrative form, and qualitative data as data expressed in numerical terms in which the numerical values could be large or small. Knowing that the data provided by the Aspen simulation are numerical and can be represented in table or a curve, the results of our research will certainly be quantitative. Qualitative data obtain from literature are also used for assessment.

The scope of the environmental study will be limited to the use of the software to illustrate production of the modular refinery. A simulation with the use of ASPEN HYSYS was performed out in order to generate enough data for the analysis. Data analyses were obtained from the simulation results.

CHAPTER 4

RESULTS AND DISCUSSION

A modular refinery with a processing capacity 12,000 bbl/day (64,409.51 kg/h) of Kutubu crude oil with CDU, FCCU, CRU and HTU in main units was designed and simulated. The design is based on tools described in the literature review and methodology, and the simulation based on Aspen Hysys simulation software procedure. Calculations were numerically simplified by the use of Microsoft Excel.

4.1. General considerations

4.1.1. Material and Energy balance

Based on the crude assay, the balance calculations were performed using Microsoft Excel as digital tool. The results of the sample characterisation of the feed data gave mass flow rate and volume flow rate shown in Table 8.

Table 8: Mass flow rate and volume flow rate balance

Cut	Mass flow rate (Kg/h)	Volume flow rate (l/h)
Gas	1495.26	2623.50
Light Naphtha	9074.32	13753.50
Heavy Naphtha	23248.53	30687.00
Kerosene	11334.79	14071.50
Diesel	8354.98	9778.50
Vacuum Gas oil	6634.514	7393.50
Vacuum residue	1267.12	1272.00
Whole crude	61409.51	79579.50

Details of mass and volume balance are provided in Appendix B.

Table 8 shows that the oil sample contains 23,248.53 kg/h of Heavy Naphtha (HN); which is the main component with 37.85% of the amount of crude oil. This was used in this study as a motivation to focus on gasoline production.

4.1.2. Thermodynamic design considerations

The thermodynamic data are provided by the crude assay (Appendix A). They are vital for CDU design.

Distillate crude oil volume data are essential because they often dictate the number of trays required for the column and the stages at which products are drowned.

To design a distillation column, the data must be expressed in terms of true boiling point (TBP), as shown in Appendix A1, but also in degree Celsius. Beforehand convert in degree Celsius (^{o}C) as represented in Table 9.

Table 9: Conversion from ^{o}F to TBP distillation

Distillation type	Conversion	Temperature (^{o}F)	Temperature (^{o}C)
IBP, F	0	12.1	-11.06
5 vol%, F	5	73.1	22.83
10 vol%, F	10	106.6	41.44
20 vol%, F	20	162.8	72.67
30 vol%, F	30	200.3	93.50
40 vol%, F	40	238.4	114.67
50 vol%, F	50	279.8	137.67
60 vol%, F	60	335.7	168.72
70 vol%, F	70	413.8	212.11
80 vol%, F	80	516.5	269.17
90 vol%, F	90	667.2	352.89
95 vol%, F	95	801.6	427.56
EP, F	100	1 162.5	628.06

Due to the calculations shown in Table 9, the test data can be represented by the Figure 11 as follow:

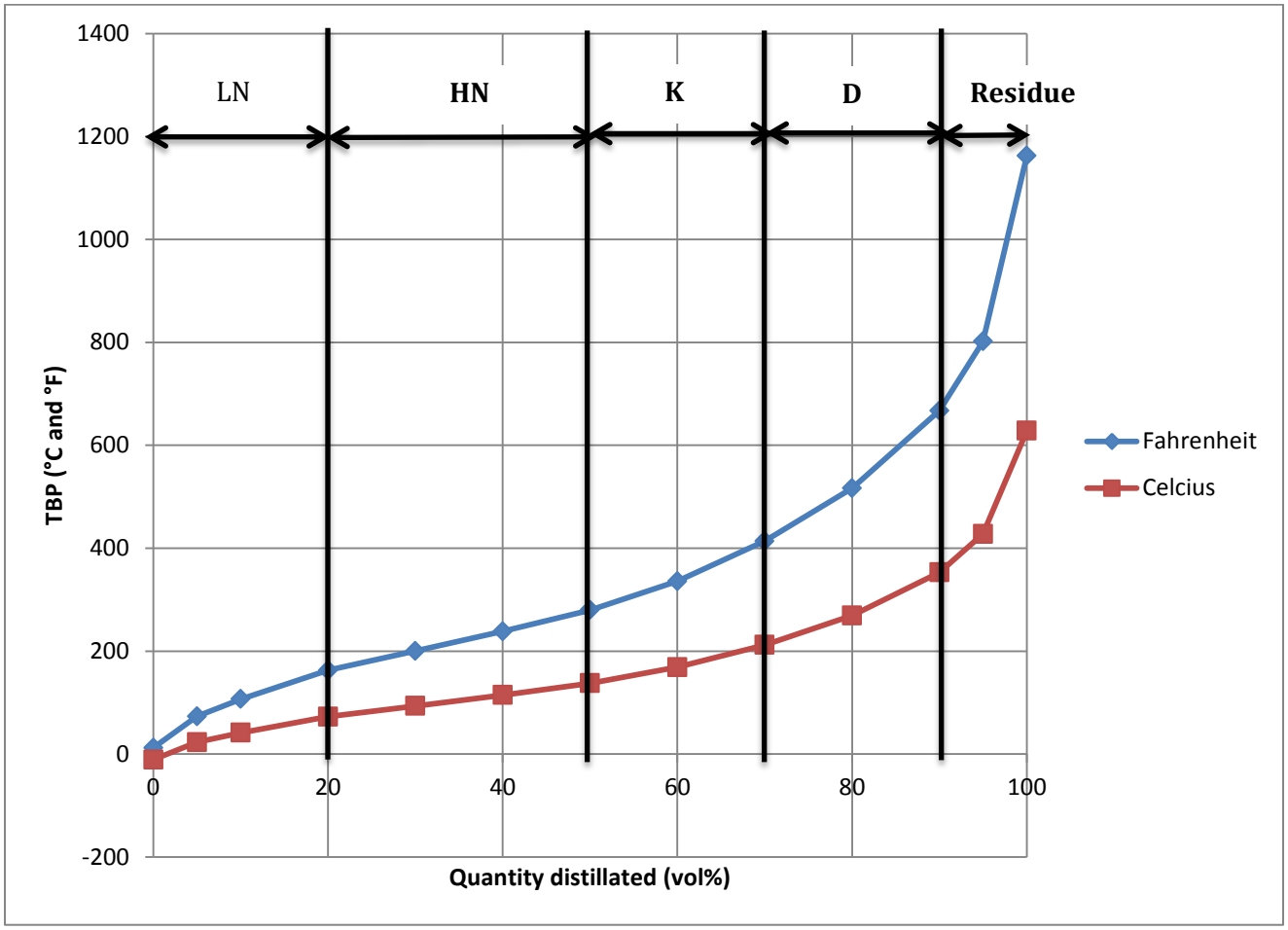

Figure 11: Representation of crude TBP

TBP data of each cut was summarized and represented in Table 10 and in Figure 12.

Table 10: TBP of each cut

Quantity distilled vol (%)	**Temperature (^{o}C)**					
	LN	**HN**	**K**	**D**	**VGO**	**Residue**
IBP	16.15	74.30	165.89	249.26	343.82	538.21
5	20.56	77.92	168.86	252.64	348.31	542.23
10	22.83	81.91	172.26	256.46	353.47	546.89
20	27.33	89.91	179.31	264.35	364.44	556.88
30	37.00	97.97	186.72	272.56	376.46	567.97
40	41.96	106.10	194.43	281.08	389.74	580.42
50	52.11	114.36	202.48	289.95	404.64	594.72
60	57.33	122.83	210.86	299.26	421.65	611.61
70	62.01	131.70	219.63	309.11	441.46	632.32
80	66.27	141.36	228.84	319.63	465.33	659.56
90	70.21	152.45	238.57	330.99	495.62	700.99
95	72.05	158.74	243.65	337.03	514.62	735.34
FBP	73.70	164.84	248.36	342.69	535.20	798.51

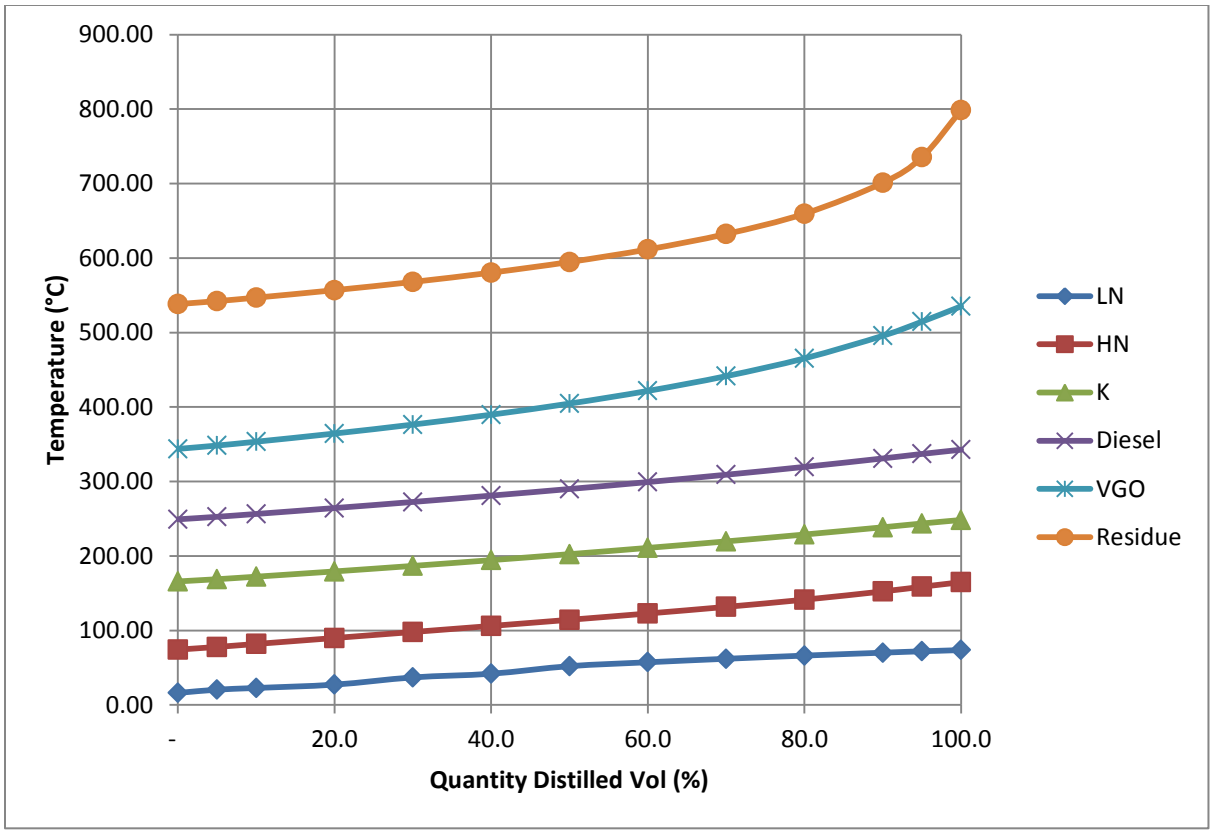

Figure 12: Representation of TBP of each cut

4.1.3. Specific Gravity and characterization factor (K)

From the crude assay data, Table 11 was designed to express the specific gravity (SG) and characterization factor (K_w) of each major product leaving the distillation column. Each SG corresponding to the cutting temperature that was to be determined by the Mean Average Boiling Point (Mid-BP) and K_w:

$$Mid - BP = \frac{Lower\ Boiling\ Point + Upper\ Boiling\ Point}{2} \quad (4.1)$$

$$K_W = \frac{\sqrt[3]{Mid-BP}}{SG} \quad (4.2)$$

Table 11: SG and Mid-BP of crude cuts

Cut	SG	Lower BP (°C)	Upper BP (°C)	Mid-BP (°C)	Mid-BP (°R)	KW
LN	0.661	15.56	37.41	26.485	539.34	12.32
HN	0.759	37.41	165.56	101.49	674.35	11.55
K	0.807	165.56	248.89	207.23	864.68	11.81
D	0.856	248.89	343.33	296.11	1024.67	11.78
VGO	0.899	343.33	537.78	440.56	1284.68	12.09
Residue	0.998	537.78	815	676.39	1709.17	11.96

The figure 13 below, show the specific gravity as function of products temperature.

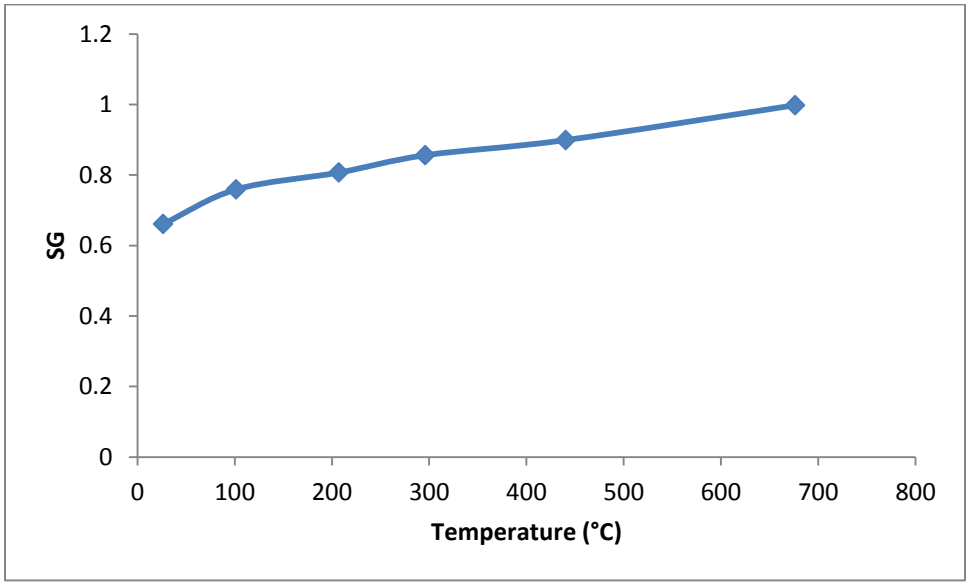

Figure 13: SG as function of temperature

4.1.4. Volume average boiling point and Energy balance (enthalpy)

Based on data represented in Table 11, data converted to ^{o}F and the average volume boiling point of each section are calculated using Equation 4.3 and shown in Table 12 below:

$$T_V = \frac{t_{10}+4\,t_{50}+t_{100}}{6} \quad (4.3)$$

Table 12: TBP (^{o}F) at 0, 50 and 100%, and TV of crude cuts

Distilled vol (%)	Temperature (^{o}F)					
	LN	HN	K	D	VGO	Residue
IBP	61.07	165.74	330.60	480.67	650.88	1000.78
50	125.80	237.85	396.46	553.91	760.35	1102.50
FBP	164.66	328.71	479.05	648.84	995.36	1469.32
TV	121.49	240.97	399.25	557.53	781.27	1146.68

Based on TV and Me-BP data, the Maxwell correlation (graphical correlation tabulated in Appendix B) and interpolation and extrapolation, the enthalpy of each cut is calculated and shown in Table 13:

Table 13: Liquid and vapour enthalpy of cuts

Cut	Liquid enthalpy		Vapour enthalpy	
	Btu/lb	kj/Kg	Btu/lb	kj/Kg
LN	39.72	92.39	134.04	311.78
HN	125.71	292.40	264.45	615.45
K	212.76	494.88	330.09	767.79
D	307.85	716.06	411.08	956.17
VGO	541.58	1259.48	464.47	1080.36
Residue	1170.83	2723.35	987.11	2296.02

4.2. Crude Oil Distillation Unit design

4.2.1. Column parameters

The design of the CDU includes parameters calculations that consider ADU and VDU as a single column. The designed distillation column must therefore work for both processes. The design of the column requires the following elements: (i) the composition of the distillates, the bottom and the feed rate; (ii) the Reflux ratio; (iii) number of trays; (iv) height and diameter of the column.

Base on Douglas method, the determination of the column height requires the actual number of trays and is determined through the McCabe graph according to a previous calculation of reflux ratio and the feed rate

a) Composition of distillate, bottom and feed rate

The composition of distillate, bottom and feed rate can be determined based on the data provided by the crude oil assay Table represented in Appendix A1. Table 14 shows the composition of distillate, bottom and feed rate.

Table 14: Composition of Distillate, Bottom and Feed rate

Elements	Feed	Distillation	Bottom
Paraffins (vol %)	51.8	86.4	2.6
Naphthenes (vol %)	29.6	13.6	10.9
Aromatics (vol %)	18.6	-	86.5

b) McCabe and Thiele graph

The determination of additional data depends on McCabe and Thiele graph. The calculations did in Appendix give us equilibrium curve and operating lines. The equilibrium curve is given by the following modified expression 3.9:

$$y = \frac{2{,}8951\,x}{1+1.8951\,x} \quad (4.4)$$

The lines can be expressed according to the equation of straight line $y = mx + p$ (4.5); where the parameters differ depending on whether it is a the lower operating line (equations 3.18 and 3.19), feed line or upper operating line. Parameters and variables of each line are represented in Table 15:

Table 15: Parameters and variables of lines

Parameter / **Line**	y	m	x	p
Lower Line	y	1.437	x	0.063
Feed Line	0.518	1	x	0
Upper Line	y	0.379	x	0.537
Minimum reflux line	y	0.3368	x	0.573

Data in Table 16 are represented in the Figure 14:

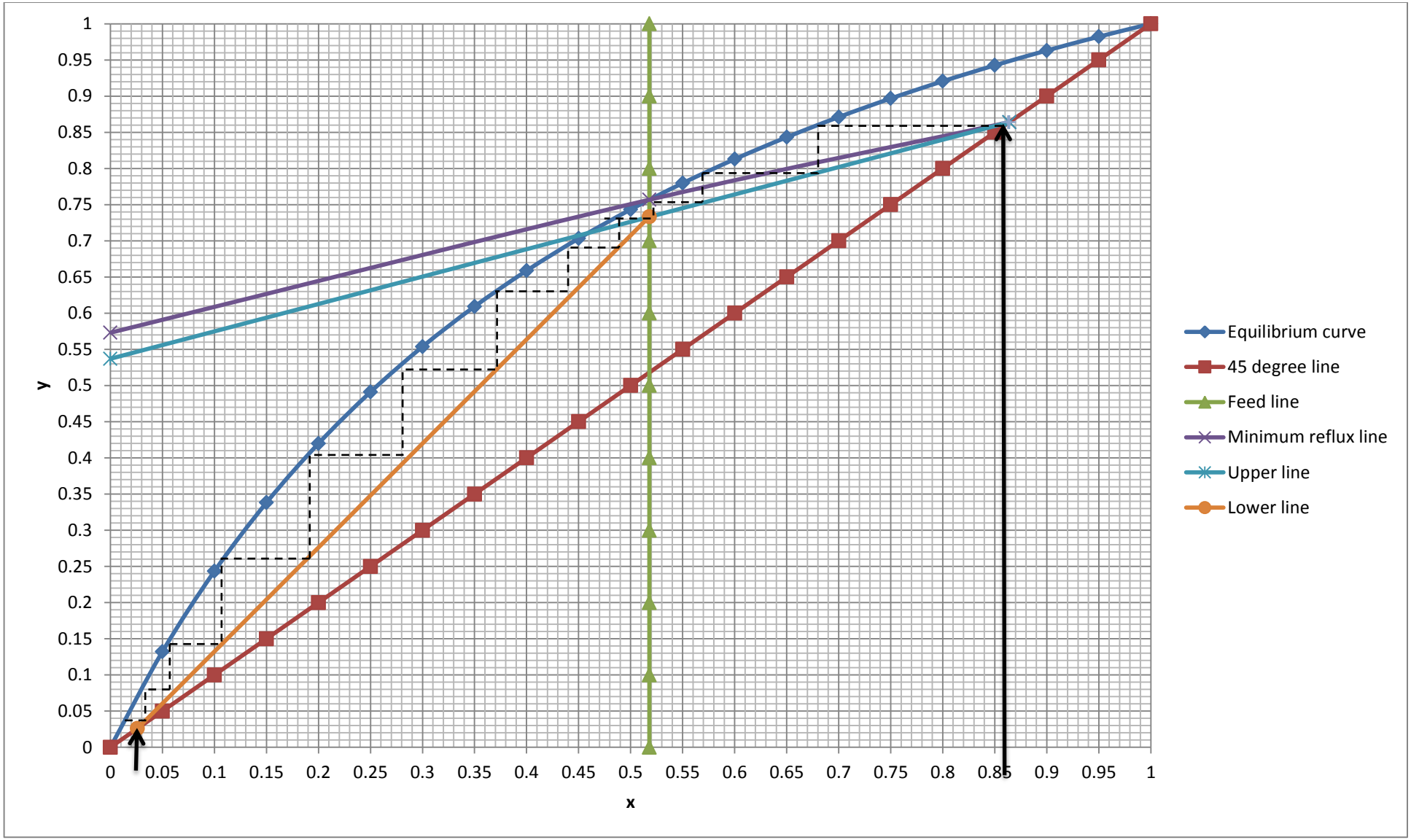

Figure 14: McCabe and Thiele graph

c) Reflux ratio

As result of McCabe and Thiele the y intercept of the minimum reflux line is 0.57. Using Equation 3.12, the minimum reflux ration is found to be equal to: $R_{min} = 0.51$.

The actual reflux ration is calculates using Equation 3.12, that gives us a value of $R_{actual} = 0.61$. The quantity of liquid will then be $L = 5531.71\ Kg/h$ after calculating with Equation 3.13.

d) Numbers of tray

The theoretical number of trays is given by the number of triangles in Figure 14 plus the reboiler, that is $N_{theory} = 12$. Selecting 0.5 as efficiency of the column, the actual number of tray is $N_{actual} = 24$.

e) Column height and diameter

As the number of tray can be related to the height of the column via Equation 3.23, the height will then be $H_{column} = 55.2\ feet = 16.83\ m$.

4.2.2. Side strippers

The side strippers of the distillation column are design in purpose to enrich product streams. They are identical to one another with a same volume that was calculated in Appendix C.2. :

$$V_{side-stripper} = 5.30\ m^3$$

According to Sinnot (2005), the side strippers conform to a height-diameter ratio of 2. Then, the calculation will give 3 m and 1.5 m respectively for height and diameter.

4.3. Reactors design

4.3.1. Trickle Bed Reactor

The design of the diesel hydro treatment unit consisted of a calculation of the catalyst volume as shown in Appendix D.1:

$$V_{HDT\ catalyst} = 6.92\ m^3$$

The volume of catalyst assisted in subsequent calculations, as showed in Table 16:

Table 16: Sizes of Trickle Bed reactor

Parameters	Value
Volume	13.84 m^3
Sectional area	4.15 m^2
Diameter	2.30 m
Length	16.10 m

4.3.2. Catalytic reforming reactors

The design of the catalytic reforming reactors unit consisted first of all of a calculation of the volume and mass of the catalyst, as done in Appendix D.2. The numbers obtained are shown in Table 17:

Table 17: Volume and mass of catalyst in each reactor

Reactor	Volume (m3)	Mass (Kg)
1	3.69	3099.60
2	5.90	4956.00
3	26.82	22528.80

Second, the catalyst volumes in each reactor contributed to the additional deduction of reactor volume, as shown in Table 18:

Table 18: Volume of each catalytic reactor

Reactor	Volume (m3)
1	7.38
2	11.8
3	53.64

4.3.3. Catalytic cracking reactor

The design of the FCC was consisted of a determination of the catalyst mass that will lead to the calculation of flowrate and rate of the catalyst, based on the discussed literature. The feed stream of 7.39 m3/h (7,393.50 l/h) equivalent to 177.44m^3/day will give the amount of catalyst circulating in the system i.e. 887.22t/day.

Using relation 3.26, the flowrate of catalyst will be calculated as follow:

$$V_{cat} = \frac{m_{cat}}{\rho_{cat}} = \frac{887.22\ t/day}{840\ kg/m^3} = 1056.21\ {}^{m^3}/_{day} = 44.009\ {}^{m^3}/_{h} \cong 44.01\ {}^{m^3}/_{h}$$

After one hour, the volume of catalyst is $44.01 m^3$

The relation 3.27 uses the value of $V_{cat}$to obtain the catalyst rate:

$$Q_{cat} = \frac{V_{cat}}{t_t} = \frac{44.009\ m^3/h}{2\ sec} = \frac{44.009\ m^3/3600 sec}{2\ sec} = 0.006\ m^3/sec \cong\ 0.01\ m^3/sec$$

Based on above data, we can calculate the catalyst to oil ratio (COR) as follow:

$$\text{COR} = \frac{44.009\ {}^{m^3}/_{h}}{7.3935\ {}^{m^3}/_{h}} = 5.95$$

4.4. Modelling

4.4.1. Modelling of distillation

Note that the trays are numbered from bottom to top. Based on assumptions set out in the methodology and data previously obtained in the design, the following steps of the procedure mentioned in the methodology are in progress:

a) Development of reflux drum's equations

Given the data obtained during design, the total material balance of the first envelope will be:

$$\frac{d(m_D)}{dt} = V_{24} - D - R \qquad (4.5)$$

where: m_D: condensed liquid in the drum

Considering the component mass balance, the following equation will be obtained:

$$\frac{d(m_D x_D)}{dt} = V_{24} y_{24} - D x_D - R x_D \qquad (4.6)$$

The development of Equation 4.6 will be as follow:

$$m_D \frac{d(x_D)}{dt} + x_D \frac{d(m_D)}{dt} = V_{24} y_{24} - D x_D - R x_D \qquad (4.7)$$

After substituting of Equation 4.5 to Equation 4.7 and simplifications we obtain:

$$\frac{d(x_D)}{dt} = \frac{V_{24}}{m_D}(y_{24} - x_D) \qquad (4.8)$$

b) Development of top stage's equations

In this section, which corresponds to the 24th stage, the total mass balance will be given by Equation 4.9 below:

$$\frac{d(m_{24})}{dt} = R + V_{23} - L_{24} - V_{24} \qquad (4.9)$$

where: m_{24}: liquid hold up in tray 24

Based on Equation 3.35 $V_{23} = V_{24}$ and relation 4.9 is simplified as follow;

$$\frac{d(m_{24})}{dt} = R - L_{24} \quad (4.10)$$

The component mass balance on this section is represented by Equation 4.11 below:

$$\frac{d(m_{24}x_{24})}{dt} = Rx_D + V_{23}y_{23} - L_{24}x_{24} - V_{24}y_{24} \quad (4.11)$$

The development of Equation 4.11 gives Equation 4.12 below:

$$m_{24}\frac{d(x_{24})}{dt} + x_{24}\frac{d(m_{24})}{dt} = Rx_D + V_{23}y_{23} - L_{24}x_{24} - V_{24}y_{24} \quad (4.12)$$

By substituting relations 4.10 to 4.12, simplifying the new equation and considering Equation 3.35, we obtain Equation 4.13 below:

$$\frac{d(x_{24})}{dt} = \frac{1}{m_{24}}[R(x_D - x_{24}) + V_{residue}(y_{23} - y_{24})] \quad (4.13)$$

c) Development of nth stage's mathematic model

The nth represents any stage of the distillation column, below and above the feed stage. The total mass balance will be given by Equation 4.14 below:

$$\frac{d(m_n)}{dt} = L_{n+1} + V_{n-1} - L_n - V_n \quad (4.14)$$

Where: m_n: liquid hold up in nth tray

Based on Equation 3.35 $V_n = V_{n-1}$ and relation 4.14 is simplified as follow;

$$\frac{d(m_n)}{dt} = L_{n+1} - L_n \quad (4.15)$$

The component mass balance on this section is represented by the Equation 4.16 bellow:

$$\frac{d(m_n)}{dt} = L_{n+1}x_{n+1} + V_{n-1}y_{n-1} - L_nx_n - V_ny_n \quad (4.16)$$

d) Feed stage mathematic model

Based on Figure 14 of the distillation design the 8th tray is the feeding stage. The total mass balance will be:

$$\frac{d(m_8)}{dt} = (L_9 + F + V_7) - (L_8 + V_8) \quad (4.17)$$

Where: m_8: liquid hold up in feed stage

The component mass balance on this section is represented by Equation 4.18 below:

$$\frac{d(m_8 x_8)}{dt} = (L_9 x_9 + F z_F + V_7 y_8) - (L_8 x_8 + V_8 y_8) \quad (4.18)$$

e) First stage mathematic model

The total mass balance will be:

$$\frac{d(m_1)}{dt} = L_2 + V_{residue} - L_1 - V_1 \quad (4.19)$$

where: m_1: liquid hold up in first stage

The component mass balance on this section is represented by Equation 4.20 bellow:

$$\frac{d(m_1 x_1)}{dt} = L_2 x_1 + V_{residue} y_{residue} - L_1 x_1 - V_1 y_1 \quad (4.20)$$

f) Bottom stage mathematic model

The total mass balance at the bottom stage is:

$$\frac{d(m_B)}{dt} = L_1 - B - V_B \quad (4.21)$$

where: m_B: liquid hold up in bottom stage

The component mass balance on this section is represented by Equation 4.22 bellow:

$$\frac{d(m_B x_B)}{dt} = L_1 x_{B1} - B x_B - V_B y_B \quad (4.22)$$

g) Determination of y and L

Knowing the relative volatility from the distillation design and based on the assumptions used, y will be determined using equilibrium relationship (Equation 4.4).

$$y = \frac{2.895179\,x}{1+(2.895179-1)\,x} \tag{4.23}$$

The liquid flow rate is calculated using the linearized form of Francis Weir equation (hydraulic relation):

$$L_n = L_{n_0} + \frac{m_n - m_{n_0}}{\beta} \tag{4.24}$$

where: L_n: Flow rate leaving the nth tray of the column
L_{n_0}: Reference value of L_n
m_n: liquid hold up in nth tray
m_{n_0}: Reference value of m_n
β: Hydraulic time constant (3 to 6 seconds per tray)

h) Degrees of freedom

First, we will determine the number of independents equations using Table 19 below:

Table 19: Independents equations

Name	Number of equations
Equilibrium equation	25
Hydraulic relationship	24
Total and composition mass balance equations	48
Reflux drum	2
Bottom column	2
Total	101

Similarly, the variables with corresponding number of equations are found in Table 20:

Table 20: Independent variables

Name	Number of equations
Liquid composition	26
Vapour composition	25
Liquid hold up	26
Liquid flow rate	24
Feed flow rate, feed composition, distillate flow rate, reflux, bottom vapour, flow rate, bottom	6
Total	107

Therefore, the degree of freedom will be given by the difference between the number of independent equations and independents variables as follow:

$$f = 107 - 101 = 6$$

Since the number of variables is greater than the number of equations, we have an underspecified process. As this process must be specified, we must make f equal to zero, it means:

- Specification of more number of disturbance variables
  This can take place by measuring following variables: Feed flow rate, feed composition
- Incorporation of more number of controller equations
  We can consider the bottom product (x_B and m_B) and the top product (x_D and m_D) as controlled variables. These variables can be used to manipulate m_B, B, R and D respectively using the following controller equations:

$$R = R_s + k_{CR}(x_{DSP} - x_D) \quad (4.25)$$

$$D = D_s + k_{CD}(m_{DSP} - m_D) \quad (4.26)$$

$$V = V_{Bs} + k_{CV}(x_{BSP} - x_B) \quad (4.27)$$

$$B = B_s + k_{CB}(m_{BSP} - m_B) \quad (4.28)$$

where: SP: set point

BS: bias point

Regarding the above, we do have two less variables amongst the independent variables and four other equations in addition of the independent equations we had before. Therefore, the degree of freedom will be zero, which makes our process specified.

4.4.2. Modelling of fluid catalytic cracking unit

The reactions involved in the fluid catalytic unit constitute a network which is represented by the reaction scheme below (Figure 15):

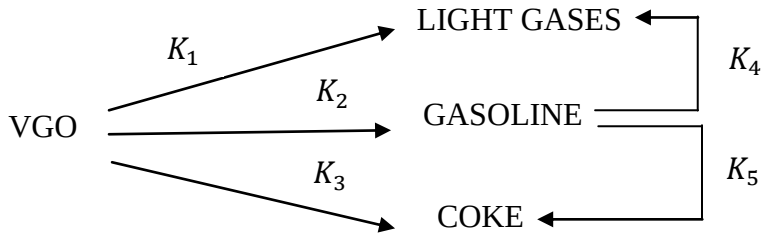

Figure 15. 4-lump reaction scheme for fluid catalytic cracking unit

On basis of Figure 15, where 4-lump kinetic is considered, the network equations are represented by Equations 4.29 to Equation 4.32 as follows:

$$\frac{dy_1}{dx} = \emptyset(t_c) f(C_{Arh}) C^{te}[-(k_1 + k_2 + k_3)y_1] \quad (4.29)$$

$$\frac{dy_2}{dx} = \emptyset(t_c) f(C_{Arh}) C^{te}[(\gamma_{VG}\, k_1\, y_2) - (k_4 + k_5)y_2] \quad (4.30)$$

$$\frac{dy_3}{dx} = \emptyset(t_c) f(C_{Arh}) C^{te}[\gamma_{VC}\, k_3 y_1 + \gamma_{GC}\, k_5 y_2] \quad (4.31)$$

$$\frac{dy_3}{dx} = \emptyset(t_c) f(C_{Arh}) C^{te}[\gamma_{VL}\, k_2 y_1 + \gamma_{GL}\, k_4 y_2] \quad (4.32)$$

In the equations above we have considered x as a dimensionless distance from the riser, y_i as weight fraction of lump under consideration (VGO, Gasoline, light gases and coke) and γ_{ij} as a molecular weight ratio of the lump i over j.

In order to satisfy the overall mass balance of the reactions, molecular weight ratios are used as stoichiometric coefficients (Heydari *et al*., 2010).

The other parameters appearing in the equations above are:

- Constant $f(C_{Arh})$ which is expressed as follow:

$$f(C_{Arh}) = \frac{1}{1+k_h C_{Arh}} \quad (4.33)$$

where: k_h: heavy aromatic ring adsorption coefficient (equal to 1.28)

C_{Arh}: Weight percentage of aromatic in VGO

- Constant of equations C^{te} can also be expressed as follow:

$$C^{te} = \frac{\overline{PMN}}{RTS_{wh}} \quad (4.34)$$

where: S_{wh} is the weight of hourly space velocity

- Catalyst activity due to coke deposition $\emptyset(t_c)$ which function depends on catalyst time t_c as shown in the Equation 3.35 below:

$$\emptyset(t_c) = \frac{1}{1+Bt_c{}^{\gamma}} \quad (4.35)$$

where: $B = 162.15$ and $\gamma = 0.76$

4.4.3. Modelling of catalytic reforming unit

Deactivation relations are developed base on reactions as follow:

- Naphthenes to paraffins:

  Rates constant at temperature T_0 and T are respectively:

- $K_{e1_{T_0}} = e^{(-7.12+\frac{8000}{T_0})}$ (4.36)
- $K_{e1_T} = e^{(-7.12+\frac{8000}{T})}$ (4.37)

Deactivation will be:

$$a = \frac{K_{e1T_0}}{K_{e1T}} = \frac{e^{(-7.12+\frac{8000}{T_0})}}{e^{(-7.12+\frac{8000}{T})}} \quad (4.38)$$

Introducing napierian logarithm, Equation 4.38 becomes:

$$lna = \ln\left[\frac{e^{(-7.12+\frac{8000}{T_0})}}{e^{(-7.12+\frac{8000}{T})}}\right] \quad (4.39)$$

$$lna = \ln\left[\frac{e^{(-7.12+\frac{8000}{T_0})}}{e^{(-7.12+\frac{8000}{T})}}\right] \quad (4.40)$$

$$lna = \frac{8000}{T_0} - \frac{8000}{T} \quad (4.41)$$

Considering T_0 as a constant, the differentiation of Equation (4.41) will give the relation below:

$$\frac{1}{a^2}\frac{da}{dt} = \frac{800}{T^2}\frac{dT}{dt} \quad (4.42)$$

- Naphthenes to aromatics:

Based on the above steps and using the Equation 2.14, the differential equation of deactivation will be given by:

$$\frac{1}{a^2}\frac{da}{dt} = \frac{-46045}{T^2}\frac{dT}{dt} \quad (4.43)$$

- Hydrocracking of naphthenes and hydrocracking of paraffins:

Using 2.16 and 2.17 or 2.18 and 2.19, and following the steps above, the differential equation of deactivation will be given by:

$$\frac{da}{dt} = 62300\frac{a^2}{T^2}\frac{dT}{dt} \quad (4.44)$$

4.4.4. Modelling of Hydrotreatment unit

Following models, Chang and Fang, Korsten and Hoffman, Murali and Voolapalli; are represented respectively by Equations 4.45, 4.46 and 4.47. These are kinetic models that give data that will be analysis in the next section for comparison.

$$r_{HDS} = K_{HDS} \frac{(C_S^S)^2 \left(C_{H_2}^S\right)^{0.6}}{1+K_{H_2S}\, C_{H_2S}^S} \quad (4.45)$$

$$r_{HDS} = K_{HDS} \frac{C_S^S \left(C_{H_2}^S\right)^{0.45}}{\left(1+K_{H_2S}\, C_{H_2S}^S\right)^2} \quad (4.45)$$

$$r_{HDS} = K_{HDS} \frac{(C_S^S)^{1.64} \left(C_{H_2}^S\right)^{0.55}}{\left(1+K_{H_2S}\, C_{H_2S}^S\right)^2} \quad (4.45)$$

4.5. Simulation and results

4.5.1. Simulation steps on Aspen

Based on the concept that the feed for each module is given and that the outputs of each module must be calculated, the Aspen simulator follows these steps respectively:

- Proprieties: Capture of components lists and fluid packages
- Design of the diagram: Capture of different modules parameters
- Simulation: Runs system and gives results

All of these with possibilities to get different curves such as petroleum assays,

4.5.2. Simulation flow diagram

Figure 14 shows the process for the CDU. It contains an atmospheric distillation unit and a vacuum distillation unit that separate crude oil into the naphtha, kerosene, gasoil (Diesel, LVGO, HVGO) and residue.

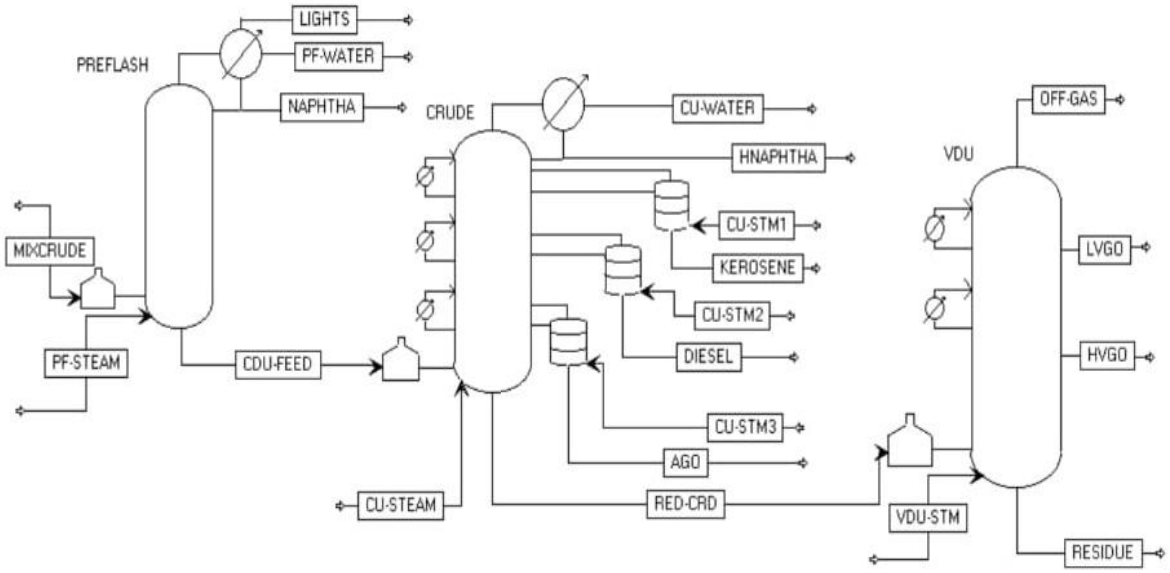

Figure 16: Process flow diagram of CDU (Aspen Hysys)

Figure 15 illustrates the FCC process. It contains reactors and a riser, as well as fractionator that processes gasoil to make gasoline.

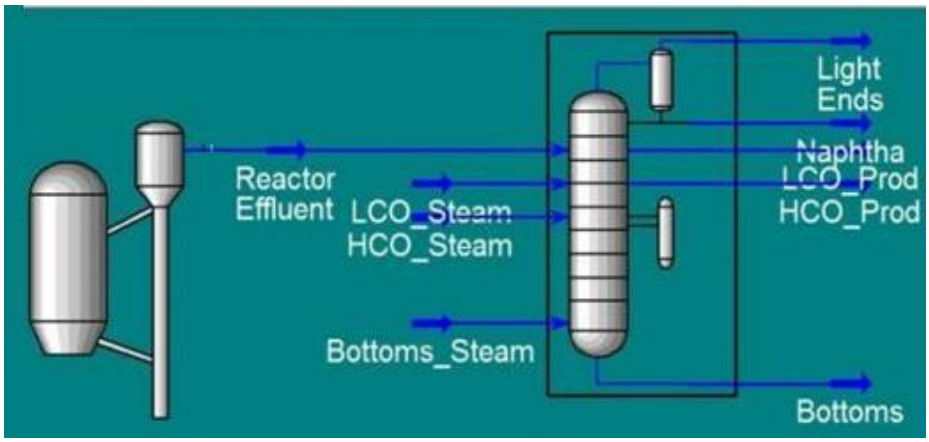

Figure 17: PFD simulation of FCC with fractionators (Aspen Hysys)

The Figure 16 illustrates the process of the CRU section. It contains three reactors that processes naphtha to produce reformate product containing gasoline.

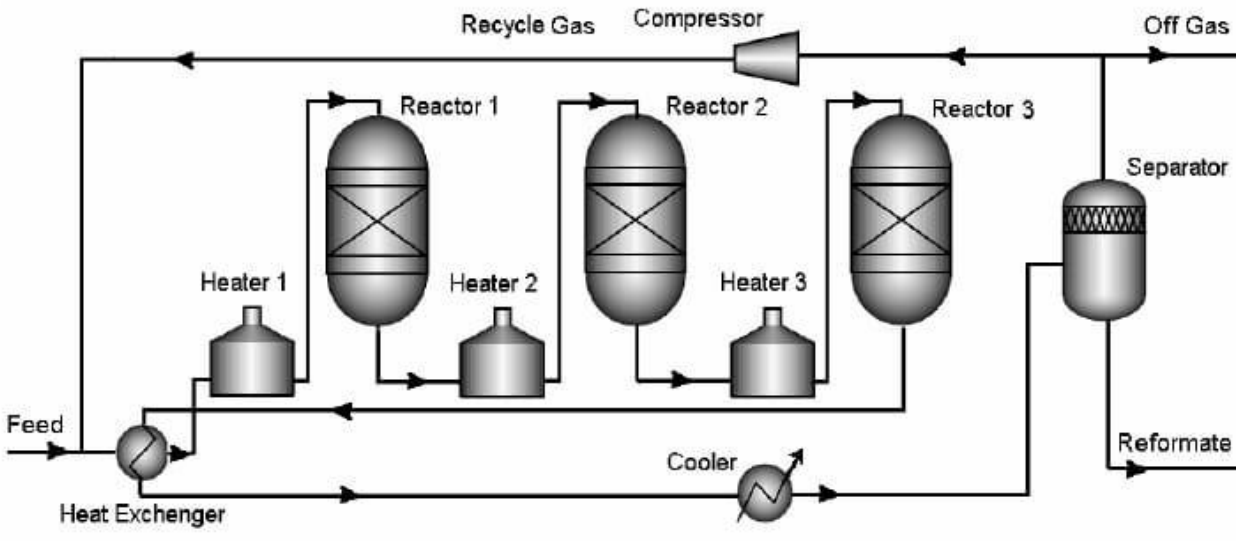

Figure 18: Process flow scheme of Catalytic Reforming Unit (Aspen Hysys)

4.5.3. Results of sulphur variation

In this section are represented results of environmental survey of this study focused on the production of low sulphur gasoline. These results were obtained with the model presented in the previous sections of our research. Results are illustrated in Table 21:

Table 21: Independent variables

Feed sulphur wt%	Gasoline / Feed ratio	Gasoline sulphur reduction (%)	COR
0.45 to 0.55	7.1	5	4.10
0.60 to 0.75	6.3	10	5.95
0.75 to 0.95	5.6	20	6.01
1.0 to 1.35	4.2	40	8.30

The new regulations which require the sulphur gasoline to be reduced to ppm is the cause of growth of the FCC process and the common point of all the research used for validation of the results represented above. The comparison between result obtained and represented in table 21 and the documentary data shows the followings elements:

- COR is also an important parameter because its increase leads to an increase in gasoline reduction. In fact, the gasoline sulphur contents were reduced from 5 to 40%, the COR

varying from 4.10 to 8.30. This joins Paul et al (2015) and Gupta (2006) who concluded that by varying the COR between 4 and 10, the reduction in sulphur increases as well as gasoline yield.

- Table 21 shows the profiles figure of some important process variables of the FCC process. Figure 19 clearly shows that as the gasoline-feed ratio increases, the reduction in sulphur decreases. The curve obtained is almost linear.

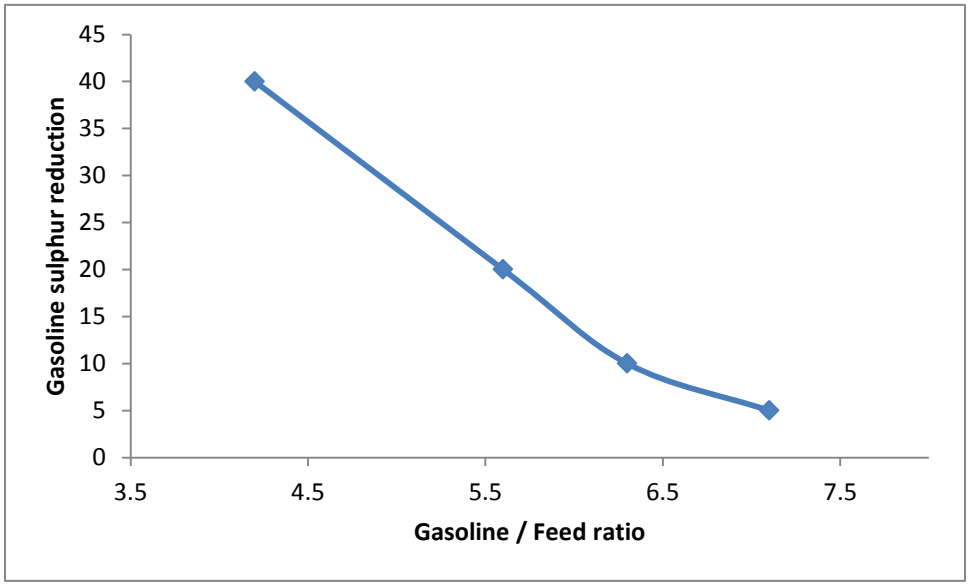

Figure 19: Sulphur variation according to gasoline/feed ratio

From these data we found that higher sulphur inputs allowed hogher levels of sulphur reduction in the gasoline.

- Figure 20 shows the representation of sulphur variation in the feed impact on the reduction sulphur in gasoline. In fact, the reduction of sulphur in gasoline is 5% when the sulphur concentration is between 0.45 and 0.55 wt% in the feed; and 40% when the sulphur is between of 1.0 and 1.35w% in the feed. The curve obtained increases and this shows that the reduction in sulphur is directly proportional to the increase of feed with sulphur content. There is a good correlation between the FCC feed sulphur and the corresponding sulphur reduction. This correlation is in agreement with a study done by Watkins et al (2011) and Watkins et al (2014).

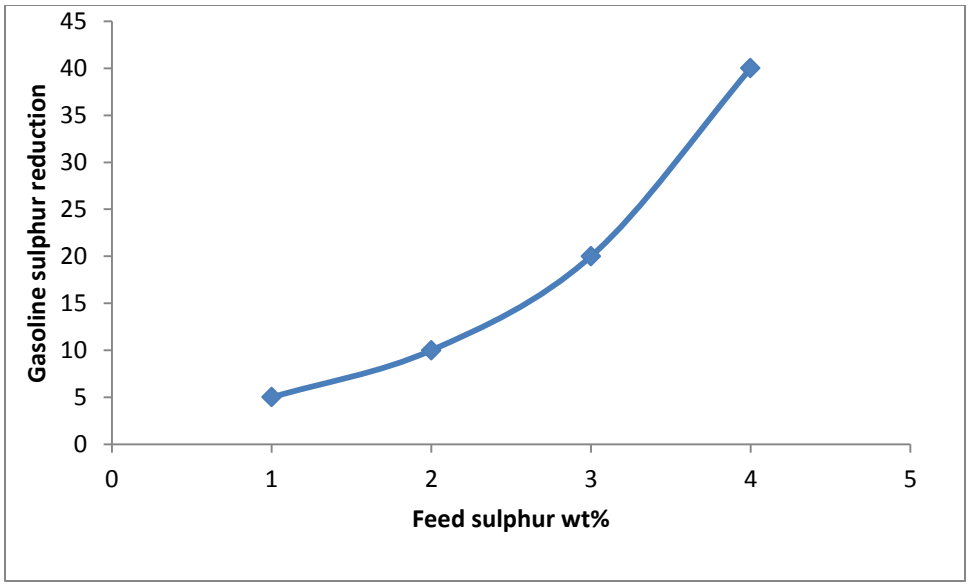

Figure 20: Sulphur variation

4.6. Discussion

The main objective of this research was the study of the environmental production of gasoline in a modular refinery. This has led to some interesting and remarkable results. However, it was important to start with a design of the required modular refinery, and a modelling for simulation.

A true boiling point curve is based on crude assay data, which is the first input into Aspen Hysys; and the mole composition of all pseudo-components. The true boiling point analysis is important for identification of the quantity and value of the crude oil (Abraham, *et al.*, 2017). The crude oil fractions are usually defined by range of 5 to 95 % temperature yield rather than 0 to 100% (Watkins, 1979). The range of 0 to 100 % may represent infinitely small amount of material.

Based on the above and referring to Figure 11 and Table 9, it is depicted 5 % of yield occurs at boiling point of the lightest hydrocarbon component, with temperature of 22.83333^{o}C. Likewise, the heaviest hydrocarbon related to 95 % yield, evaporates at the boiling point of 427.5556^{o}C.

According to Speight (2002), gasoline lower boiling point and upper boiling point are respectively -1 and 216^{o}C. Based on these assumptions, the calculation done resulted in 1.4836%

and 70.6816% as component of the lightest and heaviest gasoline respectively. Thus, this crude oil can yield up to 69.198 % gasoline.

Figure 12 shows positive disparity in the crude oil. To assert the presence of a gap between different products cuts that the separation is both viable and simple. Moreover, no significant overlap that could make distillation difficult for the crude oil studied, no significant complexity has been added to the CDU design.

For hydraulic analysis in the refinery, especially the design, evaluation and troubleshooting of piping systems, it is important to study proprieties such as density. Knowing that most crude oil can be pumped when the SG is in the range of 0.80 (45API) to 0.97 (15 API); Table 11 and Figure 13 show that LN, HN, K, D and VGO are fluid that can be pumped, excluding the residue.

The design of crude oil distillation by Manley (1993) also used by Santana and Zemp (2001) improved thermodynamics process. However, they were limited to certain difficulties such as unproven and uncertain cost. Some studies proposed short-cut modes for distillation of column, among them; Gadalla et al (2003) developed optimization approach of existing distillation processes. Although, there are a lot of studies that proposed different ways of design, some using software, others using neural network architecture or online application; this study proposed very basics design method targeting modelling and simulation.

This led us to use a graphical method of designing a distillation column, as graphical method is suitable for feasibility studies (Flores-Estrella and Iglesias-Silva, 2016). The McCabe and Thiele graph was then plotted. Published in 1925 by McCabe and Thiele, this method has been found to be of great use in variety of mass transfer operations (Lichatz, 2019). It can be used for distillation column design as well as solvent extraction. Using the McCabe and Thiele method for distillation, it is possible to calculate the number of equilibrium stages required (Gomes, 2007). This method is also convenient to determine the number of stages and reflux that assumes to be necessary.

Thus, our design of crude oil distillation column based on the graphical method above, have given expected results such as reflux ratio (0.61), number of tray (24), diameter of column (16.83 m) and side strippers volume (5.30 m^3).

Most of published information about trickle bed reactors industrial application concerns the processing with hydrogen of various petroleum fraction (Satterfield, 1975). These applications are: hydrotreating (hydrotreatment) or hydrofinishing and hydrodesulphurization or hydrocracking. Generally the trickle bed reactors are operated at high pressure. While in this work the operating pressure was inspired by Albhari (2001) as follow: 70.31 to 201.92 kg/m^2. In addition, the the weight hourly space velocity was based on previous work, Korsten and Hoffman (1996), and the value of 0.85 h^{-1} was used. Results from Askari *et al.* (2012) and Korsten Hoffman (1996) study were referenced for the catalyst and industrial bed void value. This led us first to the Equations 3.28 and 3.29 for calculation of catalyst volume (6.92 m^3) and volume of reactor (13.84 m^3); secondly to the sizes of the reactor, that are sectional area (4.15 m^2), diameter (2.3 m) and length (16.1 m).

In this study, the fluidized bed reactor was chosen as cracker to design the cracking reactor; because the fluidized bed is suitable for the production of gasoline. It has been found in the literature that more attention need to be given to the catalyst in the design as others parameters must be optimized. Based on a feedstock of 4.66 kg/l (Gary and Handwerk, 2001), the residence time of 2 second (Lee, 2016), and catalyst data from Bollas et *al.* (2007) studies; the equations 3.26 and 3.27 were used to obtain: the catalyst-oil ratio (5.95) and catalyst flowrate (44.01 m^3/h).

The design of catalytic reforming unit had involved catalyst and reactor design. Typical operating parameters were reviewed in the literature. Based on Baerns (2013) that inspired different reactors' weight hourly specific velocity, on catalyst density and industrial bed void fraction referred to Askari *et al.* (2012) and McKetta (1990); calculations could be operated in Appendix D.2 using Equation 3.28 and 3.29. These lead us to find parameters of each reactor constituting the reforming unit.

Process modelling involves process flow sheet and design; which give importance to the mathematical modelling economically process design (Khim, 2013). Based on that, this work has started with the design before carrying on to modelling of refinery's unit.

After designing a modular process refinery, this study formed mathematical models of crude oil distillation unit; hydrotreatment; catalytic reforming unit; and fluid catalytic cracking unit.

Because the pressure fluctuation makes the control of distillation unit difficult and reduce it performance; conventional or advanced distillation control system assume that the column operates at constant pressure (Minh and Rani, 2009). This was taken into account for the modelling of crude oil distillation performed in this study. The modelling has also considered two parameters, namely liquid flow rate and vapour flow rate, as control input of column distillation as stated in Minh and Rani (2009). Assumptions stated in chapter 3 were mad based on numerous studies previously published, such as Ann (2014), Jinsa and Ajeesh (2014) or Stathaki *et al*. (1985). The assumptions and their implications were applied onto mass balance and component mass balance. As result developed Equations 4.5 to 4.28 are representing the process.

The first step in modelling of catalytic cracking was to represent the scheme of reactions considered in this study. With gasoline as main focus, it was important to consider a number of lumps that will suit the purpose of this study. Different studies on modelling of FCCU have been made as of today. As results of previous researches, many have proposed models where hydrocarbons are grouped or lumped using limited number of reactions (Singh, *et al.*, 2017). These models are kinetic models that use different number of kinetics lumps: two (Weekman, 1968), three (Weekman, 1969), four (Cristina, 2015), five lumps (Ancheyta-Juarez, 2000; Bollas), six (Ancheyta, 2002), seven (Heydari, 2010) height (Sani, 2018), seventeen (Singh, *et al.*, 2017), etc. in this study 4 kinetics lumps were considered as vacuum gasoil, coke, light gases and gasoline are the considered group of hydrocarbons.

Due to the complexity of the feed coming into the catalytic reformer and various reactions that take place, kinetic models are very difficult to obtain. Thus, kinetic lumps are also used for reforming of such unit. Throughout the years several models been developed with aim to make a

better representation of the kinetics of catalytic reforming reactions. Among them we mentioned, Smith (1959), Padmavathi and Chaudhuri (1997). Referring to Ancheyta *et al.* (2001), a semi-regenerative reactor was taken into account in this study in order to allow an increase in severity.

Furthermore, focusing on gasoline the modelling of reforming has considered Smith model. The main focus on modelling of reforming unit was to develop a model based on activation. Knowing the rates constant expressions, it can be used to get deactivation; calculus devices, especially napierian logarithm have been used to develop a differential equation as model of catalytic reforming unit. Finally modelling of hydrotreatment unit was based on previous works. This gave us reasonable reduction of sulphur. Therefore, the Murali and Voolapalli kinetic model approches the experimental data.

Reducing the sulphur concentration in products is still important to comply with the regulations to reduce gas emissions emanated from combustion of fuel. This study looked onto environment impact of sulphur concentration using simulation. The data have been analyzed to find out how sulphur content changes in a specific products, for instance the gasoline.

It is clear that an appropriate study on FCCU and HTU must be carried outbefore implementing data on the process. Referring to Letzsch *et al.* (2009) that states that the range of COR is normally 4:1 to 9:1, the modular refinery simulation is a success because of the results obtained (4.10:1 to 8.30:1; with a high variation of sulphur in gasoline. This can meet different regulations mentioned in the literature.

CHAPTER 5

CONCLUSION AND RECOMMENDATION

5.1. Conclusions

The objectives of this study are the design and simulation of a modular refinery using Aspen Hysys, as well as to investigate the environmental influence of the process on the product compositions. The characterization of the fed crude oil then becomes essential, as the design of different units based on the characterized oil. Below are the designed variables used for this investigation:

- Reflux, number of trays, column height, column diameter, feed tray position and stripers volume for the CDU
- Volume, sectional area, diameter and length for HTU
- Volume and mass catalyst for CRU
- Volume and flow rate of catalyst for FCCU

The crude oil and its different cuts characterization results showed a clear variation in all properties. The refinery was successfully simulated and validated using Aspen Hysys simulation tool. This software was used to determine the amount of sulphur in gasoline for further study, such as environmental investigation of the process. The results obtained give enough information that are specifications of the crude oil required for the design.

The designs have been performed using the specifications obtained previously. The theoretical design gives a specified details and information of the main refinery units that have been targeted in this study. The data obtained after calculation represent an advantage and useful results for the design, in particular material and energy balances.

A modular refinery with a processing capacity of 12,000.00 bbl/day was designed and a detailed equipment design using numerical calculations was carried out. Although the simulation gave more detailed and effective results, numerical design technique made possible to better compare

the Aspen Hysys simulation. Equipment design includes column (number of trays 24, reflux ratio 0.51 and column height: 16.83m), side strippers (volume 5.30 m^3), trickle bed reactor (catalyst volume 6.92 m^3, reactor volume 13.84 m^3, sectional area 4.15 m^3, diameter 2.30 m^3 and length 16.1m), catalytic reforming reactor (reactor 1 catalyst volume 3.69 m^3, reactor 2 catalyst volume 5.90 m^3, reactor 1 catalyst volume 26.82 m^3, reactor 1 volume 7.38 m^3, reactor 2 volume 11.80 m^3 and reactor 3 volume 53.64 m^3) and catalytic cracking reactor (catalyst flowrate 44.01 m^3/h, catalyst rate 0.006 m^3/sec and catalyst to oil ratio 5.95).

The Aspen Hysys simulation of the model obtained by designing helps to provide a complete evaluation of the equipment. This survey increased the production of gasoline using Aspen Hysys software and provided details on the environmental impact.

Environmental results presented in this study are in good agreement with results presented by author mentioned in literature review and methodology.

The improvement of refineries definitely needs techniques such as modelling and simulation. The use of modelling in different studies always adds useful data in this field. High subjective errors in evaluation of refinery project are avoided when simulation is coupled with modelling.

5.2. Recommendations

During the course of this study, various considerations were made to study the environment effects of sulphur in products. The data obtained in this research was not focused entirely on all environmental aspects. However, data on influence of sulphur on the environment were sufficient, although some empirical calculations were made from the beginning. In this respect, future studies are recommended to implement a pilot plant, in order to find the best parameter values for maximum production and an advanced environmental study on refinery.

This study performed a specific case study provided by the design. Because refineries have different configurations and give differences in products, more cases of modular refineries should be investigated. It is even very important to consider the configuration of a large-scale refinery. The configuration and scale can influence the concentration of sulphur in gasoline. The catalyst amount must be designed according to the feedstock data. It is possible to study the

influence of configuration and scale by analysing different cases with different modular refineries.

Deviations from the design specifications and changes operating parameters may occur due to the state of feed mixture and feed composition of crude oil. This can jeopardize the purpose of the refinery. It is then recommended to consider this factor in future studies.

REFERENCES

Abdullah, Z., Aziz, N. and Ahmad, Z. (2007) "Nonlinear Modelling Application in Distillation Column", *Chemical Product and Process modelling*, **2**(3), p.12.

Abraham, J.M., Babu, A., Manoj, K., Ahamed, K., Raj, G., Arunachaleswara, P.R. and Kanna, R. (2017) "Correlation of True Boiling Point of Crude Oil", *International Refereed Journal of Engineering and Science (IRJES)*, pp. 45-49.

Abubakar, A.; Mohammed-Dabo, I.A. and Ahmed, A.S. (2016) "reduction of Sulphur Content of urals Crude Oil Prior to Processing using Oxidative Desulphurization", *Nigerian journal of Basic and apllied Science*, 24(1): 19-24.

Adefarati, F. and Chigbu, P. (2017) The continuous advocacy for Modular refineries in Nigeria: time for all hands to be on deck, *Energy & Natural Resources Department*, SPA Ajibade & Co, Lagos, Nigeria.

Akpa, J.G. and Umuze, O.D. (2013) "Simulation of a Multi-component Crude Distillation Column", *American J. of Scientific and Industrial Research*, **4**(4), pp.366-377.

Alattas, A.M., Grossmann, I.E. and Palou-Rivera, I. (2012) "Refinery production planning: Multiperiod MNLP With CDU model", *Industrial & Engineering Chemistry Research*, **51**(39), pp.12852–12861.

Albahri, T (2001) "Petroleum refining-Chapter 8: Desulfurization", Kuwait University.

Albhari, T (2008) "Petroleum refining-chapter 8: Desulphurization" www.albhari.info/Refinery/Chapter08%20-%20Desulfurization.pdf [2017, June 25].

Al-Malki, A. (2004) "*Desulfurization of Gasoline and diesel Fuels, Using Non-Hydrogen consuming Techniques*", Master of Science Dissertation, King Fahed University of Petroleum and Minerals.

Ancheyta, J (2011) "*Modelling and Simulation Catalytic Reactors for Petroleum Refining"*, John Wiley & Sons, Inc, Hoboken, New Jersey.

Ancheyta, J. and Sotelo, R. (2002) "Kinetic modeling of vacuum gas oil catalytic cracking", *Revista de la Sociedad Química de México*, **46**(1), pp.38-42.

Ancheyta, J; Villafuerte, ME; Díaz, G.L; González, AE (2001) "Modelling and Simulation of Four Catalytic Reactors in Series for Naphtha Reforming", *Energy Fuels*, **15**, 887-893.

Ancheyta-Juarez, J. and Sotelo-Boyas, R. (2000) "Estimation of kinetic constants of a five-lump model for fluid catalytic cracking process using simpler sub-models", *Energy & fuels*, **14**(6), pp.1226-1231.

Ann, I.W.F. (2014) "*Modelling and simulation of distillation column*", BEng Chem Thesis, Universiti Malaysia Pahang.

Arani, HM, Shokri, S and Shirvani (2010) "Dynamic Modelling and Simulation of Catalytic Naphtha Reforming", *International Journal of Chemical Engineering and Applications*, 1(2), p.159.

Askari, A; Karimi, H; Rahimi, MR and Ghanbari M (2012) "Simulation and modelling of catalytic reforming process", *Petrol. Coal*, 54(1), pp.76-84.

AspenTech (2009) "*Getting Started Modelling Petroleum Processes*", Aspen Technology, Inc. Burlington, USA.http://www.aspentech.com [2017, May 16].

Backhurst, J. R., Coulson, J. M., Harker, J. H., & Richardson, J. F. (1999) "*Fluid Flow, Heat Transfer and Mass Transfer*", Oxford: Butterworth-Heinemann.

Barbosa, AC; Lopes GC; Rosa LM; Mori, M and Martignoni, WP (2013) "Three dimensional simulation of catalytic cracking reactions in an industrial scale riser using a 11-lump kinetic", *In AIDIC Conference Series*, 11, 31-40.

Barletta, T., White, S. and Chunangad, K. (2012) “Designing a crude unit heat exchanger network”, *Petroleum Technology Quarterly*, **16**, p.3.

“Basic knowledge Distillation”, http://www.gunt.de/images/download/distillation_rectification_english.pdf [2017, January 02].

Behmiri, NB and Manso, JPR (2014) “The linkage between crude oil consumption and economic growth in Latin America: The panel framework investigations for multiple regions”, *Energy*, vol. 72, no. 1, pp. 233-241.

Bhende, SG and Patil, KD (2014) “Modelling and simulation for FCC unit for the estimation of gasoline production”, *International Journal of Chemical Sciences and Applications*, Vol 5, Issue 2, pp 38-45.

Bollas, G.M., Lappas, A.A., Iastridis, D.K. and Vasalos, I.A. (2007) “Five-lump Kinetic model with selective catalyst deactivation for the prediction of the product selectivity in the fluid catalyst process”, *Catalysis Today*, Volume 127, pp. 31-43.

Boston, J. F. and Sullivan, S. L. (1974) “A New Class of Solution Methods for Multi-component, Multistage Separation Processes”, *The Canadian Journal of Chemical Engineering*, 52(1), pp.52-63.

Brooks, B. A. (1993) “*Modelling of a Distillation Column Using Bond Graphs*”, M.Sc. Thesis, University of Arizona, 70-88.

Brown, K.B.; Maxwell, R.V. and Shumwau, M.D. (2003), Modular Oil Refinery, US. Patent WO2003031012A1.

Bunse, K; Vodicka, M; Schönsleben, P; Brülhart, M and Ernst, FO (2011) “Integrating energy efficiency performance in production management–gap analysis between industrial needs and scientific literature”, *Journal of Cleaner Production*, 19(6), pp.667-679.

Caballero S.B. (2014) “*Logic hybrid simulation-optimization algorithm for distillation design*”, Computers & Chemical Engineering.

CenAm Energy Partners (2012) "The Case for Modular Mini-Refineries", *Internal Company Report. CenAm Energy Partners S.A*, Panama City, Panama

Cheremisinoff, NP and Rosenfeld, P.E (2009) "*Handbook of pollution prevention and cleaner production Vol. 1: Best practices in the petroleum industry*", William Andrew.

Cristina, P. (2015) "Four–Lump Kinetic Model vs. Three-Lump Kinetic Model for the Fluid Catalytic Cracking Riser Reactor", *Procedia Engineering*, **100**, pp.602-608.

Couper, J.R., Penney W.R, Fair, J.R. and Walas, S.M. (2012) "*Chemical Process Equipment Selection and Design*", Butterworth-Heinemann, Third Edition.

Cournoyer, A., Couture, G., Couture, J-F., Ferland, M., Fontaine, A., Gervais, O., Giroux, F., Laplante, A., Lapointe-Garant, P-P., Morin, V. and Vallières, S. (2005) "Rapport Final- Équipe A - Raffinerie intégrée'', Final Report, Département de génie chimique, Université de Sherbrooke, Quebec, Canada.

Cross, P; Desrochers, P and Shimizu, H (2013) "The economics of Petroleum Refining, Understanding the business of processing crude oil into fuels and other value products", *Canadian Fuels Association*, Ottawa, Canada.

Daneshvar, MR and Fatemi, S (2011) "Mathematical Modelling and Simulation of Hydrotreating (HDS, HDN and HAD) of Gas oil in Commercial Trickle-bed Reactor", *In 7th International Chemical Engineering Congress & Exhibition*.

De la Paz-Zavala, C., Burgos-Vázquez, E., Rodríguez-Rodríguez, J.E. and Ramirez-Verduzco (2013) "Ultra low sulfur diesel simulation. Application to commercials units", *Fuel 110,* pages 227-234.

DEA- RSA (2010) "National Climate Change Response Green Paper", *Department of Environmental Affairs*.

Doronin, VP and Sorokina, TP (2007) "Chemical design of cracking catalysts", *Russian Journal of General Chemistry,* 77(12), pp.2224-2231.

Douani, M., Ouadjenia, F. and Terkhi, S. (2007a) "Distillation of a complex mixture. Part I: High Pressure Distillation Coulmn analysis: Modelling and simulation", *Entropy*, **9**, (2), 58-72.

Douani, M., Terkhi, S. and Ouadjenia F. (2007b) "Distillation of a Complex Mixture. Part II: Performance Analysis of a Distillation Column Using Exergy", *Entropy*, **9**, pp 137-151.

Douglas, J. (1988) "*Conceptual Design of Chemical Process*", MacGraw-Hill, Inc, section A-3.

Dreher, T. (2016) "Electrostatic Desalter Optimisation", *MI lecture note series*, 67, pp.24-29.

Ejikeme-Ugwu, E (2012) "*Planning for the integrated refinery subsystems*", Ph.D. Thesis, Cranfield University, United Kingdom.

El-Hadi, D (2015) "Comparative Study of the Characterization Factors for Hydrocarbon Types of Petroleum Fluids Fractions", *Journal of Petroleum Science Research*.

Energy Information Administration "EIA" (2014) "Independent statistics and analysis", *US Department of Energy*.

Energy Information Agency "EIA" (2014) "Products made from a Barrel of Oil", *US Department of Energy*.

Environmental Protection Agency "EPA" (1995) "Compilation of air pollutant emissions factors Volume 1: Stationary Point and Area Sources", *US Department of Environment*, AP 42, Fifth edition.

Eβer, J.; Wasserсheid, P and Jess, A (2004) "*Deep desulfurization of oil refinery streams by extraction with ionic liquids*", Green Chemistry.

Fagan, A (1991) "*An Introduction to the petroleum industry*",Terminology, vol. 1, p. 1.

Fahim, MA; Al-Sahhaf, TA and Elkilani, A (2010) "*Fundamentals of petroleum refining*", Elsevier, pp.1-32.

Ferreira, C; Marques, J; Tayakout, M; Guibard I; Lemos, F; Toulhoat H and Ramoa Ribeiro, F (2009) "Modelling residue hydrotreating", In 20th International Symposium in Chemical Reaction, *Chemical Engineering science: Engineering—Green Chemical Reaction Engineering for a Sustainable Future*, pp. 322–329.

Fetter-Pruneda, E., Borrell Escobedo, E.R. and Garfias Vázquez, F.J. (2005) "Optimum temperature in the electrostatic desalting of Maya crude oil", *Journal of the Mexican Chemical Society*, **49**(1), pp.14-19.

Flores-Estrella, R.A. and Iglesias-Silva, G.A. (2016) "Reactive McCabe-Thiele: Short cut method including reactive vapor-liquid efficiency", *Revista Mexicana de Ingeniería Química*, **15**(1), pp.193-207.

Fuente, J. R. (2015) "*Equipment Sizing and Costing*", In J. R. Fuente, Chemical Process Design, Cantabria: open course ware, pp. 2-30.

Gadalla, M., Jobson, M. and Smith, R. (2003) "Optimization of existing heat-integrated refinery distillation systems", *Chemical Engineering Research and Design*, **81**(1), pp.147-152.

Gañí, R., Ruiz, C.A. and Cameron, I.T. (1986) "A generalized model for distillation columns-I: Model description and applications", *Computers & chemical engineering*, 10(3), pp.181-198.

Gary, JH and Handwerk, GE (2001) "*Petroleum Refining Technology and Economics*", Marcel Dekker Inc. New York.

Gary, JH; Handwerk, GE and Kaiser, MJ (2007) "*Petroleum refining: technology and economics.4th*", CRC press.

Green D. and Perry R. (2007) "*Perry's Chemical Engineer's Handbook*", Eight Edition, McGraw-Hill.

Gomes, J.F.P. (2007) "Reflections on the use of the Mccabe and Thiele method", *Revista Ciências & Tecnologia*, Ano 1, n. 1.

Gupta, R.S. (2006) "*Modelling and Simulation of Fluid Catalytic Cracking Unit*", PhD Thesis, Thapar Institute of Engineering and Technology, India.

Han, IS; Riggs, J.B and Chung, CB (2000) "Modelling of a fluidized catalytic process", *Computers & Chemical Engineering and Processing*, 24(2000), pp.1681-1687.

Harbert, W.D. (1978) "Preflash saves heat in crude unit", *Hydrocarbon Processing*, **57**(7), pp.123-125.

Haydary, J and Pavlík, T (2009) "Steady-state and dynamic simulation of crude oil distillation using Aspen Plus and Aspen Dynamics", *Petroleum and Coal*, **51**(2), p.100.

Heydari, M., AleEbrahim, H. and Dabir, B., 2010. Study of seven-lump kinetic model in the fluid catalytic cracking unit *American Journal of Applied Sciences*, **7**(1), p.71.

Heydari M., AleEbrahim H. and Dabir B. (2010) "Study of seven-Lump Kinetic Model in the Fluid Catalytic Cracking Unit", *American Journal of Applied Sciences*, **7** (1): 71-76.

Hug, I (1998) "*Design Control Studies on the Fluid Catalytic Cracking Process*", Thesis in partial fulfilment of the requirement of Doctor of philosophy, California Institute of Technology, Pasadena, California, pp. 1234.

Ibrahim, H.A.H. (2014) "Design of Fractionation Columns", In MATLAB Applications for the Practical Engineer, DOI: 10.5772/57249.

Ibsen, K (2006) "Equipment Design and Cost Estimation for small Modular Biomass Systems, Synthesis Gas Cleanup, and Oxygen Separation Equipment - Task 1: Cost Estimates of small Modular Systems", *National Renewable Energy Laboratory*, Midwest Research Institute, Battellle, Subcontract report NREL/SR-510-39943. Contract No, Sans Francisco, California.

Ilkhaani, S (2009) "*Modelling and optimization of crude oil desalting*". Master thesis, University of Waterloo, Department of Chemical Engineering, Waterloo, Ontario, Canda.

International Energy Agency "IEA" (2016) "CO2 emissions from fuel combustion-highlights", www.iea.org/statistics/onlinedataservice/ [2017, July 29].

Ivakpour, J. and Kasiri, N. (2008) "Improve speed and convergence of distillation column simulation", *Hydrocarbon Process*, **87**(10), pp.75-79.

Jaroslav, J., Hlavacek, V. and Kubicek, M. (1973) "Calculation of Multistage Countercurrent Separation Processes-I. Multi-component Multi-stage Rectification by Differentiation with Respect to an Actual Parameter (J)", *Chem. Eng. Sci.*, **28**(10), 1555-1563.

Jarullah, A.T., (2012) "*Kinetic Modelling Simulation and Optimal Operation of Trickle Bed Reactor for Hydrotreating of Crude Oil. Kinetic Parameters Estimation of Hydrotreating Reactions in Trickle Bed Reactor (TBR) via Pilot Plant Experiments; Optimal Design and Operation of an Industrial TBR with Heat Integration and Economic Evaluation*", Doctoral dissertation, University of Bradford.

Jechura, J (2017) "*Refinery Feedstocks and Products–Proprieties and Specifications*", Colorado School of mines, USA.

Jelinet J. and Hlavecek V. (1975) "Mathematical Modelling of the Rectification Process", *International Chemical Engineering*, **15**(3) 487-494.

Jinsa M. and Ajeesh K.N. (2014) "Distillation composition control of binary distillation column", *Journal Impact Factor*, Volume 5, Issue 3, pp 79-85.

Jones, D.S. and Pujadó, P.P. eds. (2006) "*Handbook of petroleum processing*", Springer Science & Business Media, p.p. 1-109.

Kane, RD (2006) "Corrosion in Petroleum Refining and Petrochemical Operations", *Corrosion: Environments and Industries, vol 13C*, p 967-1014.

Kemp, I. C. (2007) "*Pinch Analysis and Process Integration-A User Guide on Process Integration for the Efficient Use of Energy*", Oxford.Butterworth-Heinemann.

Khim, TW (2013) "*Dynamic modelling of crude distillation unit*", Bachelor of Engineering dissertation, Universiti Malaysia Pahang.

Kister, H. (1992) "*Distillation design (vol1)*", McGraw-Hill Professional.

Kodjak, D (2015) "Policies to reduce fuel consumption, air pollution, and carbon emissions from vehicles in G20 nations", *The International Council on Clean Transportation*, Washington, D.C. http://www.theicct.org/policies-reduce-fuel-consumption-air-pollution-andcarbon-emissions-vehicles-g20-nations [2017, October 10].

Kolmetz, K. and Sari, R.M. (2016) "*Refinery atmospheric crude tower selection and sizing (Engineering Design Guideline)*", Kolmetz Handbook of Process Equipment Design, Malaysia, pp 1-164.

Kumar, V., Sharma, A., Chowdhury, I.R., Ganguly, S. and Saraf, D.N. (2001) "A crude distillation unit model suitable for online applications", *Fuel processing technology*, **73**(1), pp.1-21.

Lee, Q.F (2016) "*Fluid Catalytic cracking*", Chemical and Biological Engineering, University of British Columbia, Canada.

Leffler, W.L. (1985) "*Petroleum refining for nontechnical person, 2nd Edition*", PennWell Books, ISBN 0-87814-280-0.

Lekan, T.P., Gutti, B. and Alfred, A.S. (2013) "A review of an expert system design for crude oil distillation column using the neural networks model and process optimization and control using genetic algorithm framework", *Advances in Chemical Engineering and Science*, **3**, pp.164-170.

Letzsch, W., Santner, C. and Tragesser, S. (2009) "FCC reactor design: Part II", *Petroleum Technology Quarterly*, (**1**), p.25-29.

Li, W; Hui, CW and Li, A (2005) "Integrating CDU, FCC and product blending models into refinery planning", *Computers & chemical engineering*, **29**(9), pp.2010-2028.

Liang, KM; Guo, HY and Pan, SW (2005) "A study on naphtha catalytic reforming reactor simulation and analysis", *Journal of Zhejiang University*, Science.B, **6**(6), p.590.

Lichatz, T.A., "Dr. "Angelo Lucia's Tutorials on Distillation", *National Science Foundation*, accessed 2019-12-16, https://personal.egr.uri.edu/lucia/tutorials/tutorial2.html

Linninger, A., Senior Design CHE 396, Innovations Solutions.

Liu, L (2015) "*Molecular Characterization and Modelling for Refining Processes*", Ph.D. Thesis, University of Manchester, England.

López, D.C., Mahecha, C.A., Hoyos, L.J., Acevedo, L. and Villamizar, J.F. (2009) "Optimization model of a system of crude oil distillation units with heat integration and metamodelling", *CT&F-Ciencia,Tecnología y Futuro*, **3**(5), pp.159-173.

Manjumdor, S.K. and Das, C. (2012) "*Mass transfer operation 1-Distillation*", National programme on Technology Enhanced Learning,s Indian Institute of Technology Guwahati. Assam, India.

Manley, D.B., 1(993) "Waste minimization through improved process thermodynamics: crude oil fractionation", *The University of Missouri*, Rolla, Missouri.

McCabe, W.L., Smith, J.C. and Harriott, P (1993) "*Unit Operations of Chemical Engineering Fifth Edition*", MacGraw-Hill.

McCabe-Thiele, VAXA Software, PTTD, Version 1.8.0, www.vaxasoftare.com

McCain, WD (1990) "*The properties of petroleum fluids*", PennWell Books, Tulsa.

McSweeney, R. and Timeperley, J. (2018) "The Carbon Brief Profile: South Africa", https://www.carbonbrief.org/the-carbon-brief-profile-south-africa.

Merdrignac, I and Espinat, D (2007) "Physicochemical characterization of petroleum fractions: the state of the art", *Oil & Gas Science and Technology-Revue de l'IFP*, **62**(1), pp.7-32.

Minh, V.T. and Rani, A.M.A. (2009) "Modelling and Control of Distillation Column in Petroleum Process", *Mathematical Problems in Engineering*, Article ID 404702

Moses, J.R.L. (2011) "*Petroleum Refining: Modular versus Conventional Refineries*", www.vanguardngr.com/2011/10/petroleum-refining-modular-versus-conventional-refineries/ [2017, January 2011]

Mustapha, D., Fatima, O. and Sabria, T. (2007) "Distillation of a Complex Mixture. Part I: High Pressure Distillation Column Analysis: Modelling and Simulation", *Entropy*, **9**(2), pp.58-72.

Muhsin, W.A.S.; Zhang, J. and Lee, J. (2016) Modelling and Optimisation of Crude oil Hydrotreating Process Using neural network, *Chemical Engineering transactions*, 52, 211-216, DOI: 10.3030 ICET1652036.

Naré, H and Kamakaté, F (2017) "Developing a roadmap for adoption of clean fuel and vehicle standards in Southern and Western Africa", *International Council on Clean Transportation*.

Odebunmi, E.O.; Ogunsakin, E.A. and Ilukhor, P.E.P. (2002) "Characterization of crude oils and petroleum products: elution liquid chromatographic separation and gas chromatographic analysis of crude oils and petroleum products", *Bulletin of the Chemical Society of Ethiopia*, **16**(2), pp.115-132.

Ogundari, IO; Akinwale, Y; Adepoju AO and Akarakiri, JB (2012) "The modular Petroleum Alternative as an Energy Security and Environmental Sustainability Strategy in Nigeria: A Technology Policy Assessment", *3rd Technology Management for Directors of Science and Technology*, Bayelsa State, Nigeria.

Pahwa, R and Gupta, R (2016) "CFD Modelling of FCC Riser Reactor", *Int. Res. J. eng. Technol.*, 3(2), pp. 206-209.

Pant, K.K. and Kunzru, D. (2015) "*Pretroleum refinery engineering-Design concept of crude oil distillation column design*", National programme on Technology Enhanced Learning. Indian Institute of Technology Delhi.

Parkash, S (2003) "*Refinning Process Handbook*", Gulf publishing, New York.

Partnership for Clean Fuels and Vehicles "PCFV" (2015) "Clean fuels and vehicles regulatory toolkit", *United Nations-Environmental Protection agency (UNEP),* Naerobi, Kenya.

Paul, D; Thakur, R.S. and Chaudhari, P.K. (2015) Simulation of FCC Riser Reactor Using Five Lump model, *International Journal of ChemTech Research,* ISSN: 0974-4290, vol. 8, No 6, pp 750-758.

PetroWiki, Oil demislsification, viewed 14th Frbruary, 2017, <http://petrowiki.org/Oil_demulsification>

Prince, R.M. (2003) "Distillation, retrieved from lectures", http://facstaff.cbu.edu/rprice/lectures/distill7.html

Putter, A (2015) "*The Need for Southern African Liquid Fuels Production*", www.otctoolkits.com/the-need-for-southern-african-liquid-fuels-production/ [2017, October 02].

Rahim, K and Ben-Rahla, S. (2012) "*Calcul de vérification et optimisation des paramètres de fonctionnement de la colonne de Stabilisation PX0-CB-21-01 de l'UTBS*", Mémoire de Master, University Mohamed KhiderBiskar, Algeria.

Ramesh, K., Aziz, N., Shukor, S.A. and Ramasamy, M. (2007) "Dynamic rate-based and equilibrium model approaches for continuous tray distillation column", *Journal of Applied Science Research*, **3**(12), pp.2030-2041.

Rao, R.M., Rengaswamy, R; Suresh, A.K. and Balaraman, KS (2004) "Industrial experience with object-oriented modelling: FCC case study", *Chemical Engineering Research and Design*, **82**(4), pp.527-552.

Ratshomo, K. and Nembahe, R. (2015) "Overview of petroleum and diesel market in South Africa between 2002 and 2013", *Energy data collection management and analysis*, 1st Edition.

Reyes-Labarta, J.A. (2010) "*Métodos para el cálculo de operaciones de separaciónmultietapa en mezclasmulticomponentes*", University of Alicant.

Riazi, M.R. (2005) "*Characterization and properties of petroleum fractions (vol. 50)*", ASTM international.

Richmond, B. (2006), "*Introduction to Data analysis Handbook*", Academy for Educational development, Washington.

Rivotti, P.M.N. (2009) "*Modelling of vacuum residue hydrotreatment. Impact of the feedstock description on model output*", Master degree Dissertation, Instituto Superior Técnico, page 16.

Rosendo, M. L. (2003) "Simulation of Multi-component Multistage Vapor-Liquid Separations, An Improved Algorithm using the Wang-Henke Tridiagonal Matrix Method", *Ind. Eng. Chem. Res.*, **4**2(1), 175-182.

Sadeghbeigi, R. (2000) "*Fluid catalytic cracking handbook: Design, Operation and Troubleshooting of FCC Facilities*", Butterworth-Heinemann, 2nd Edition.

Sadeghbeigi, R. (2012) "*Fluid catalytic cracking handbook: An expert guide to the practical operation, design, and optimization of FCC units*", Elsevier, Waltham.

Sani, A.G., Ebrahim, H.A. and Azarhoosh, M.J. (2018) "8-Lump kinetic model for fluid catalytic cracking with olefin detailed distribution study', *Fuel*, **225**, pp.322-335.

Santana, E.I. and Zemp, R.J. (2001) "Thermodynamic Analysis of a Crude-Oil Fractionating Process", *In 4th Mercosur Congress on Process Systems Engineering*, vol. **21**, pp. 523-528.

SAPIA (2016) "South African Petroleum Industry Association, cleaner fuels II", http://www.sapia.org.za/Key-Issues/Cleaner-fuels-II, [2017, June 17]

Satterfield, C.N. (1975), "Trickle-bed reactors", *AIChE Journal*, vol 21, no2.

Saunders, M., Lewis, P. and Thornhill, A. (2009), "*Research methods for business students.5th Edition*", Harlow, England: Prentice Hall. https://is.vsfs.cz/el/6410/leto2014/BA_BSeBM/um/Research_Methods_for_Business_Students__5th_Edition.pdf [25/10/2018].

Seader, JD, Henley, EJ and Roper, DK (2011) "*Separation process principles, 3rd Edition*", John Wiley & Sons Incorporated, pp. 1-2.

Sharma, P. (2018) "*Developing an Online Predictor to Predict Sulfur Concentration for HDS Unit*", Master of Engineering Dissertation, Memorial University of Newfoundland.

Sharma, S. and Ghosh, R. (2016) "Designing and Process Simulation of A Single Column Crude Distillation Unit for Refineries", *Imperial Journal of Interdisciplinary Research (IJIR),* Vol 2, P. 985.

Shokri, S., Marvast, M.A. and Tajerian, M. (2007) "Production of ultra low sulphur diesel: Simulation and software development", *Petroleum and Coal*, ISSN 1337-7027.

Singh, B., Sahu, S., Dimri, N., Dasila, P.K., Parekh, A.A., Gupta, S.K. and Das, A.K. (2017) "Seventeen-lump model for the simulation of an industrial fluid catalytic cracking unit (FCCU)", *Sādhanā,* **42**(11), pp.1965-1978.

Sinnot, R. K. (2005) "*Chemical Engineering Design*", Oxford: Elsevier Butterworth-Heinemann.

Sittig, M. (1978) "*Petroleum Refining Industry Energy Saving and Environmental Control*", Noyes Data Corporation, New Jersey.

Smith, R.B. (1959) "Kinetic analysis of naphtha reforming with platinum catalyst", *Chem. Eng. Prog*, **55**(6), pp.76-80.

Solomon, A. F. (1981) "*Recent Advances in the Study of Multicomponent Distillation"*, B.Sc. Thesis, Chemical Engineering Department, University of Lagos, Nigeria.

Song, C. (2003) "An overview of new approaches to deep desulfurization for ultra-clean gasoline, Diesel Fuel and Jet Fuel", *Catalyst today*, Volume 86, issues 1-4, pages 211-263.

Souck, J.B. (2012) "*Modelling of crude oil distillation*", MSc Thesis, KTH Royal Institute of Technology, Stockholm, Sweden.

Speight, JG (2002) "*Handbook of petroleum product analysis*", New York, John Wiley & Sons, pp. 1-66.

Speight, JG (2006) "*The chemistry and technology of petroleum*", Laramie, CRC press, pp. 31-46.

Sridhar, L.N. and Lucia, A. (1990) "Tearing algorithms for separation process simulation (J)", *Computer Chemical Engineering*, **14**(8), 901-905.

Stathaki, A., Mellichamp, D.A. and Seborg, D.E. (1985) "Dynamic Simulation of a Multicomponent Distillation Column with Asymetric Dynamics", The Canadian Journal of Chemical Engineering, volume 63.

Taskar, UM (1996) "*Modelling and optimization of a catalytic naphtha reformer*", Ph.D. dissertation, Texas Tech University.

Thambiran, T. and Diab, R.D. (2011) "Air pollution and climate change co-benefit opportunities in the road transportation sector in Durban, South Africa", *Atmospheric Environment*, **45**(16), pp. 2683-2689. doi:10.1016/j.atmosenv.2011.02.059

Tissot, B.P .and Welte, D.H. (1984) "*From kerogen to petroleum-In Petroleum Formation and Occurrence*", Springer Berlin Heidelberg, pp. 160-198.

Vafajoo, L., Ganjian, K. and Fattahi, M. (2012) "Influence of key parameters on crude oil desalting: An experimental and theoretical study", *Journal of Petroleum Science and Engineering*, **90**, pp.107-111.

Vanmali, KH (2014) "*Improving refinery productivity through better utilization of crude oil blending using linear programming*", MSc research report, University of the Witwatersrand, Johannesburg.

Vathi, G.P. and Chaudhuri, K.K. (1997) "Modelling and simulation of commercial catalytic naphtha reformers", *The Canadian Journal of Chemical Engineering*, **75**(5), pp.930-937.

Wakeford, JJ (2012) "*Socioeconomic implications of global oil depletion for South Africa: vulnerabilities, impacts and transition to sustainability*", Doctorat of Philosophy Dissertation. Stellenbosch University.

Watkins, B; Haley, J. and Schiller, R. (2014) Meeting Tier 3 Gasoline Sulfur Regulations, *Grace Catalysts Technologies Catalagram*, Issue No 114/2014, p. 36-39.

Watkins, B; Olsen, C. and Hunt, D. (2011) Balancing the Need for low sulphur FCC Products and Increasing FCC LCO Yields by Applying Advanced Technology for Cat Feed Hydrotreating, *NPRA Annual Meeting*, Issue No 109/2011, p. 38-48.

Watkins, R. N. (1979) "*Petroleum Refinery Distillation*", Second Edition, Gulf Publishing Company, Houston.

Wauquier, JP (1994) "*Le raffinage du pétrole-Tome 1-Pétrole brut, Produits pétroliers. Schémas de fabrication (Vol. 1)* ", Editions Technip, Paris.

Weekman Jr, V.W. (1968) "Model of catalytic cracking conversion in fixed, moving, and fluid-bed reactors", *Industrial & Engineering Chemistry Process Design and Development*, **7**(1), pp.90-95.

Weekman Jr, V.W. (1969) "Kinetics and dynamics of catalytic cracking selectivity in fixed-bed reactors" *Industrial & Engineering Chemistry Process Design and Development*, **8**(3), pp.385-391.

Wlazlowski, S; Hagströmer, B. and Giulietti, M. (2001) "Causality in crude oil prices", *Applied Economics*, vol. 43 issue **24**, p. 3337-3347.

World Bank Development Indicators, http://data.worldbank.org/indicator/EN.ATM.CO2E.PC?end=2013&locations=ZA&start=1960&view=chart [2017, July 28].

Yang, Y and Barton, PI (2015) "Refinery Optimization Integrated with a Nonlinear Crude Distillation Unit Model", *IFAC-PapersOnLine*, **48**(8), pp.205-210.

Yasin, G., Bhanger, M.I., Ansari, T.M., Naqvi, S.M.S.R., Ashraf, M; Ahmad, K. and Talpur, F.N. (2013) "Quality and chemistry of crude oils", *Journal of Petroleum Technology and Alternative Fuels*, **4**(3), pp.53-63.

Yusuf, A.Y. (2013) "*Green Petroleum Refining - Mathematical Models for Optimizing Petroleum Refining Under Emission Constraints*", MASc, University of waterloo.

APPENDIX

Appendix A: Feedstock data

A.1. Thermodynmic properties data of the feedstock

The crude oil used is named Kutubucrude, it has the composition properties given in the Table A.2 below.

Table A1 Kutubu crude assay (Exxon Mobil, 2017)

KUTUB16F	Whole crude	Butane and Lighter IBP - 60F	Light Naphtha C5 - 165F	Heavy Naphtha 165 - 330F	Kerosene 330 - 480F	Diesel 480 - 650F	Vacuum Gas Oil 650 - 1000F	Vacuum Residue 1000F+
Cut volume, %	100,0	3,3	17,3	38,6	17,7	12,3	9,3	1,6
API Gravity,	51,4	116,4	82,5	54,9	43,9	33,7	26,0	10,3
Specific Gravity (60/60F),	0,774	0,571	0,661	0,759	0,807	0,856	0,899	0,998
Carbon, wt %	86,0	82,6	83,8	86,2	86,1	87,0	87,1	87,3
Hydrogen, wt %	14,0	17,4	16,2	13,8	13,9	13,0	12,8	12,0
Pour point, F	(3,7)			(95,6)	(47,6)	24,1	103,2	126,8
Neutralization number (TAN), MG/GM	0,020	0,000	0,001	0,003	0,009	0,053	0,075	0,101

Sulfur, wt%	0,021	0,000	0,0001	0,0001	0,002	0,028	0,107	0,254
Viscosity at 20C/68F, cSt	1,2	0,4	0,5	0,8	1,6	5,3	73,2	3 879 326,2
Viscosity at 40C/104F, cSt	1,0	0,4	0,4	0,6	1,2	3,3	27,8	146 810,5
Viscosity at 50C/122F, cSt	0,9	0,3	0,4	0,6	1,1	2,7	18,9	39 976,4
Mercaptansulfur, ppm	0,6	0,0	0,0	0,1	0,3	0,2	0,0	0,0
Nitrogen, ppm	161,7	-	-	0,0	0,3	33,0	728,6	3865,9
CCR, wt%	0,3						0,2	13,0
N-Heptane Insolubles (C7 Asphaltenes), wt%	0,0						-	0,4
Nickel, ppm	0,2							10,9
Vanadium, ppm	0,0							0,1
Calcium, ppm	0,5							
Reid Vapour Pressure (RVP) Whole Crude, psi	7,1							
Hydrogen Sulfide (dissolved), ppm	-							
Salt content, ptb	0,5							
Paraffins, vol %	51,8	100,0	86,4	43,1	46,3	42,7	39,3	2,6
Naphthenes, vol %	29,6	-	13,6	37,8	33,8	33,5	27,0	10,9
Aromatics (FIA), vol %	18,6	-	-	19,1	19,9	23,8	33,7	86,5
Distillation type, TBP								

IBP, F	12,1		61,1	165,7	330,6	480,7	650,9	1 000,8
5 vol%, F	73,1		69,0	172,3	336,0	486,8	659,0	1 008,0
10 vol%, F	106,6		73,1	179,4	342,1	493,6	668,2	1 016,4
20 vol%, F	162,8		81,2	193,8	354,8	507,8	688,0	1 034,4
30 vol%, F	200,3		98,6	208,3	368,1	522,6	709,6	1 054,3
40 vol%, F	238,4		107,5	223,0	382,0	537,9	733,5	1 076,8
50 vol%, F	279,8		125,8	237,8	396,5	553,9	760,4	1 102,5
60 vol%, F	335,7		135,2	253,1	411,6	570,7	791,0	1 132,9
70 vol%, F	413,8		143,6	269,1	427,3	588,4	826,6	1 170,2
80 vol%, F	516,5		151,3	286,5	443,9	607,3	869,6	1 219,2
90 vol%, F	667,2		158,4	306,4	461,4	627,8	924,1	1 293,8
95 vol%, F	801,6		161,7	317,7	470,6	638,6	958,3	1 355,6
EP, F	1 162,5		164,7	328,7	479,0	648,8	995,4	1 469,3
Freeze point, F				(85,6)	(35,1)	37,3		
Smoke point, mm				27,8	21,0	14,4		
Naphthalenes (D1840), vol%					3,1	11,8		
Viscosity at 100C/212F, cSt	0,6	0,3	0,3	0,4	0,6	1,3	4,9	510,7

Viscosity at 150C/302F, cSt	0,4	0,2	0,2	0,3	0,4	0,8	2,2	49,9
Cetane Index 1990 (D4737),				25,3	43,0	51,4		
Cloud point, F				(91,2)	(43,9)	28,7		
Aniline pt, F					133,6	158,5	185,3	

A.2. Physical, Chemical and thermodynamic properties

Calculation of density, molecular weight of each fraction and molecular weight of pseudo-component were done using respectively equation A.1, A.2, A.3, A.4 and A.5 (Souck, 2012; Riazi, 2005). Base on the calculation of density and molecular, Adapted from Sinnot (2005) and Buck *et al*. (1999) the Table A.2. gives physical, chemical and thermodynamic data.

$$Density\ \left(\frac{kg}{m^3}\right) = 1000 \text{ x } SG \qquad \text{A.1}$$

$$Molecular\ Weight_{fraction}(\frac{g}{mol}) = 42.965\ (T_b^{1.26007} * SG^{4.98308}) e^{\left(2.097*10^{-4}\right)T_b - 7.78712SG + \left(2.08476*10^{-3}\right)T_b SG} \qquad \text{A.2}$$

$$Molecular\ Weight_{paraffin}\left(\frac{g}{mol}\right) = \left(\frac{1}{0.02013}(6.98291 - \ln(1070 - T_b))\right)^{\frac{3}{2}} \qquad \text{A.3}$$

$$Molecular\ Weight_{naphthene}\left(\frac{g}{mol}\right) = \left(\frac{1}{0.02239}(6.98291 - \ln(1070 - T_b))\right)^{\frac{3}{2}} \qquad \text{A.4}$$

$$Molecular\ Weight_{aromatic}\left(\frac{g}{mol}\right) = \left(\frac{1}{0.02247}(6.98291 - \ln(1070 - T_b))\right)^{\frac{3}{2}} \qquad \text{A.5}$$

Where

T_b Is the characteristic boiling point of the petroleum fraction (K)

$SG$is the specific gravity of the petroleum fraction at 15.56^{o}C (60^{o}F)

The mean average boiling point (MEABP) is commonly used for characterisation of a mixture boiling point. However, the boiling point at 50 vol% distilled may be considered as the characteristic boiling point instead of MEABP (Riazi, 2005). This study is going to use this knowledge for further calculations.

Noted that the pseudo-components (naphtenes, paraffins and aromatics) have the same density as the fraction in which it is contained (Liang, Guo and Pan, 2005).

Table A.2: Physical, Chemical and thermodynamic property

Component	**Boiling point (K)**	**Average molecular weight (g/mol)**	**SG**	**Density (Kg/m3)**
Whole crude			0.774	774
Gases	277.36	54.50077	0.571	571
G: Paraffins	277.36	59.7157		
G: Naphthenes	277.36	50.90648		
G: Aromatics	277.36	50.63486		
Light Naphtha	325.26	77.90992	0.661	661
LN: Paraffins	325.26	78.76196		
LN: Naphthenes	325.26	60.8815		
LN: Aromatics	325.26	66.78479		
Heavy Naphtha	387.48	107.7519	0.759	759
HN: Paraffins	387.48	108.2124		
HN: Naphthenes	387.48	92.24898		
HN: Aromatics	387.48	91.75677		
Kerosene	475.65	160.0617	0.807	807
K: Paraffins	475.65	160.8767		
K: Naphthenes	475.65	137.1443		
K: Aromatics	475.65	136.4125		
Diesel	563.09	226.6347	0.856	`856
D: Paraffins	563.09	229.5035		
D: Naphthenes	563.09	195.6473		
D: Aromatics	563.09	194.6034		
VGO	677.82	349.3105	0.899	899
VGO: Paraffins	677.82	356.027		
VGO: Naphthenes	677.82	306.5061		
VGO: Aromatics	677.82	301.8867		

Residue	867.87	659.9901	0.998	998
Sulphur		32.06		
Hydrogen Sulphide		34.8		
Hydrogen		2.02		
Water		18.01		
Argon		39.948		
Oxygen		31.999		
Nitrogen		28.013		
Carbon Dioxide		44.01		
Ethanol		46.07		
MTBE		88.15		
Natural Gas		16.04		

A.3. Property data pertaining to select representative compounds (adapted from Sinnot (2005) and Buck *et al.* (1999))

In purpose to simplify modelling, the pseudo-components of the different fractions were represented by molecules according to molecular weight similarities between pseudo-components and reprehensive molecules as shown the Table A.3.

Table A.3: Representation of pseudo-component of different fractions

Component	Pseudo-component	Representative Molecule	Chemical Formula of representative Molecule	Molecular weight of pseudo-components (kg/kmol)	Molecular weight of representative molecule (kg/kmol)	Relative error between molecular weight (%)	RON
Light Naphthas	LN Paraffins	n-Hexane	C6H14	78.76196	86.18	8.61	
	LN Naphtenes	Cyclopentane	C5H10	60.8815	70.13	13.19	
	LN Aromatics						
Heavy Naphtha	HN Paraffins	n-Octane	C8H18	108.2124	114.23	5.27	
	HN Naphtenes	Ethylcyclopentane	C7H14	92.24898	98.19	6.05	
	HN Aromatics	Toluene	C7H8	91.75677	92.14	0.42	
Reformate	R Paraffins	n-Pentane					61.80
	R Naphtenes	Cyclopentane					101.60

	R Aromatics	Benzene					98.00
Kerosene	K paraffins	n-Undecane	C11H24	160.8767	156.31	-2.92	
	K Naphtenes	Hexylcyclopentane	C11H22	137.1443	154.30	11.12	
	K Aromatics	Methyl Naphtalene	C11H10	136.4125	142.20	4.07	
Diesel	D Paraffins	n-Hexadecane	C16H34	229.5035	226.45	-1.35	100.00
	D Naphtenes	n-Decyclohexane	C16H32	195.6473	224.45	12.83	70.00
	D Aromatics	n-Nonylbenzene	C15H24	194.6034	204.36	4.77	50.00
Ethanol							123.00
MTBE							118.00

A.4. Feed Items

Crude oil: Imported from Papua New Guinea, the Kutubu crude is stored at 15.56^{o}C and 1.01bar. The compositional proprieties of this crude oil are listed in Table A.4:

Hydrogen: use to supported hydrotrating operations, is kept at 25oC and 20 bar.

Air: kept at 20oC and 1.01 bar with the average molar composition given in the Table A.4.

Table A.4: Composition of air (Mackenzie and Mackenzie, 1995)

Component	Amount (%)
Nitrogen	78.04
Oxygen	20.947
Argon	0.934
Carbon dioxide	0.035

Blending agents: Use of Ethanol and MTBE for research of better octane number during blending of gasoline, both agents at 25oC and 20 bar.

Appendix B: Material Balance and heat balance

B.1. Material balance

Equations of material balance:

- $Volume\ Flowrate\ (F_i) = \frac{Cut\ Vol\ (\%)\ \text{x}\ Feed\ Flowrate}{100}$ [bbl/day] B.1

  Where i representing different cut

- $Mass\ Flowrate(M_i) = F_i$ x 42 x 8.33 x $S.G.$ [lbs/day] B.2

  Where SG is the specific gravity, 42 and 8.33 are conversion constant

- $Sulfur\ Flowrate = \frac{M_i\ \ Sulfur,wt\%}{100}$ [lbs/day] B.3
- $Molar\ Flowrate = \frac{M_i}{24\ \ Molecular\ Weight}$ [lbs-mole/h] B.4

Table B.1: Materials balance of refinery products

KUTUB16F	Whole crude	Butane and Lighter IBP-60F	Light Naphtha C5 - 165F	Heavy Naphtha 165 - 330F	Kerosene 330 - 480F	Diesel 480 - 650F	Vacuum Gas Oil 650 - 1000F	Vacuum Residue 1000F+
Cut volume, %	100	3,3	17,3	38,6	17,7	12,3	9,3	1,6
API Gravity,	51,4	116,4	82,5	54,9	43,9	33,7	26	10,3
Specific Gravity (60/60F),	0,774	0,571	0,661	0,759	0,807	0,856	0,899	0,998
Sulfur, wt%	0,021	0	0	0	0,002	0,028	0,107	0,254
volume flow rate (bbl/day)	12000	396	2076	4632	2124	1476	1116	192
volume flow rate (liter/h)	79579,5	2623,5	13753,5	30687	14071,5	9778,5	7393,5	1272
mass flow rate (lb/day)	3249500	79108,94	480090,5	1229999	599683,8	442032,7	351008,9	67038,77
mass flow rate (Kg/h)	61409,51	1495,259	9074,32	23248,53	11334,79	8354,979	6634,514	1267,118
sulphur flow rate (lb/day)	682,3949	0	0	0	11,99368	123,7692	375,5796	170,2785
sulphur flow rate (Kg/h)	12,87506	0	0	0	0,226547	2,337862	7,094281	3,216371
molecular weight	1636,16	54,5008	77,9099	107,752	160,062	226,635	349,311	659,99
molar flow rate(lbs-mole/h)	1076,341	60,47999	256,7551	475,6291	156,1075	81,26748	41,86926	4,232309

B.2. Energy Balance

Without knowing the enthalpy of petroleum vapour/liquid fractions, it is not possible to estimate the condenser and re-boiler duties and conduct energy balances. Maxwell (1950) presents about 13 graphs that can be conveniently used to estimate the enthalpy of vapour/liquid fractions as functions of refinery stream characterization factor and system temperature. These graphical correlations are tabulated and presented in Tables B.2 – B.13. Using these Tables, the enthalpy of refinery process streams is estimated using interpolation and extrapolation procedures.

Table B.2.: Hydrocarbon liquid enthalpy data for MEABP = 200^{o}F and K = 11 – 12

T (^{o}F)	Hydrocarbon Enthalpy (Btu/lb) for various values of K					
	11	11.2	11.4	11.6	11.8	12
0	0.49	0.41	0.33	0.24	0.16	0.07
20	8.12	8.34	8.56	8.78	9.00	9.22
40	17.98	18.29	18.60	18.91	19.22	19.54
60	27.90	28.32	28.74	29.16	29.58	30.00
80	37.59	38.15	38.71	39.27	39.82	40.38
100	47.38	48.16	48.94	49.71	50.49	51.27
120	57.74	58.76	59.79	60.81	61.83	62.85
140	68.52	69.61	70.70	71.79	72.88	73.96
160	78.81	80.25	81.69	83.13	84.56	86.00
180	88.86	90.77	92.68	94.60	96.51	98.42
200	99.60	101.54	103.47	105.40	107.33	109.27
220	110.37	112.46	114.55	116.64	118.73	120.82
240	122.05	124.37	126.70	129.03	131.36	133.68
260	133.69	136.21	138.72	141.23	143.75	146.26
280	144.74	147.54	150.35	153.15	155.95	158.75
300	156.43	159.66	162.90	166.13	169.36	172.59
320	168.98	172.47	175.95	179.43	182.91	186.39
340	180.43	184.26	188.09	191.92	195.75	199.59
360	192.85	197.02	201.18	205.34	209.51	213.67
380	207.06	211.34	215.62	219.91	224.19	228.47
400	220.58	225.00	229.42	233.84	238.26	242.67
420	234.17	238.93	243.69	248.45	253.21	257.97
440	247.78	253.05	258.32	263.59	268.86	274.13
460	262.39	268.04	273.68	279.33	284.98	290.62
480	277.45	283.60	289.75	295.91	302.06	308.21
500	293.22	300.01	306.80	313.59	320.38	327.17

Table B.3: Hydrocarbon vapour enthalpy data for MEABP = 200°F and K = 11 – 12.

T (°F)	Hydrocarbon Enthalpy (Btu/lb) for various values of K					
	11	11.2	11.4	11.6	11.8	12
0	182.29	179.55	176.81	174.07	171.32	168.58
20	187.88	185.37	182.86	180.36	177.85	175.34
40	194.67	192.23	189.79	187.36	184.92	182.48
60	201.76	199.36	196.97	194.57	192.17	189.78
80	208.69	206.47	204.26	202.04	199.82	197.60
100	215.52	213.65	211.79	209.92	208.05	206.18
120	222.35	220.76	219.16	217.56	215.97	214.37
140	229.24	227.77	226.29	224.82	223.35	221.88
160	236.45	235.14	233.83	232.52	231.21	229.90
180	243.96	242.89	241.81	240.74	239.67	238.59
200	251.70	250.84	249.97	249.11	248.25	247.38
220	260.16	259.65	259.13	258.62	258.11	257.60
240	267.77	267.64	267.51	267.38	267.25	267.12
260	275.72	275.81	275.89	275.98	276.06	276.15
280	284.69	284.87	285.06	285.24	285.42	285.61
300	293.23	293.64	294.06	294.47	294.89	295.30
320	302.34	302.96	303.57	304.18	304.80	305.41
340	311.03	312.03	313.03	314.03	315.02	316.02
360	320.06	321.42	322.77	324.13	325.48	326.84
380	329.97	331.47	332.97	334.46	335.96	337.46
400	339.71	341.41	343.10	344.80	346.49	348.19
420	349.78	351.83	353.88	355.92	357.97	360.02
440	360.60	362.80	365.00	367.20	369.39	371.59
460	370.59	373.18	375.77	378.36	380.94	383.53
480	381.21	384.16	387.12	390.07	393.03	395.98
500	392.13	395.17	398.21	401.25	404.29	407.34
520	404.19	407.12	410.06	412.99	415.92	418.86
540	414.90	418.19	421.48	424.77	428.06	431.35
560	424.77	428.72	432.67	436.63	440.58	444.53
580	437.34	441.54	445.74	449.93	454.13	458.33
600	447.85	452.59	457.34	462.09	466.83	471.58
620	459.48	464.45	469.42	474.39	479.35	484.32
640	470.59	476.04	481.50	486.95	492.40	497.86
660	481.81	488.00	494.19	500.38	506.57	512.76
680	494.36	500.86	507.36	513.85	520.35	526.84
700	507.41	513.71	520.02	526.33	532.64	538.95
720	519.67	526.24	532.81	539.38	545.95	552.52
740	532.34	539.21	546.07	552.93	559.80	566.66
760	545.20	552.41	559.62	566.84	574.05	581.26
780	557.96	565.55	573.14	580.74	588.33	595.92
800	571.08	578.89	586.70	594.52	602.33	610.15
820	584.25	592.40	600.55	608.70	616.85	625.00
840	597.11	605.50	613.88	622.27	630.65	639.03
860	609.73	618.42	627.10	635.78	644.46	653.14
880	622.88	631.97	641.05	650.13	659.21	668.29
900	637.09	646.43	655.76	665.09	674.43	683.76
920	651.13	660.64	670.14	679.65	689.16	698.67
940	664.71	674.57	684.44	694.30	704.17	714.04
960	678.71	689.03	699.34	709.66	719.97	730.29
980	692.89	703.63	714.38	725.12	735.87	746.61
1000	706.48	717.70	728.92	740.14	751.35	762.57
1020	720.64	732.32	743.99	755.67	767.34	779.02
1040	734.09	746.28	758.46	770.64	782.83	795.01
1060	748.40	760.93	773.46	785.99	798.52	811.05
1080	763.68	776.50	789.33	802.16	814.99	827.81
1100	777.76	791.17	804.57	817.97	831.37	844.77
1120	791.62	805.53	819.44	833.36	847.27	861.18

Table B.4: Hydrocarbon vapour enthalpy data for MEABP = 300°F and K = 11 – 12

T (°F)	Hydrocarbon Enthalpy (Btu/lb) for various values of K					
	11	11.2	11.4	11.6	11.8	12
0	175.25	172.59	169.93	167.28	164.62	161.96
20	180.93	178.59	176.25	173.90	171.56	169.22
40	186.86	184.86	182.86	180.86	178.86	176.86
60	192.94	191.25	189.56	187.88	186.19	184.51
80	199.18	197.80	196.42	195.04	193.66	192.29
100	205.84	204.73	203.62	202.51	201.41	200.30
120	213.09	212.06	211.04	210.01	208.98	207.96
140	220.02	219.20	218.39	217.57	216.75	215.93
160	227.41	226.82	226.24	225.66	225.08	224.50
180	235.52	235.07	234.62	234.17	233.71	233.26
200	243.15	242.92	242.70	242.48	242.26	242.03
220	250.07	250.32	250.57	250.82	251.07	251.32
240	258.30	258.73	259.17	259.60	260.04	260.47
260	266.78	267.32	267.86	268.40	268.94	269.48
280	275.06	275.86	276.66	277.46	278.26	279.06
300	284.19	285.19	286.20	287.20	288.20	289.20
320	292.73	293.93	295.12	296.31	297.50	298.69
340	302.24	303.59	304.94	306.30	307.65	309.00
360	312.58	314.02	315.46	316.90	318.34	319.77
380	322.63	324.18	325.73	327.27	328.82	330.37
400	332.11	333.90	335.68	337.46	339.24	341.03
420	341.54	343.57	345.59	347.61	349.63	351.65
440	351.73	353.86	355.99	358.11	360.24	362.37
460	362.34	364.62	366.89	369.17	371.44	373.72
480	373.42	375.94	378.47	380.99	383.52	386.04
500	384.62	387.29	389.97	392.65	395.32	398.00
520	395.29	398.41	401.53	404.65	407.77	410.89
540	406.19	409.58	412.97	416.36	419.75	423.14
560	416.87	420.52	424.17	427.82	431.47	435.12
580	428.01	431.96	435.91	439.86	443.81	447.76
600	439.69	443.76	447.83	451.90	455.97	460.04
620	451.80	456.19	460.57	464.96	469.35	473.74
640	463.34	468.06	472.77	477.49	482.21	486.93
660	474.93	479.97	485.02	490.06	495.10	500.14
680	487.16	492.61	498.05	503.50	508.95	514.39
700	499.64	505.47	511.30	517.13	522.96	528.79
720	512.30	518.29	524.29	530.29	536.29	542.29
740	524.92	531.22	537.52	543.82	550.12	556.42
760	537.61	544.28	550.96	557.63	564.31	570.98
780	550.17	557.13	564.09	571.05	578.01	584.96
800	562.83	570.00	577.18	584.35	591.52	598.69
820	576.66	584.05	591.43	598.81	606.19	613.57
840	589.01	596.92	604.84	612.76	620.67	628.59
860	601.61	609.89	618.16	626.44	634.71	642.99
880	615.56	623.98	632.41	640.83	649.25	657.68
900	628.88	637.84	646.80	655.76	664.72	673.68
920	641.84	651.41	660.98	670.55	680.12	689.70
940	655.92	665.68	675.43	685.19	694.94	704.70
960	669.92	679.95	689.98	700.02	710.05	720.08
980	683.56	694.03	704.50	714.97	725.43	735.90
1000	697.91	708.57	719.23	729.89	740.55	751.21
1020	711.62	722.83	734.04	745.26	756.47	767.68
1040	725.70	737.23	748.76	760.29	771.82	783.35
1060	740.84	752.50	764.16	775.82	787.48	799.13
1080	755.66	767.71	779.75	791.80	803.85	815.89
1100	769.42	782.09	794.76	807.44	820.11	832.78
1120	784.49	797.57	810.64	823.71	836.78	849.85
1140	798.91	812.31	825.71	839.11	852.51	865.91

Table B.5: Hydrocarbon liquid enthalpy data for MEABP = 300°F and K = 11 – 12.

T (°F)	Hydrocarbon Enthalpy (Btu/lb) for various values of K					
	11	11.2	11.4	11.6	11.8	12
0	0.20	0.24	0.29	0.33	0.37	0.41
20	7.75	8.17	8.60	9.03	9.45	9.88
40	16.77	17.34	17.91	18.48	19.05	19.62
60	25.55	26.36	27.16	27.97	28.77	29.57
80	34.35	35.31	36.28	37.24	38.20	39.17
100	43.94	44.85	45.76	46.67	47.58	48.48
120	52.97	54.19	55.40	56.62	57.83	59.05
140	62.57	64.05	65.52	67.00	68.47	69.94
160	72.21	73.96	75.71	77.46	79.21	80.96
180	81.92	83.86	85.80	87.73	89.67	91.61
200	92.43	94.35	96.27	98.19	100.11	102.03
220	102.56	104.89	107.23	109.56	111.89	114.23
240	113.48	115.99	118.49	121.00	123.50	126.01
260	124.52	127.09	129.65	132.21	134.77	137.33
280	135.07	137.91	140.75	143.59	146.42	149.26
300	146.03	149.19	152.36	155.52	158.68	161.85
320	157.82	161.19	164.55	167.92	171.28	174.65
340	169.58	173.29	177.00	180.71	184.42	188.13
360	181.80	185.77	189.75	193.72	197.69	201.67
380	194.68	198.70	202.72	206.75	210.77	214.79
400	207.56	211.67	215.77	219.87	223.98	228.08
420	220.69	224.98	229.28	233.58	237.88	242.18
440	234.11	238.57	243.04	247.50	251.96	256.43
460	246.65	251.52	256.40	261.28	266.16	271.04
480	261.11	266.38	271.66	276.93	282.21	287.48
500	274.84	280.16	285.47	290.78	296.10	301.41
520	288.40	293.89	299.37	304.85	310.33	315.81
540	304.29	310.08	315.88	321.67	327.46	333.25
560	319.00	325.04	331.08	337.12	343.16	349.20
580	335.13	341.51	347.89	354.27	360.66	367.04
600	350.68	357.81	364.93	372.06	379.19	386.31

Table B.6: Hydrocarbon vapour enthalpy data for MEABP = 400°F and K = 11 – 12

T (°F)	Hydrocarbon Enthalpy (Btu/lb) for various values of K					
	11	11.2	11.4	11.6	11.8	12
0	167.62	165.22	162.82	160.42	158.02	155.62
20	174.02	171.96	169.91	167.86	165.81	163.76
40	179.94	178.13	176.32	174.51	172.69	170.88
60	186.39	184.72	183.06	181.40	179.74	178.08
80	192.50	191.12	189.73	188.35	186.96	185.58
100	199.48	198.21	196.95	195.69	194.42	193.16
120	206.21	205.32	204.44	203.55	202.66	201.78
140	213.27	212.35	211.44	210.53	209.61	208.70
160	221.95	220.89	219.83	218.77	217.71	216.65
180	228.82	228.13	227.43	226.74	226.04	225.35
200	236.82	236.41	236.00	235.58	235.17	234.76
220	244.23	243.93	243.62	243.32	243.01	242.71
240	252.48	252.21	251.93	251.65	251.37	251.10
260	261.24	261.07	260.90	260.73	260.57	260.40
280	270.09	270.06	270.02	269.99	269.95	269.92
300	278.61	278.96	279.30	279.65	279.99	280.33
320	288.11	288.36	288.61	288.85	289.10	289.35
340	297.17	297.81	298.44	299.07	299.71	300.34
360	306.84	307.54	308.24	308.95	309.65	310.36
380	316.15	316.96	317.76	318.57	319.37	320.18
400	325.50	326.72	327.93	329.15	330.37	331.58
420	336.12	337.18	338.23	339.28	340.34	341.39
440	347.06	348.41	349.77	351.12	352.47	353.82
460	356.74	358.66	360.58	362.50	364.42	366.35
480	367.24	369.30	371.35	373.41	375.46	377.52
500	378.94	380.98	383.02	385.05	387.09	389.13
520	389.90	392.33	394.75	397.17	399.59	402.02
540	400.52	403.20	405.88	408.57	411.25	413.93
560	410.40	413.67	416.95	420.22	423.50	426.77
580	422.91	426.22	429.53	432.84	436.15	439.47
600	433.45	437.00	440.55	444.10	447.65	451.20
620	445.20	448.77	452.34	455.91	459.47	463.04
640	457.32	461.21	465.09	468.98	472.86	476.75
660	469.16	473.55	477.95	482.34	486.74	491.14
680	481.18	486.07	490.96	495.85	500.74	505.63
700	492.79	497.98	503.17	508.36	513.54	518.73
720	506.17	511.35	516.53	521.71	526.89	532.06
740	517.71	523.50	529.30	535.09	540.89	546.69
760	530.52	536.53	542.54	548.55	554.56	560.57
780	543.76	549.79	555.82	561.85	567.88	573.92
800	558.15	564.11	570.07	576.04	582.00	587.96
820	570.49	576.97	583.46	589.94	596.43	602.92
840	583.01	589.92	596.82	603.72	610.62	617.53
860	596.52	603.73	610.93	618.14	625.35	632.55
880	610.01	617.44	624.87	632.30	639.74	647.17
900	622.48	630.53	638.57	646.61	654.65	662.69
920	636.94	645.05	653.15	661.26	669.36	677.46
940	649.30	657.97	666.64	675.31	683.97	692.64
960	662.75	671.74	680.73	689.72	698.72	707.71
980	677.17	686.61	696.05	705.49	714.92	724.36
1000	690.46	700.27	710.08	719.88	729.69	739.50
1020	705.18	715.34	725.51	735.67	745.84	756.00
1040	720.34	730.57	740.79	751.01	761.24	771.46
1060	735.34	745.63	755.93	766.23	776.53	786.83
1080	749.35	760.34	771.34	782.33	793.32	804.32
1100	763.82	775.04	786.25	797.47	808.69	819.90
1120	778.70	790.46	802.22	813.99	825.75	837.52
1140	793.54	805.70	817.85	830.00	842.15	854.30

Table B.7.: Hydrocarbon liquid enthalpy data for MEABP = 400°F and K = 11 – 12

T (°F)	Hydrocarbon Enthalpy (Btu/lb) for various values of K					
	11	11.2	11.4	11.6	11.8	12
0	0	0	0	0	0	0
20	7.70	7.90	8.10	8.30	8.50	8.70
40	15.46	15.93	16.39	16.86	17.32	17.79
60	24.16	24.88	25.59	26.31	27.02	27.74
80	31.58	32.54	33.50	34.46	35.42	36.39
100	39.75	40.86	41.97	43.08	44.18	45.29
120	49.31	50.57	51.83	53.09	54.35	55.62
140	58.42	59.89	61.36	62.84	64.31	65.78
160	67.37	69.02	70.67	72.31	73.96	75.60
180	77.24	78.95	80.65	82.36	84.07	85.78
200	86.99	88.87	90.75	92.62	94.50	96.38
220	96.32	98.37	100.41	102.46	104.51	106.56
240	107.95	109.93	111.91	113.89	115.86	117.84
260	118.58	120.66	122.74	124.82	126.91	128.99
280	129.36	131.66	133.96	136.26	138.56	140.86
300	140.21	142.89	145.56	148.23	150.91	153.58
320	151.32	154.05	156.78	159.51	162.24	164.97
340	163.26	166.17	169.08	171.99	174.90	177.81
360	175.32	178.44	181.56	184.68	187.80	190.92
380	187.16	190.23	193.30	196.37	199.45	202.52
400	200.18	203.39	206.60	209.82	213.03	216.25
420	213.59	216.77	219.95	223.13	226.31	229.50
440	225.94	229.45	232.95	236.46	239.97	243.48
460	238.23	242.03	245.83	249.63	253.43	257.23
480	251.00	255.12	259.23	263.35	267.46	271.57
500	264.20	268.52	272.83	277.15	281.47	285.79
520	277.65	282.44	287.23	292.02	296.81	301.60
540	291.31	296.15	300.98	305.81	310.65	315.48
560	305.20	310.51	315.82	321.13	326.44	331.75
580	320.08	325.59	331.10	336.62	342.13	347.64
600	334.63	340.57	346.51	352.45	358.38	364.32
620	349.72	356.08	362.45	368.81	375.17	381.53
640	365.41	372.19	378.96	385.73	392.50	399.27
660	380.81	387.91	395.02	402.12	409.22	416.32
680	397.78	404.95	412.13	419.31	426.48	433.66

Table B.8: Hydrocarbon vapour enthalpy data for MEABP = 500°F and K = 11 – 12

T (°F)	Hydrocarbon Enthalpy (Btu/lb) for various values of K					
	11	11.2	11.4	11.6	11.8	12
0	165.62	162.14	158.65	155.17	151.69	148.20
20	171.50	168.21	164.92	161.62	158.33	155.04
40	177.35	174.38	171.42	168.45	165.49	162.52
60	184.01	181.21	178.40	175.60	172.79	169.98
80	190.03	187.57	185.10	182.63	180.17	177.70
100	197.11	194.84	192.58	190.31	188.04	185.77
120	203.34	201.23	199.12	197.01	194.90	192.79
140	210.66	208.55	206.45	204.34	202.23	200.13
160	217.84	216.02	214.20	212.39	210.57	208.76
180	225.78	224.08	222.39	220.69	218.99	217.30
200	233.16	231.55	229.94	228.33	226.71	225.10
220	241.18	239.96	238.73	237.51	236.29	235.06
240	249.49	248.36	247.22	246.09	244.96	243.82
260	257.24	256.31	255.39	254.46	253.54	252.61
280	265.65	265.00	264.34	263.69	263.03	262.38
300	275.16	274.42	273.67	272.93	272.19	271.45
320	285.10	284.30	283.50	282.70	281.90	281.11
340	294.83	293.99	293.16	292.32	291.49	290.65
360	304.42	303.73	303.04	302.35	301.65	300.96
380	313.71	313.39	313.08	312.77	312.46	312.15
400	323.59	323.49	323.39	323.30	323.20	323.11
420	332.69	333.01	333.32	333.64	333.95	334.26
440	342.76	343.11	343.46	343.81	344.16	344.50
460	352.66	353.38	354.09	354.80	355.52	356.23
480	364.52	365.34	366.17	366.99	367.82	368.64
500	375.06	376.31	377.57	378.82	380.08	381.33
520	385.70	387.30	388.90	390.50	392.10	393.70
540	397.51	399.10	400.70	402.30	403.89	405.49
560	409.14	410.90	412.66	414.42	416.18	417.94
580	419.94	421.95	423.96	425.96	427.97	429.98
600	431.32	433.56	435.80	438.05	440.29	442.53
620	443.43	445.72	448.01	450.30	452.59	454.88
640	455.04	457.57	460.09	462.62	465.14	467.67
660	467.10	469.93	472.76	475.59	478.42	481.25
680	477.88	481.32	484.75	488.19	491.62	495.05
700	490.28	493.91	497.55	501.18	504.81	508.45
720	502.85	506.65	510.45	514.24	518.04	521.83
740	514.89	519.07	523.24	527.42	531.60	535.77
760	527.83	532.18	536.53	540.87	545.22	549.57
780	539.95	544.71	549.47	554.23	558.99	563.75
800	553.32	558.47	563.62	568.77	573.91	579.06
820	566.16	571.68	577.19	582.71	588.22	593.73
840	578.50	584.25	590.00	595.75	601.50	607.25
860	592.13	597.94	603.74	609.55	615.35	621.16
880	606.12	612.25	618.39	624.52	630.66	636.79
900	618.17	625.11	632.04	638.98	645.91	652.85
920	632.49	639.38	646.27	653.16	660.05	666.94
940	645.97	653.16	660.35	667.54	674.72	681.91
960	660.26	667.76	675.27	682.77	690.27	697.77
980	675.02	682.68	690.34	698.00	705.66	713.32
1000	689.02	696.98	704.95	712.91	720.88	728.84
1020	704.02	712.26	720.50	728.74	736.97	745.21
1040	718.15	726.74	735.33	743.93	752.52	761.11
1060	731.92	741.08	750.24	759.41	768.57	777.74
1080	748.06	757.47	766.88	776.28	785.69	795.09
1100	762.00	772.00	781.99	791.98	801.98	811.97
1120	775.97	786.43	796.89	807.35	817.81	828.27
1140	790.71	801.52	812.34	823.15	833.97	844.78
1160	806.26	817.36	828.45	839.55	850.65	861.74

Table B.9: Hydrocarbon liquid enthalpy data for MEABP = 500°F and K = 11 – 12

T (°F)	Hydrocarbon Enthalpy (Btu/lb) for various values of K					
	11	11.2	11.4	11.6	11.8	12
0	0	0	0	0	0	0
20	8.34	8.55	8.76	8.97	9.18	9.40
40	16.33	16.42	16.51	16.60	16.70	16.79
60	24.17	24.34	24.51	24.69	24.86	25.03
80	32.51	32.93	33.34	33.76	34.18	34.59
100	40.09	40.74	41.40	42.06	42.71	43.37
120	48.80	49.68	50.56	51.44	52.33	53.21
140	58.68	59.62	60.57	61.51	62.46	63.41
160	67.31	68.39	69.48	70.57	71.65	72.74
180	77.26	78.24	79.22	80.20	81.18	82.16
200	86.56	87.86	89.15	90.45	91.75	93.04
220	95.50	97.15	98.80	100.45	102.10	103.76
240	106.01	107.79	109.58	111.36	113.15	114.93
260	117.04	118.85	120.65	122.45	124.25	126.05
280	127.04	129.10	131.16	133.22	135.28	137.33
300	137.82	140.09	142.36	144.63	146.90	149.17
320	149.33	151.47	153.61	155.74	157.88	160.02
340	159.02	161.68	164.34	167.00	169.66	172.32
360	171.17	173.89	176.62	179.35	182.07	184.80
380	182.97	185.66	188.34	191.03	193.72	196.40
400	194.53	197.33	200.13	202.93	205.73	208.53
420	205.53	208.75	211.97	215.19	218.41	221.63
440	218.36	221.56	224.75	227.94	231.14	234.33
460	230.10	233.59	237.09	240.58	244.08	247.57
480	242.83	246.37	249.92	253.47	257.02	260.57
500	255.38	259.05	262.73	266.40	270.07	273.74
520	268.39	272.46	276.54	280.62	284.70	288.77
540	283.06	287.09	291.11	295.14	299.17	303.19
560	295.46	300.25	305.04	309.82	314.61	319.40
580	310.38	315.43	320.48	325.53	330.59	335.64
600	325.04	330.17	335.31	340.45	345.59	350.73
620	339.59	345.05	350.51	355.96	361.42	366.88
640	353.23	358.89	364.56	370.22	375.88	381.55
660	367.88	373.80	379.71	385.62	391.54	397.45
680	383.10	389.41	395.73	402.04	408.36	414.68
700	398.75	405.14	411.53	417.93	424.32	430.71
720	413.92	420.81	427.69	434.58	441.46	448.35
740	430.95	438.00	445.05	452.10	459.15	466.20
760	446.71	454.06	461.41	468.76	476.11	483.46
780	463.72	471.16	478.61	486.06	493.51	500.95
800	479.61	487.70	495.78	503.87	511.96	520.05

Table B.10: Hydrocarbon liquid enthalpy data for MEABP = 600°F and K = 11 – 12

T (°F)	Hydrocarbon Enthalpy (Btu/lb) for various values of K					
	11	11.2	11.4	11.6	11.8	12
0	0	0	0	0	0	0
20	7.92	8.06	8.20	8.33	8.47	8.61
40	15.09	15.52	15.94	16.36	16.78	17.20
60	23.22	23.76	24.30	24.85	25.39	25.93
80	32.36	32.87	33.39	33.91	34.42	34.94
100	39.91	40.75	41.59	42.43	43.27	44.11
120	48.39	49.37	50.34	51.32	52.30	53.27
140	56.84	57.94	59.05	60.15	61.25	62.36
160	65.97	67.13	68.29	69.45	70.61	71.76
180	75.95	77.08	78.20	79.33	80.45	81.57
200	85.29	86.55	87.80	89.05	90.31	91.56
220	94.60	96.04	97.48	98.92	100.36	101.80
240	104.68	106.13	107.58	109.03	110.48	111.93
260	114.30	115.96	117.62	119.28	120.94	122.61
280	123.68	125.66	127.65	129.63	131.62	133.61
300	134.60	136.55	138.51	140.46	142.42	144.37
320	145.15	147.36	149.56	151.76	153.96	156.16
340	156.17	158.55	160.93	163.31	165.69	168.07
360	167.38	169.90	172.42	174.94	177.47	179.99
380	178.42	181.16	183.89	186.63	189.37	192.11
400	189.95	192.82	195.69	198.56	201.43	204.30
420	201.97	204.94	207.91	210.88	213.85	216.82
440	214.53	217.58	220.64	223.69	226.75	229.80
460	226.92	230.02	233.13	236.23	239.34	242.44
480	239.57	242.96	246.36	249.76	253.15	256.55
500	252.55	255.81	259.06	262.32	265.58	268.84
520	264.31	267.69	271.07	274.44	277.82	281.20
540	277.65	281.20	284.75	288.30	291.85	295.40
560	290.79	294.62	298.46	302.29	306.13	309.96
580	303.45	307.57	311.68	315.80	319.92	324.03
600	317.22	321.17	325.11	329.05	333.00	336.94
620	331.49	335.58	339.67	343.76	347.85	351.95
640	345.88	350.23	354.59	358.94	363.30	367.65
660	359.94	364.60	369.25	373.90	378.56	383.21
680	374.04	379.04	384.04	389.04	394.04	399.04
700	388.85	394.13	399.42	404.70	409.98	415.26
720	403.65	409.19	414.74	420.28	425.83	431.37
740	419.07	424.95	430.83	436.72	442.60	448.48
760	434.54	440.80	447.07	453.34	459.61	465.88
780	449.97	456.58	463.19	469.79	476.40	483.00
800	466.08	472.93	479.78	486.63	493.48	500.33
820	481.86	489.12	496.37	503.63	510.88	518.14
840	497.97	505.71	513.46	521.20	528.95	536.69
860	515.04	523.28	531.53	539.77	548.01	556.26
880	530.48	539.65	548.81	557.97	567.14	576.30
900	548.65	558.02	567.40	576.77	586.15	595.52

Table B.11: Hydrocarbon vapour enthalpy data for MEABP = 600°F and K = 11 – 12

T (°F)	Hydrocarbon Enthalpy (Btu/lb) for various values of K					
	11	11.2	11.4	11.6	11.8	12
0	159.95	156.45	152.95	149.45	145.95	142.45
20	166.78	163.39	160.00	156.61	153.22	149.83
40	172.72	169.52	166.33	163.13	159.93	156.73
60	178.50	175.62	172.73	169.84	166.96	164.07
80	184.91	182.23	179.55	176.87	174.19	171.51
100	192.18	189.47	186.76	184.05	181.34	178.63
120	199.43	196.84	194.24	191.65	189.06	186.47
140	206.08	203.70	201.31	198.93	196.55	194.17
160	213.33	211.14	208.95	206.75	204.56	202.37
180	221.11	219.07	217.04	215.00	212.96	210.93
200	228.41	226.52	224.63	222.74	220.85	218.96
220	236.70	234.92	233.14	231.37	229.59	227.81
240	244.40	242.89	241.38	239.87	238.36	236.85
260	252.48	251.10	249.72	248.34	246.96	245.58
280	261.25	259.93	258.62	257.31	256.00	254.69
300	269.74	268.74	267.74	266.74	265.74	264.74
320	279.44	278.43	277.42	276.41	275.40	274.39
340	288.20	287.18	286.16	285.14	284.12	283.11
360	297.15	296.45	295.75	295.05	294.35	293.65
380	306.77	306.44	306.11	305.78	305.45	305.12
400	315.66	315.65	315.63	315.61	315.60	315.58
420	326.10	326.28	326.47	326.65	326.84	327.02
440	336.49	336.54	336.60	336.65	336.70	336.76
460	346.54	346.85	347.15	347.46	347.77	348.07
480	357.46	358.19	358.93	359.67	360.40	361.14
500	369.03	369.66	370.28	370.91	371.53	372.16
520	380.07	380.92	381.78	382.63	383.49	384.34
540	390.63	391.82	393.00	394.19	395.38	396.56
560	401.89	403.19	404.49	405.79	407.09	408.39
580	413.01	414.50	416.00	417.50	418.99	420.49
600	423.35	425.15	426.95	428.75	430.54	432.34
620	436.02	437.74	439.47	441.19	442.92	444.65
640	448.66	450.51	452.35	454.20	456.05	457.90
660	459.97	462.29	464.61	466.94	469.26	471.58
680	471.32	474.02	476.72	479.43	482.13	484.83
700	484.30	487.00	489.70	492.40	495.09	497.79
720	497.51	500.36	503.20	506.05	508.89	511.73
740	509.77	513.11	516.44	519.78	523.12	526.46
760	522.35	526.05	529.75	533.44	537.14	540.84
780	535.36	539.25	543.15	547.05	550.94	554.84
800	547.58	551.93	556.29	560.64	565.00	569.35
820	561.05	565.64	570.23	574.83	579.42	584.01
840	574.27	578.95	583.62	588.30	592.97	597.65
860	587.07	592.07	597.07	602.07	607.06	612.06
880	600.32	605.69	611.07	616.45	621.82	627.20
900	613.87	619.47	625.08	630.68	636.29	641.89
920	626.79	632.93	639.07	645.20	651.34	657.48
940	640.17	646.58	652.99	659.40	665.80	672.21
960	654.83	661.39	667.96	674.52	681.09	687.65
980	669.29	676.16	683.02	689.89	696.75	703.62
1000	682.24	689.52	696.80	704.08	711.36	718.64
1020	696.85	704.36	711.87	719.37	726.88	734.39
1040	711.12	718.94	726.75	734.56	742.38	750.19
1060	725.03	733.23	741.43	749.63	757.83	766.03
1080	739.54	748.10	756.65	765.21	773.76	782.31
1100	753.82	762.86	771.90	780.93	789.97	799.00
1120	768.44	777.86	787.28	796.71	806.13	815.55
1140	783.69	793.25	802.80	812.36	821.91	831.47

Table B.12: Hydrocarbon liquid enthalpy data for MEABP = 800°F and K = 11 – 12

T (°F)	Hydrocarbon Enthalpy (Btu/lb) for various values of K					
	11	11.2	11.4	11.6	11.8	12
0	0	0	0	0	0	0
20	7.74	7.81	7.87	7.94	8.00	8.07
40	15.25	15.41	15.56	15.72	15.87	16.02
60	22.46	22.76	23.06	23.35	23.65	23.95
80	30.81	31.15	31.48	31.82	32.16	32.50
100	38.70	39.22	39.73	40.25	40.76	41.27
120	46.46	47.15	47.84	48.53	49.22	49.91
140	54.20	55.07	55.95	56.82	57.69	58.57
160	63.97	64.75	65.53	66.31	67.08	67.86
180	72.44	73.29	74.13	74.98	75.83	76.67
200	81.27	82.28	83.30	84.31	85.32	86.34
220	89.89	91.19	92.48	93.78	95.08	96.38
240	100.40	101.50	102.59	103.69	104.78	105.88
260	110.69	111.64	112.58	113.52	114.46	115.41
280	120.32	121.50	122.68	123.87	125.05	126.23
300	130.81	132.05	133.29	134.53	135.77	137.01
320	140.10	141.58	143.05	144.52	145.99	147.47
340	151.40	152.88	154.36	155.84	157.32	158.80
360	161.59	163.42	165.25	167.09	168.92	170.75
380	172.03	173.82	175.61	177.40	179.20	180.99
400	183.51	185.38	187.24	189.10	190.97	192.83
420	195.52	197.35	199.17	201.00	202.83	204.65
440	205.96	208.14	210.33	212.51	214.70	216.89
460	218.32	220.59	222.85	225.12	227.38	229.65
480	230.42	232.78	235.14	237.50	239.87	242.23
500	242.71	245.17	247.62	250.08	252.54	255.00
520	254.97	257.53	260.09	262.65	265.21	267.77
540	267.83	270.54	273.26	275.98	278.70	281.42
560	280.18	283.23	286.27	289.31	292.35	295.40
580	293.20	296.48	299.76	303.05	306.33	309.61
600	305.91	309.51	313.12	316.72	320.33	323.93
620	318.91	322.70	326.49	330.28	334.07	337.86
640	332.82	336.78	340.74	344.70	348.66	352.63
660	346.82	350.78	354.74	358.69	362.65	366.60
680	360.05	364.35	368.66	372.97	377.28	381.59
700	373.72	378.30	382.88	387.46	392.04	396.63
720	387.57	392.24	396.91	401.57	406.24	410.91
740	402.54	407.32	412.11	416.90	421.69	426.48
760	417.13	422.11	427.09	432.07	437.05	442.04
780	431.65	436.84	442.03	447.23	452.42	457.61
800	447.21	452.47	457.73	462.98	468.24	473.50
820	461.39	466.85	472.30	477.75	483.20	488.66
840	477.79	483.40	489.00	494.60	500.20	505.81
860	493.26	499.13	504.99	510.86	516.72	522.58
880	509.35	515.19	521.03	526.87	532.72	538.56
900	524.08	530.32	536.56	542.81	549.05	555.29
920	540.55	546.99	553.43	559.87	566.32	572.76
940	557.03	563.65	570.27	576.89	583.51	590.13
960	573.65	580.53	587.41	594.30	601.18	608.06
980	589.75	597.06	604.37	611.67	618.98	626.29
1000	606.56	614.20	621.83	629.47	637.11	644.75
1020	623.47	631.27	639.07	646.87	654.66	662.46
1040	641.90	650.25	658.59	666.94	675.29	683.64
1060	659.93	668.58	677.23	685.87	694.52	703.17
1080	677.10	686.52	695.95	705.38	714.81	724.23
1100	695.64	705.56	715.48	725.40	735.32	745.24

Table B.13: Hydrocarbon vapour enthalpy data for MEABP = 800°F and K = 11 – 12

T (°F)	Hydrocarbon Enthalpy (Btu/lb) for various values of K					
	11	11.2	11.4	11.6	11.8	12
0	147.65	143.99	140.33	136.67	133.01	129.35
20	152.66	149.20	145.74	142.29	138.83	135.38
40	159.17	155.88	152.58	149.29	145.99	142.70
60	165.75	162.48	159.20	155.92	152.64	149.36
80	171.83	168.66	165.49	162.32	159.15	155.98
100	178.70	175.74	172.77	169.81	166.85	163.89
120	185.20	182.35	179.49	176.64	173.79	170.93
140	192.28	189.64	187.00	184.36	181.72	179.07
160	199.87	197.35	194.84	192.32	189.81	187.29
180	207.11	204.67	202.24	199.80	197.37	194.93
200	215.73	213.29	210.85	208.41	205.97	203.53
220	223.77	221.47	219.17	216.87	214.57	212.27
240	231.59	229.44	227.30	225.16	223.01	220.87
260	239.35	237.48	235.61	233.74	231.87	230.00
280	248.35	246.60	244.85	243.10	241.35	239.60
300	257.59	255.83	254.08	252.32	250.57	248.81
320	266.19	264.51	262.82	261.13	259.45	257.76
340	275.31	273.71	272.10	270.49	268.88	267.27
360	285.00	283.47	281.93	280.39	278.85	277.31
380	294.05	292.81	291.58	290.34	289.10	287.87
400	303.97	302.92	301.88	300.84	299.79	298.75
420	312.78	311.94	311.10	310.26	309.41	308.57
440	323.67	322.70	321.72	320.75	319.77	318.80
460	334.13	333.45	332.78	332.10	331.43	330.76
480	344.19	343.63	343.07	342.51	341.95	341.39
500	356.14	355.67	355.20	354.73	354.26	353.79
520	367.42	367.63	367.84	368.05	368.26	368.47
540	377.61	377.95	378.28	378.62	378.95	379.29
560	388.30	388.94	389.58	390.22	390.86	391.50
580	401.02	401.48	401.95	402.42	402.89	403.36
600	410.89	411.83	412.77	413.71	414.65	415.59
620	422.64	423.84	425.05	426.25	427.45	428.66
640	434.21	435.63	437.04	438.45	439.86	441.28
660	445.97	447.57	449.17	450.77	452.37	453.97
680	458.16	459.94	461.73	463.51	465.29	467.08
700	470.66	472.55	474.45	476.34	478.23	480.13
720	482.53	484.77	487.00	489.23	491.46	493.69
740	495.57	497.91	500.26	502.61	504.95	507.30
760	508.08	510.65	513.22	515.79	518.36	520.93
780	520.96	523.72	526.49	529.25	532.01	534.77
800	534.29	537.22	540.15	543.08	546.02	548.95
820	547.30	550.54	553.77	557.00	560.24	563.47
840	560.83	564.13	567.42	570.72	574.01	577.31
860	574.74	578.08	581.41	584.75	588.09	591.43
880	587.02	590.80	594.59	598.37	602.16	605.94
900	600.30	604.39	608.49	612.59	616.68	620.78
920	613.85	618.38	622.91	627.45	631.98	636.52
940	628.26	633.00	637.74	642.49	647.23	651.97
960	642.25	647.20	652.16	657.12	662.08	667.04
980	655.83	661.14	666.45	671.76	677.07	682.38
1000	670.38	675.96	681.54	687.13	692.71	698.29
1020	684.46	690.48	696.51	702.54	708.56	714.59
1040	698.46	704.76	711.06	717.36	723.66	729.96
1060	712.70	719.35	726.00	732.65	739.29	745.94
1080	727.97	734.95	741.94	748.92	755.91	762.89
1100	741.39	748.93	756.48	764.02	771.56	779.11
1120	756.85	764.55	772.26	779.97	787.67	795.38
1140	771.12	779.40	787.67	795.95	804.23	812.50
1160	787.50	796.00	804.50	813.00	821.50	830.01

Appendix C: Crude Oil Distillation Uni design

C.1. Column

Distillation column design was based on Mac Cabe and Thiele method. To be able to use that method, calculation of relative volatility was done using Antoine equation.

$$\boldsymbol{Log\ P = A - \frac{B}{C+T\ (C^o)}} \quad \text{C.1.}$$

With P: Saturated vapour pressure (mmHg)
A, B and C: Antoine coefficients

Usage of Antoine equation on the LK, D and HK of the crude oil helped to find different values of relative volatility, and the average of all values gave us the relative volatility needed which was: $\alpha = 2.895179$

Table C.1: Calculation of relative volatility using Antoine equation

T (oC)	Log P			P			α
	LK	D	HK	LK	D	HK	
13.3	1.339849	1.161551	0.736817	21.87002	14.5061	5.455281	4.008963
14.5	1.370248	1.190877	0.769533	23.4557	15.51946	5.882115	3.987631
15	1.382816	1.203007	0.783064	24.1444	15.95904	6.068257	3.978803
15.7	1.400315	1.219902	0.801908	25.1371	16.59212	6.337348	3.966501
20	1.505404	1.321511	0.915184	32.01873	20.96576	8.225919	3.892419
25	1.62263	1.435147	1.04177	41.9401	27.23622	11.00956	3.809427
30	1.734837	1.544209	1.163161	54.30466	35.0114	14.55999	3.729719
35	1.842342	1.648969	1.279671	69.55721	44.56245	19.04018	3.65318
40	1.945434	1.749675	1.391589	88.19305	56.19211	24.63705	3.579691
45	2.04438	1.846559	1.49918	110.7592	70.23591	31.56314	3.509131
50	2.139424	1.939834	1.602692	137.8555	87.0631	40.05822	3.441377
55	2.230793	2.029698	1.702351	170.1347	107.0775	50.39075	3.376309
60	2.318696	2.116335	1.798369	208.3032	130.7179	62.85918	3.313807
65	2.403326	2.199915	1.890941	253.12	158.4584	77.79317	3.253756
70	2.484864	2.280598	1.980251	305.3964	190.8087	95.55449	3.196044
75	2.563475	2.358532	2.066467	365.9947	228.3136	116.5379	3.140563
80	2.639314	2.433854	2.149748	435.8268	271.5526	141.1718	3.087209
85	2.712525	2.506694	2.23024	515.8524	321.1398	169.9184	3.035883
90	2.783243	2.577173	2.308083	607.0765	377.7225	203.2743	2.986489
95	2.851593	2.645403	2.383403	710.5477	441.9806	241.7704	2.938936
100	2.917692	2.711491	2.456323	827.3549	514.6251	285.9714	2.893139
105	2.981649	2.775536	2.526954	958.6249	596.3971	336.4759	2.849015

110	3.043566	2.83763	2.595403	1105.519	688.0663	393.9158	2.806485
115	3.10354	2.897863	2.66177	1269.23	790.4291	458.9554	2.765476
120	3.161661	2.956316	2.726149	1450.979	904.307	532.2904	2.725916
125	3.218013	3.013067	2.788626	1652.013	1030.545	614.6475	2.68774
130	3.272676	3.068189	2.849286	1873.598	1170.01	706.7824	2.650884
135	3.325725	3.121752	2.908206	2117.021	1323.587	809.4794	2.615288
140	3.37723	3.173821	2.96546	2383.582	1492.179	923.5492	2.580894
145	3.427258	3.224457	3.021118	2674.593	1676.707	1049.828	2.547649
150	3.47587	3.273719	3.075246	2991.372	1878.101	1189.175	2.515501
155	3.523128	3.321662	3.127906	3335.244	2097.305	1342.473	2.484403
157.7	3.548103	3.347021	3.155752	3532.666	2223.416	1431.371	2.46803
160	3.569085	3.368338	3.179156	3707.534	2335.273	1510.623	2.454308
160.2	3.570897	3.370179	3.181178	3723.035	2345.195	1517.671	2.453124
165	3.613796	3.413796	3.229053	4109.565	2592.963	1694.546	2.425172
170	3.65731	3.458085	3.27765	4542.657	2871.341	1895.178	2.396955
175	3.699675	3.501248	3.324997	5008.119	3171.375	2113.472	2.369617
180	3.740935	3.543327	3.37114	5507.254	3494.035	2350.393	2.34312
185	3.781134	3.584364	3.416127	6041.347	3840.288	2606.916	2.31743
190	3.820311	3.624396	3.459999	6611.67	4211.102	2884.027	2.292513
195	3.858506	3.66346	3.502798	7219.477	4607.438	3182.717	2.268337
200	3.895754	3.70159	3.544562	7866	5030.252	3503.985	2.244873
205	3.932091	3.738819	3.585329	8552.452	5480.491	3848.832	2.22209
210	3.967549	3.77518	3.625134	9280.017	5959.095	4218.262	2.199962
215	4.00216	3.810702	3.66401	10049.86	6466.992	4613.279	2.178463
217.3	4.017805	3.826769	3.68159	10418.49	6710.713	4803.854	2.168778
220	4.035954	3.845414	3.701989	10863.11	7005.097	5034.883	2.157569

Relative volatility value can then be substitute in equation C.2. That makes possible the drawing of the equilibrium curve. Substituting X with numbers between 0 and 1 in equation C.2 and C.3, both curve and line can be plotted using data obtained and represented in Table C.3 below.

$$Y = \frac{\alpha X}{1+(\alpha-1) X} \quad \text{C.2}$$

$$Y = X \quad \text{C.3}$$

Table C.3: Data representing points that assisted to plot equilibrium curve and 45^{o} line

X	C.2	C.3
0	0	0
0.05	0.132229	0.05
0.1	0.243391	0.1
0.15	0.338149	0.15
0.2	0.419885	0.2
0.25	0.49111	0.25
0.3	0.553729	0.3
0.35	0.609214	0.35
0.4	0.658717	0.4
0.45	0.703157	0.45
0.5	0.743272	0.5
0.55	0.779665	0.55
0.6	0.812831	0.6
0.65	0.843181	0.65
0.7	0.871058	0.7
0.75	0.896753	0.75
0.8	0.920513	0.8
0.85	0.942549	0.85
0.9	0.96304	0.9
0.95	0.982146	0.95
1	1	1

C.2. Side strippers

The following assumptions were made in the design of side strippers' column:

- 100% removal of hydrogen sulphide
- 100% efficient
- No stripping gas is lost
- Operations are isothermal
- Minimal to negligible drop in stripper

The side stripes are identical to one another each having same dimensions with a ratio height-diameter of3:1.5 (Sinnot, 2005). The volume is evaluated using equation C.2 below:

$$V_{side-stripper} = h_{side-stripper}\ \pi\ \frac{\left(Diameter_{stripper}\right)^2}{4} = 3m\ \pi\ \frac{(1.5m)^2}{4} = 5.30\ m^3$$

Appendix D: Design of reactors

D.1. Design of Hydrotreatment Unit reactor

For diesel hydrotrearting a trickle bed reactor is with a WHSV 0.85 h^{-1} was assumed as applied by Korsten and Hoffman (1996).

Following data are used for calculation (Askani *et al.*, 2012; Korsten and Hoffman)

- Catalyst density: $\rho_{CoMo/Al_2O_3\ catalyst} = 1420\ kg/m^3$
- Industrial bed void fraction ε = 0.5

Catalyst volume calculation:

$$WHSV_{diesel} = 0.85h^{-1} = \frac{83540979\ kg/h}{1420\frac{kg}{m^3}\ V_{HDTcatalyst}(m^3)} \text{ (D.1)}$$

$$\rightarrow V_{HDT\ catalyst} = 6.92\ m^3 (D.1\ bis)$$

Reactor volume calculation:

$$V_{HDT\ reactor\ volume} = \frac{6.92\ m^3}{1-0.5} = 13.84\ m^3 \text{ (D.2)}$$

The volume is also determinate by using the following formula $V = \pi\frac{D^2}{4}L + 4\frac{\pi D^3}{24}$ (D.3) with diameter-length ratio equal to 7 (from what $L = 7 * D$ (D.4)). By substituting D.4 into the volume relation D.3, we extract the value of the diameter which is 2.3m and this can also be substitute in the relation D.4 to find the value of the length 16.1m.

Knowing the diameter, the sectional area can be calculated using following formula:

$$A = \frac{\pi D^2}{4} = \frac{\pi(2.33)^2}{4} = 4.15m^2 \text{ (D.5)}$$

D.2. Design of catalytic reforming reactors

In this section reactors are in serie, its then receive the same flow rate in term of mass. Reactors used are semi regeneration catalytic reforming reactors. Referring to Baerns (2013) these are the following WHSV use for the three reactors:

- Catalytic reactor 1: WHSV1 = $8h^{-1}$
- Catalytic reactor 2: WHSV2 = $5h^{-1}$
- Catalytic reactor 3: WHSV3 = $1h^{-1}$

Following data are used for calculation (Askani *et al.*, 2012; McKetta, 1990):

- Catalyst density: $\rho_{bimetallic} = 788\ kg/m^3$
- Industrial bed void fraction $\varepsilon = 0.5$
- Catalyst volume calculation:

$$WHSV_1 = 8h^{-1} = \frac{23248.53\ kg/h}{788\frac{kg}{m^3} V_{CR1\ catalyst}(m^3)} \text{ (D.6)}$$

$$\rightarrow V_{CR1\ catalyst} = 3.69\ m^3 \text{ (D.6 bis)}$$

$$WHSV_2 = 5h^{-1} = \frac{23248.53\ kg/h}{788\frac{kg}{m^3} V_{CR2\ catalyst}(m^3)} \text{ (D.7)}$$

$$\rightarrow V_{CR2\ catalyst} = 5.90\ m^3 \text{ (D.7 bis)}$$

$$WHSV_3 = 1.1h^{-1} = \frac{23248.53\ kg/h}{788\frac{kg}{m^3} V_{CR31\ catalyst}(m^3)} \text{ (D.8)}$$

$$\rightarrow V_{CR3\ catalyst} = 26.82\ m^3 \text{ (D.8bis)}$$

Reactor volume calculation:

$$V_{CR1\ reactor} = \frac{3.69\ m^3}{1-0.5} = 7.38\ m^3 \text{ (D.9)}$$

$$V_{CR2\ reactor} = \frac{5.90\ m^3}{1-0.5} = 11.80\ m^3 \text{ (D.10)}$$

$$V_{CR3\ reactor} = \frac{26.82\ m^3}{1-0.5} = 53.64\ m^3 \text{ (D.11)}$$